Automatic volume inspection for glass blow moulds

Master degree in Product Design Engineering

Tiago André Roriz Ferreira

Leiria, November of 2020

Automatic volume inspection for glass blow moulds

Master degree in Product Design Engineering

Tiago André Roriz Ferreira

Project Report under the supervision of Professor Carlos Neves and Professor Fábio Simões.

Leiria, November of 2020

Originality and Copyright

This dissertation/project report is original, made only for this purpose, and all authors whose studies and publications were used to complete it are duly acknowledged.

Dedication

I dedicate this thesis to my family, the special people inside my group of friends and co-workers who allowed its fulfilment.

Acknowledgments

This section has the purpose of thanking the individuals who helped me face and develop this project.

A big thank you to my supervisors Carlos Neves and Fábio Simões for all their help, advice and guidance throughout the project's duration.

I would also like to thank Flávio Domingues, Hélder Morais, Pedro Pereira, from Micronsense, and Ricardo Ferreira, from Intermolde, for proposing such an engaging project and for providing the material necessary for its development. A special thanks to Flávio Domingues for the mentorship and suggestions to execute the project development.

Furthermore, I would like to thank my colleagues João Fonseca and Mariana Agostinho for the help given during the laser scanning of the moulds. I would also like to thank Mariana Ramos for the time and patience given in the CMM department.

In addition, I wish to leave my deepest appreciation towards my family, for the constant support, love and trust given to reach this point in my life. A special mention to my brother for his ability to cheer me up and make me go back to work.

A word of gratitude to my friends and Carolina Serra for the constant joys in life and making me who I am. I would like to specifically thank Carolina Serra, a very special persosn, for appearing in my life and pushing me towards fulfilling my goals in life and for all her love and support.

A final thanks to all my co-workers in Micronsense for all their support and good times spent together.

Abstract

In the glass bottle mould making industry, volume control is done by measuring the amount of water needed to fill the mould. This process has several issues. Firstly, it requires a trained operator to properly seal the mould. Secondly, different operators will lead to different volume values. Another issue is related to the time and work necessary for the procedure, which can take up to 20 minutes for a single mould, making it unsuitable to inspect several moulds of the same series. These issues can be solved by automating the procedure. By using reverse engineering systems to obtain the internal cavity surfaces, comparative studies can be done, such as wear study, enabling the optimization of the moulds. The goal of this project is to establish a system to automate the inspection of the moulds which will result in the acquisition of the moulding surfaces. Then, the volume of the moulds and surface deviations in specific areas can be measured. The development of this project focused in two main areas: the development of a script, where the volume is calculated and the surface is inspected, from cloud points, to determine if the mould is in an acceptable state; and the study of technologies capable of acquiring the mould's surface while simultaneously being automatable. As for this study, several case studies using laser and structured light are performed to understand the abilities and limitations of these technologies. The first study was done using polished cast iron moulds to determine the ability to acquire the surface and obtain the volume. Then, the ability to present proper comparative results is explored by using a set of unpolished cast iron moulds and then these same moulds once polished to verify if the used systems can obtain the deviations between the two situations. Finally, the validation of the technologies was done using a demo bronze mould, where surface deviations were inspected as well as a ring gauge where the inner cylinder was used for inspection. From these cases, the used laser scanner was able to obtain the volumes of the moulds as well as proper comparative results without spray. As for the used structured light system, it proved unable to acquire the surfaces of the moulds and of the ring gauge, requiring spray. Despite this performance, the system is quite automatable and a state-of-the-art structured light system, using blue light, could be used for this purpose. The laser is also a viable solution, but the cost and complexity to automate can be higher than the structured light system.

Keywords: Automatic inspection, laser scanning, reverse engineering, bottle moulds

List of Figures

Figure 1 - Wide mouth press and blow process [1] 2

Figure 2 - Narrow neck press and blow process [1] 2

Figure 3 - Glass manufacturing schematic [2] 8

Figure 4 - Plunger action in the blank mould [9] 9

Figure 5 - Appearance of spikes on the container's surface [10] 10

Figure 6 - Reverse Engineering basic steps [20] 14

Figure 7 - Reflection behaviour for different surfaces [25] 15

Figure 8 - Schematic of a structured light system [40] 17

Figure 9 - Example of a structured light system being used to inspect a part a) System setup; b) Aligned point clouds; c) STL model of the part [37] 17

Figure 10 - Structured light scanning of a metallic part: a) The part; b) Reflected pattern with an exposure time of 16.7 ms; c) Reflected pattern with an exposure time of 100 ms [33] 17

Figure 11 - Scan of the part with different exposure times [36] 19

Figure 12 - Comparison between scans: a) Without spray; b) With spray c) Error map with a nominal tolerance of +0.06/0.00 mm and a critical tolerance of ±1.00 mm, adapted from [36] 19

Figure 13 - Inspection of an aluminium part using conventional phase-shifting method; a) The part; b) Projection of stripes; c) High reflectivity regions; d) Absolute phase map [35] 21

Figure 14 - Scanning results using phase-shifting method: a) Point cloud; b) Point cloud from a scan at a different angle; c) 3D reconstruction [35] 21

Figure 15 - Inspection of aluminium part using the proposed adjusting fringe pattern method; a) Adapted pattern; b) Projection of stripes; c) details under projection with high frequency adapted stripe pattern; d) Absolute phase map [35] 21

Figure 16 - Scanning results using the proposed method: a) Point cloud; b) Point cloud from a scan at a different angle; c) 3D reconstruction [35] 22

Figure 17 - Surface comparison between both methods: a) Conventional phase-shifting; b) Proposed method, adapted from [35] 22

Figure 18 - 3D scanning flowchart, adapted from [42] 24

Figure 19 - a) 3D acquisition of a skull through photogrammetry; b) 3D surface scan with laser scanning [41]. 24

Figure 20 - Triangulation principle: a) Measurement principle; b) Resulting field of view [43] 25

Figure 21 – Laser scanning parameters [44] 26

Figure 22 - Scanning orientations [46] 28

Figure 23 - Outlier percentage for variation in scanning orientations for the mixed reflections model [46] ... 28

Figure 24 - Outlier percentage for variation in scanning orientations for the multi-path reflections model [46] ... 30

Figure 25 - Scanning of an object with the proposed method: a) 45° IIA and 0° EOA; b) 45° IIA and 30° EOA [47] ... 31

Figure 26 - Scanning of an aluminium part with concave cylindrical surfaces a) The part; b) Scan from a poorly planned path; c) Scan obtained from rotating scans; d) Point cloud after applying outlier filters [47]. 32

Figure 27 - Layout of marked points on part, together with scale rulers [51] ... 33

Figure 28 - Creation of digital model through photogrammetry [41] ... 34

Figure 29 - Scanning of a dental tooth key [50] ... 34

Figure 30 - Deflectometry schematic [61] ... 35

Figure 31 - Dimensions of simplified case in millimetres ... 39

Figure 32 - Project development roadmap ... 40

Figure 33 - Equipment used: a) X-Orbit 55-7 b) FARO Quantum M with the blue scanner attached c) Cronos 3D Dual ... 41

Figure 34 - Overview of script workflow ... 42

Figure 35 - CAD guide script diagram ... 43

Figure 36 - Initiation of the dialogue: a) First version; b) Second version ... 44

Figure 37 - Feature creation example ... 45

Figure 38 - Feature deletion example ... 45

Figure 39 - Prompt for file saving ... 45

Figure 40 Scanned point clouds: a) Points clouds; b) Global registration of the points ... 48

Figure 41 - Resulting mesh with the created features ... 49

Figure 42 – STL mesh: a) Trimmed mesh; b) User selecting extra geometry to be trimmed ... 50

Figure 43 – Final trimmed mesh ... 50

Figure 44 - Deviation map with the point cover over the mesh ... 51

Figure 45 - Misaligned meshes ... 52

Figure 46 - Final bottle mesh ... 52

Figure 47 - Overall test methodology ... 55

Figure 48 – Set of cast iron moulds: a) Cast iron mould halves; b) Cast iron mould bottom ... 56

Figure 49 - Diagram for the cast iron mould acquisition test ... 57

Figure 50 - Cast iron mould STL obtained from laser scanning: a) Mould bottom; b) Mould half ... 58

Figure 51 - Plane nomenclature for the moulds 59
Figure 52 - Unpolished bronze mould set 60
Figure 53 - Test plan for the scanning of the unpolished bronze moulds 60
Figure 54 - Point clouds of the bottom mould part: a) Scan without spray; b) Scan with spray 62
Figure 55 - STL of the mould halves: a) Without spray; b) With spray 62
Figure 56 - Polished and unpolished scanning study flow chart 64
Figure 57 - Unpolished cast iron mould set 65
Figure 58 - Unpolished cast iron mould being scanned by structured light 65
Figure 59 - Polished cast iron moulds 66
Figure 60 - Polished cast iron mould being scanned by structured light 66
Figure 61 - Surface comparisons of mould cavity 16 from the laser scans 69
Figure 62 - Surface comparisons of mould cavity 16 from the SLS scans 69
Figure 63 – Ring gauge 72
Figure 64 - Flow diagram for the validation test 72
Figure 65 - Results from the CMM measurement 73
Figure 66 – Ring gauge STL mesh: a) Obtained from laser scanning; b) Obtained from SLS scanning 74
Figure 67 - Demo bronze mould 75
Figure 68 - Flow chart of the case study procedure 76
Figure 69 - Bronze mould being scanned by structured light 77
Figure 70 - Mould fixed on the CMM 77

List of Tables

Table 1 – European glass container production per year per country in tonnes [3] 6

Table 2 - Voice of the customer 37

Table 3 - Product features using a Kano analysis 38

Table 4 - Volume tolerance table for the moulds 39

Table 5 – Initial volumes obtained from laser scanning and water testing of the initial cast iron moulds 59

Table 6 - Corrected volume values 59

Table 7 - Volumes obtained from the bronze mould scanning using the light systems 61

Table 8 - Results from the point spacing test 68

Table 9 - Volumes obtained from each method in the unpolished and polished condition 70

Table 10 - Volume deviation between the unpolished and polished condition from each method 71

Table 11 - Comparison of the ring gauge inspection 74

Table 12 - Mean Absolute Error for the light systems 78

Table 13 - Comparison between the used systems 79

Table 14 - Benchmark comparison between the equipment 80

Table 15 - Benefits and limitations of the project 81

Table 16 - Comparison between the conventional and the developed method 82

List of Abbreviations and Acronyms

2D	Two-Dimensional
3D	Three-Dimensional
API	Application Programming Interface
CAD	Computer Aided Design
CCD	Charge-Coupled Device
CMM	Coordinate Measuring Machine
DoF	Depth of Field
EOA	Edge Orientation Angle
FoV	Field of View
HDR	High Dynamic Range
IIA	In-Plane Incident Angle
IS	Individual Section
LCD	Liquid Crystal Display
LED	Light-Emitting Diode
MAE	Mean Absolute Error
NNPB	Narrow Neck Press and Blow
OIA	Out-Plane Incident Angle
PMD	Phase Measuring Deflectometry
RE	Reverse Engineering
RMS	Root-Mean-Square
SLS	Structured Light Systems
SNR	Signal-To-Noise Ratio

Contents

Originality and Copyright ..... **iii**

Dedication ..... **v**

Acknowledgments ..... **vii**

Abstract ..... **ix**

List of Figures ..... **xi**

List of Tables ..... **xv**

List of Abbreviations and Acronyms ..... **xvii**

1. Introduction **1**

1.1. Project goals and motivation **1**

1.2. Work structure **3**

2. Literature review **5**

2.1. Glass production **5**

2.1.1. Production 7

2.1.2. Narrow Neck Press and Blow 8

2.2. Moulds **11**

2.2.1. Mould materials for glass container production 11

2.2.2. Mould wear 11

2.3. Reverse engineering systems **12**

2.3.1. Structured light 16

2.3.2. Laser scanning 23

2.3.3. Photogrammetry 32

2.3.4. Deflectometry 34

3. Product development **37**

3.1. Design methodology **37**

3.1.1. Design constraints 38

3.1.2. Roadmap 40

3.2. Technology **40**

3.3. Script development **41**

3.3.1. User CAD guide 42

3.3.2. Volume Assessment Script 47

4. Validation and results 55

4.1. Surface acquisition of moulds using light systems 55
4.1.1. Cast iron mould surface acquisition using laser scanner..... 56
4.1.2. Acquisition of unpolished bronze moulds using laser and structured light 59

4.2. Differences in the acquisition of unpolished and polished moulds 62
4.2.1. Procedure..... 63
4.2.2. Unpolished moulds..... 64
4.2.3. Polished moulds 66
4.2.4. Results 67

4.3. Validation of equipment – Ring gauge and bronze mould 71
4.3.1. Validation using ring gauge 71
4.3.2. Bronze mould acquisition..... 74

4.4. Study conclusions 78

5. Conclusions and Future Work 83

Bibliographic References 85

Appendix A – Programmer's manual: function descriptions 93

Appendix B – User manual..... 97

Appendix C – Input/output function blocks: User CAD guide script 105

Appendix D – Diagram for the workflow of the volume assessment script 107

Appendix E – Input/output function blocks: Volume Assessment script 109

1. Introduction

Currently, in the glass bottle mould making industry, to control the volume of the produced moulds, the moulds are closed, sealed, and then filled with water. The amount of water used is then measured, which will give the volume of the internal cavities of the mould. This process has several issues. First of all, it requires a trained operator to properly seal the mould. Next, different operators will imply differences in sealing the mould which will also lead to differences in the measurement of the volume. Another issue is related to the time and work necessary for the procedure, which can take up to 20 minutes for a single mould, making it unsuitable to inspect several moulds of the same series. These issues can be properly solved by automating the whole procedure thus decreasing the time and human error which in turn will increase the quality of the product. By using reverse engineering systems to obtain the internal cavity surfaces, there is also an opportunity for wear inspection. This data can then be used for optimization of the moulds themselves.

1.1. Project goals and motivation

This project results from a real industrial need posed by Intermolde, a prominent Portuguese mould making company specialized in moulds for the glass industry. The moulds they manufacture can each be used to produce between 800000 and 1000000 bottles. These moulds will typically be used over the course of 18 weeks, replacing the moulds to spread their wear. From the point of view of their customers, it is important to have tight tolerances for the volume of the mould. For this reason, it is important for them to meet these quality demands.

Depending on the product, a different process and mould type are used:

- Pressing will be used to obtain lenses, pots and tableware;
- Centrifugal casting has the objective of producing plates and cathode tubes;
- The press and blow method is mainly used to manufacture bottles and other lightweight hollow glass containers, Figure 1.

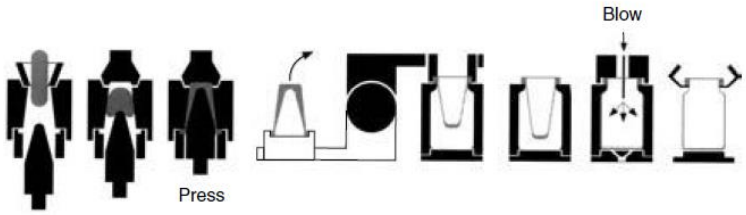

Figure 1 - Wide mouth press and blow process [1]

Narrow Neck Press and Blow (NNPB) is a subset of press and blow moulding. This process uses a plunger to obtain the glass preform before the final blow stage, Figure 2. Through this process, it is possible to obtain a great amount of lightweight glass containers and have a better glass distribution control. To be optimal, the uniformity of the glass gob masses must be constant throughout. However, due to the process being constantly ran, this uniformity is not possible. To control this issue, one can install a camera system to obtain images of the gob, which provide a way to calculate the volume and thus the mass [1], [2].

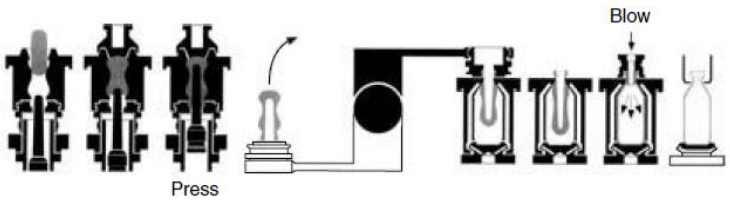

Figure 2 - Narrow neck press and blow process [1]

Intermolde produces moulds for these purposes and, as such, this project aims to develop a solution capable of automating the volume inspection procedure while also inspecting the deviations between the real mould and the virtual model in its cavity. This can be used not only for automatic volume inspection and surface inspection in the glass bottle mould making industry, but also applied to other part inspections. It could be applied to automatically acquire the surface of plastic parts and conduct their surface inspection, for example. Another aspect related to this project is that it enables further studies into the mould wear which enables improved process quality.

To accomplish these purposes, tests are done with suitable technologies, such as laser scanning and structured light to obtain the surface of the mould and achieve the required data.

1.2. Work structure

- In chapter 2 three main subjects are addressed: glass production to understand the methods used to produce glass containers, moulds related to the production of these glass objects and reverse engineering systems;
- Then, chapter 3 concerns to the product development part of the project. Here, the development constraints and overall roadmap are set. Then, the equipment used to develop the project is shown. Finally, the script development is discussed, showing the benefits and limitations of each script;
- In chapter 4, the results of the technology studies are shown. This will have the discussion and analysis of three separate case studies: surface acquisition of bronze and cast iron moulds, differences found in moulds after polishing and the validation of the used equipment;
- Finally, in chapter 5 the conclusions of the overall project are drawn, and future development directions are proposed and discussed.

2. Literature review

To properly control the glass container production, there are several factors to account for. Since the goal of the project is related to a mould manufacturer, mould wear and inspection technologies for metallic surfaces are investigated in this chapter. It starts with the description of the production process, followed by the explanation of the wear mechanism for the type of moulds used and ending with a study on the possible inspection systems that could be used for the desired application.

2.1. Glass production

Glass is a versatile material capable of being shaped for different applications. This material results from the mixture of fused silicates, lime and soda at a temperature range between 1500 Cº and 1600 Cº [1]–[3]. In this state, the material presents a structure similar to a liquid, allowing it to be shaped in several forms, depending on the application. Among these, it can be used to produce optics, containers, automotive parts and electric equipment screens [3].

An issue regarding the production of glass products is related to the large amount of energy and non-renewable resource consumption. For this reason, to make the process more efficient and cheaper, by lowering the mixture's melting point, glass cullet is reintroduced in the process cycle to decrease the use of virgin raw material [3]–[5]. According to the European Glass Container Federation in 2016, through the recycling of glass cullet, inside the EU, 670 kilograms (kg) of CO_2 are saved for each tonne of glass being reintroduced to the furnace [6]. It must also be noted that, with continuous recycling, the main properties of the material remain. However, in the case of producing colourless glass products, recycled cullet cannot be used due to coloured glass carrying impurities to the mix [4], [6].

In Graph 1, the amount of glass produced per sector in Europe in Megatons (MT) is shown. The two main sectors are clearly glass for containers and flat glass, accounting for a market share of around 70% and 25%, respectively. The container glass industry in Europe is fundamental to its packaging sector due to glass having the ability to be recycled several times. This means that glass is a good candidate for sustainable production and consumption. In Table 1, the amount of glass packaging produced is detailed per country in Europe. Portugal is the 6th country which most produces this type of glass product and also shows

signs of growth in this industry, reaching a growth of 10% in 2014 [1], [3]. Inside the glass container sector, the beverage sector accounts for around 75% of the total tonnage, where food products are responsible for 20% and cosmetics, pharmaceutical and technical products have the remaining share [4].

In this section, the main aspects related to glass production are discussed. The production of glass containers is explained, including the main processes behind their forming.

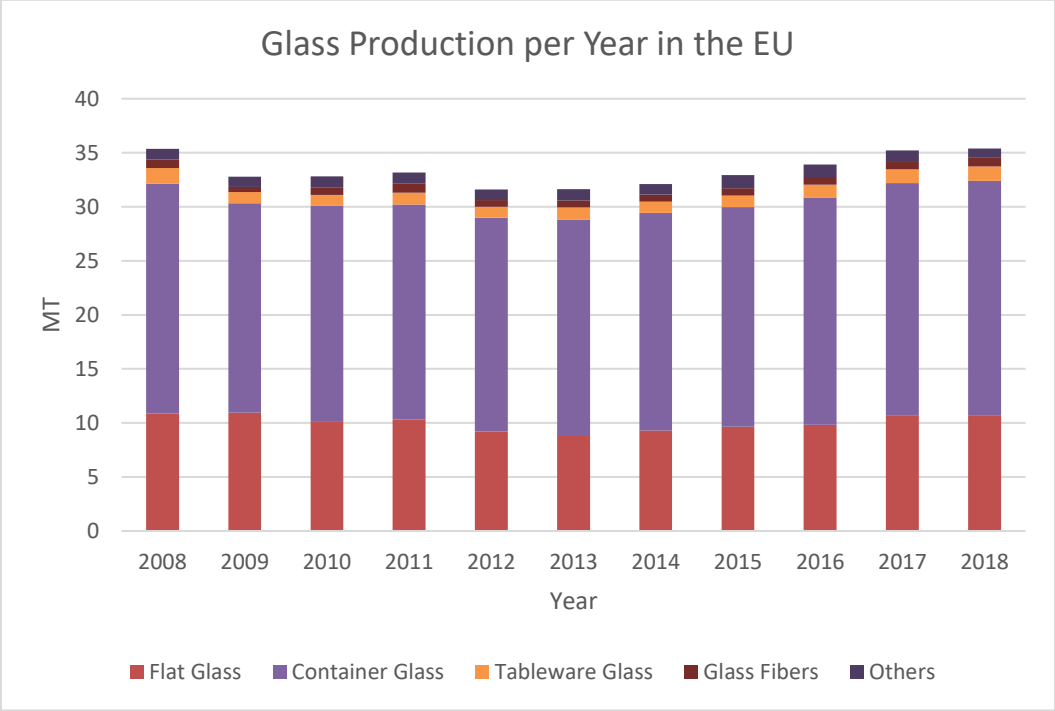

Graph 1 - Glass production per sector per year in the EU [7]

Table 1 – European glass container production per year per country in tonnes [3]

Country	2010	2011	2012	2013	2014	Growth %
Germany	3,787,750	4,065,452	3,934,844	3,933,641	3,973,786	4,9
Italy	3,506,532	3,568,710	3,391,637	3,445,302	3,467,462	-1,1
France	3,152,023	3,310,186	3,146,755	3,030,949	3,097,473	-1,7
United Kingdom	2,316,604	2,310,667	2,226,321	2,240,759	2,245,986	-3,0
Other North-Central	1,950,400	2,041,404	2,096,753	2,093,984	2,138,703	9,6
Spain	1,979,957	2,067,016	2,012,381	2,087,000	2,099,236	6
Portugal	1,312,909	1,351,919	1,441,962	1,439,429	1,451,735	10,6
Other South-East	1,068,659	1,186,726	1,198,207	1,364,601	1,403,563	31,3
Turkey	779,462	822,502	950,000	1,021,000	1,172,313	50,4
Poland	986,347	986,750	996,660	1,003,551	1,078,071	9,3
Europe	20,840,643	21,711,331	21,395,520	21,660,216	22,128,328	6,2
Total EU28	19,956,884	20,783,077	20,333,593	20,533,216	20,858,515	4,5

2.1.1. Production

To produce glass, the raw materials ought to have minimal humidity, constant chemical composition, and optimal granulation. In terms of raw materials, silica sand, soda, calcite, dolomite, and feldspars are used. Some auxiliary raw materials are also used, such as dyes, melt clarifiers and glass cullet obtained from the crushing of discarded glass products. The main process to produce containers, which can be seen schematically in Figure 3, is described as follows:

- Firstly, the materials are transported and fed into compound mixers where they are mixed;
- Then, through conveyor belts, the mixture is fed into furnaces at a temperature up to 1650 ºC, resulting in glass melt;
- From the furnace, the glass melt forms up to four parallel streams which are supplied to a feeder via specific channels which also work as heat exchangers to better homogenize the composition and the temperature of the melt;

In the next step, through a mechanical plunger, each stream is cut by a shear, obtaining gobs with the correct length and mass. These gobs are then fed into the blank mould in the individual section (IS) machine where they obtain their preform shape. The IS machine will be considered a single, double, triple, or quadruple gob machine according to how many gobs it will be forming simultaneously in one section.

Finally, the preform is inverted and transferred to the final mould in the IS machine. In this stage, the preform sags due to gravity, but does not touch the mould. Pressurized air is used to inflate the preform to obtain the final shape [2], [4], [8].

Achieving the final form of the part, it must go through visual inspection. If the part is approved, it will then move to the tempering furnace where coatings of ceramic material are applied to protect the glass product's external surface. These coatings are applied after forming to promote better adhesion and strength. In the case the glass product fails the visual inspection, it will be discarded, and the glass will be reintroduced to the process in the form of glass cullet. With the coating applied, the product possesses high friction surfaces which require lubrication. As such, the product is cooled down in a controlled environment, inside the lehr, to relieve residual stress and a lubricant is applied. As the final step, the products are subjected to several tests, rejecting those with defects [1], [2], [4].

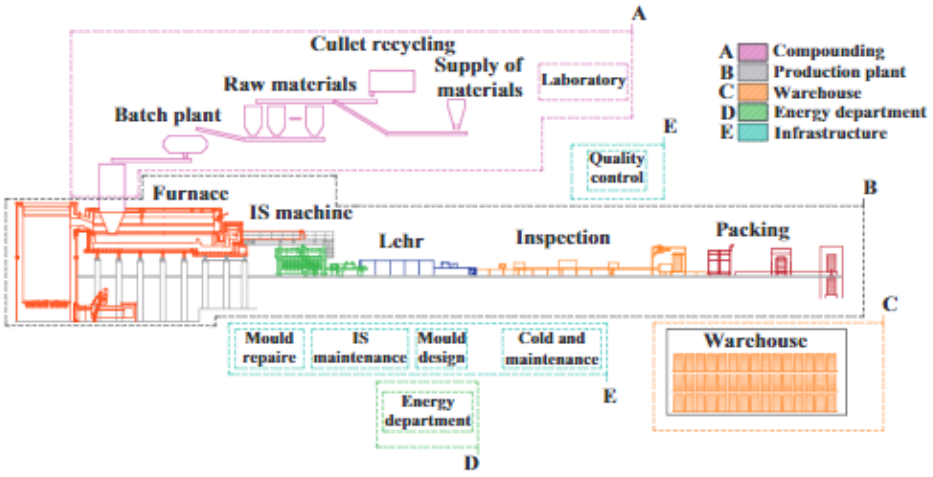

Figure 3 - Glass manufacturing schematic [2]

Through this whole process, it is possible to produce one million parts per mould, where 20 moulds are used per production set [1]. The IS machine is an assembly of individual container forming units placed side-by-side where each section has a given number of mould cavities for the preform and final shape production. By using the IS machine, the operator can retrieve sections out of production to conduct maintenance without compromising the production of the other sections. This machine has the added advantage of fast production, being able to have up to 20 sections where each section can produce between 1 to 4 bottles simultaneously. This allows a production rate that can reach 700 bottles/minute [2], [4].

2.1.2. Narrow Neck Press and Blow

To obtain a glass container with reduced weight while maintaining strength, it is necessary to have an even glass distribution throughout the walls of the container. The NNPB appears as a solution to this requirement. By using a metallic plunger, it is able to evenly distribute the glass in the blank mould. It also prevents the glass from distorting due to its own weight by removing the thermal energy from its surface [9], [10].

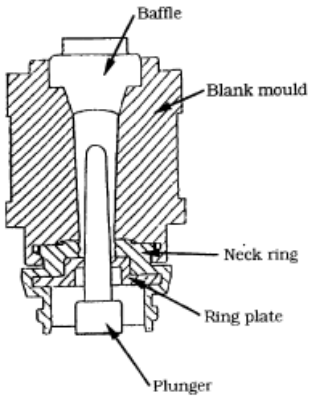

Figure 4 - Plunger action in the blank mould [9]

This process involves three different moulds:

- **Blank mould**: The gob is fed to the blank mould, whereby action of the plunger and the baffle (responsible for pressing against the preform at the same time as the plunger) the preform is formed;
- **Neck-ring mould**: This mould is responsible for forming the neck and thus allowing the transfer from the blank mould to the blowing mould;
- **Blow mould**: The final mould, where the final shape of the container is formed [2], [9].

This process differs at the feeding stage, where after the gob is fed into the blank mould, a plunger presses against the gob to produce its preform shape. After this pressing stage, the process continues with the transfer of the preform to the blow mould to obtain the final shape and proceeding further to the coating and annealing stages of the product [2].

2.1.2.1. Process issues

Despite being an adequate process to obtain better glass distribution in glass containers, it presents some challenges due to being exposed to harsh environments. The glass container forming process involves subjecting the tools, the plunger and the moulds, to high temperatures where there will also occur mechanical contact between the tools and hot abrasive glass. These conditions decrease the tools' lifespan which further leads to product defects and process instability.

The main failure mode of the plunger is typically related to its material selection, which when inappropriate, can lead to issues to the adherence between the substrate and its coatings. The coatings must be absent of porosity, otherwise the plunger will suffer higher

wear rates and some distortion. Wear of the plunger is another concern which happens due to mechanical contact and the abrasion from the glass. These problems further lead to process instability and product defects. Regarding product defects due to material failure of the plunger, this will involve material loss into the glass which can lead to the appearance of spikes in the containers, as seen in Figure 5 [9], [10].

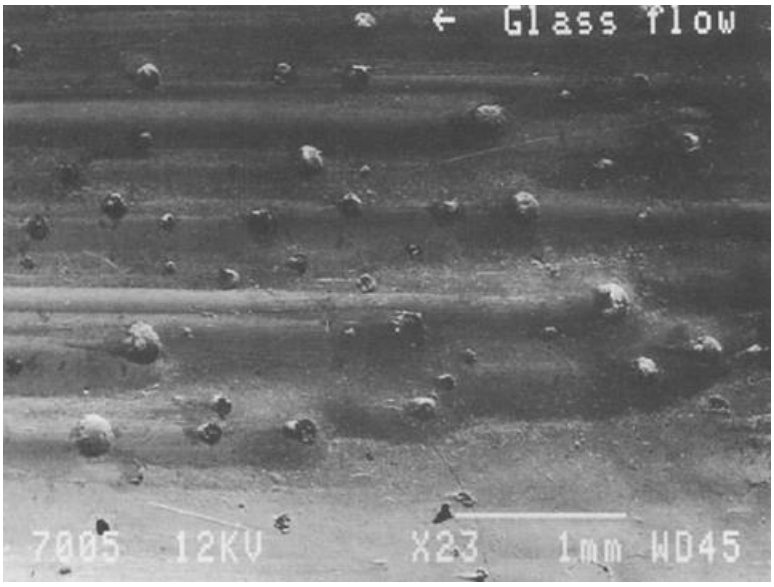

Figure 5 - Appearance of spikes on the container's surface [10]

2.1.2.2. Process requirements

The plunger's main task in the NNPB process is to create the preform by evenly distributing the glass of its walls, as well as removing some thermal energy to prevent the shape's distortion before the transfer to the blow mould. To produce glass containers through this method, the toolset must fulfil some requirements:

- Volumetric control of both the blank mould and the blow mould;
- Accurate tolerancing between interfacing components;
- Appropriate plunger materials;
- Reduction of the wear rate by spray welding the neck ring mould cavities;
- Reduction of repair need by seam welding the blow moulds.

The NNPB process offers some benefits, namely the possibility of obtaining thin walls with tight dimensional tolerances, weight reduction of up to 30% and an increase in production speed. Nonetheless, it has some issues with the plunger's wear rate, the production downtime due to replacing the failed parts and the produced products' inner surface having a lower impact resistance. The weaker inner surface is caused by the high

temperatures in the glass-mould interface which affect the microstructure, leading to surface discontinuities in the inner surface [9].

2.2.Moulds

This section aims to showcase the types of moulds used for the process and to explain how they get worn and damaged. Firstly, the mould materials are explored, following the mould wear mechanisms.

2.2.1. Mould materials for glass container production

An important aspect to produce glass containers is the contact between the glass and the mould. When the glass hits the mould walls, there will be rapid local cooling with an increase of the glass' viscosity accompanied with stretching and thinning. The flow of the glass is also affected by the contact between the mould and the glass [11], [12]. By appropriately selecting the mould material, it is possible to improve the mould lifetime, reduce the cost of production (reduced wear rate) and improve the quality of the container's surface. For the material selection, it is important to consider resistance to thermal cycling, corrosion, wear, sticking and good machinability. The most typical mould materials are cast iron, bronze and stainless steel [5], [12], [13].

Metallic materials are the most appropriate to mitigate corrosion, thermal and mechanical loading, and wear for moulds. As the mould's surface becomes worn, marks begin to appear on the product's surface and the glass begins to stick to the mould's walls. To solve these issues, the mould should be polished. Ideally, the mould's surface should be inert when in contact with the glass to avoid corrosion, sticking and adhesion. To promote inert behaviour and improve protection, coatings which are resistant to oxidation and abrasion are used.

2.2.2. Mould wear

To successfully produce good quality products for a longer period of time, mould damage must be reduced. Mould damage comes from different sources such as: wear, thermal fatigue, and crystal growth. In terms of abrasive wear, it mainly occurs in two interfaces: in the contact zone between the molten glass and the surface of the mould's wall; and between the molten glass and the plunger. Some measures can be taken to mitigate these effects, such as material selection and by applying coatings. Through the application of

coatings, resistance to wear and corrosion is promoted, while also reducing the sticking of the glass to glass moulds [5], [14].

Grey cast irons are a commonly used mould material to produce glass packaging products. They have good resistance to wear, oxidation and are cheap to produce [14], [15]. For high-carbon cast irons, the material has a high thermal conductivity, however, it has lower resistance to oxidation and wear due to its coarse-grained surface. As for nodular cast irons, they have low thermal conductivity, which leads to process time issues. They require more time to extract the product. By increasing the amount of graphite present in the microstructure, it is possible to improve the cast irons' performance [15].

Bronze alloyed with aluminium has high wear resistance but has some issues. Due to its high cost, its use is only justified when there is a very high production of parts, otherwise it will not be economically feasible. Another problem is related to its thermal cycling, its temperature rises and cools down quickly. This can lead to deformations in the produced product [16].

Due to being in most contact with the molten glass, the bottle neck is the area where the most wear occurs. For this reason, the chosen material for the neck ring must be more resistant to thermal fatigue than the remaining body, which is why aluminium and bronze are typically used. [13], [17].

Lubricants are an important agent that should be used to extend the service life of the moulds. They improve the process by limiting the heat exchange between molten glass and steel, minimizing the sticking and promoting a lower friction coefficient, consequently reducing the abrasion caused by the glass. Nonetheless, care should be taken as the lubricants chemically attack the mould and the plunger, polluting the production environment as well[18].

2.3. Reverse engineering systems

Reverse engineering (RE) is the process which converts a product from the physical realm to a virtual model. This process enables a thorough analysis of the product and obtains proper documentation of the actual product [19]–[21]. Seeing as most production processes use Computer Aided Design (CAD) models, the aim of this process is to obtain a CAD model

so it can interface with these processes. The main needs for RE can be summarised as follows:

- **Product design:** Some product designs often start as a physical prototype, without CAD information. Obtaining the CAD model from this prototype allows for proper analysis and optimization of the design;
- **Modifying existing products:** Products often suffer several iterations for optimization, requiring the new CAD model after the modifications are applied;
- **Loss of product information:** Occasionally, the CAD file for a part is not available, requiring RE of the part to retrieve it;
- **Product verification:** RE can be used to obtain product dimension information [19].

At the start of the RE process, a CAD model is not available. Therefore, the process starts with the acquisition of the product's geometric information. Digitisation is the technique of taking several discrete coordinate points from the product's three-dimensional (3D) surface and obtaining a point cloud which can then be used to produce the CAD model [19], [20]. It must be noted that the repeatability and the accuracy of the digitisation will be critical to the accuracy of the CAD model [20]. The steps for RE can be seen in Figure 6.

Digitisation techniques can be classified into three main classes:

Contact: Encompasses the most traditional methods, manual and coordinate measuring machine (CMM). This machine can obtain points with very high accuracy; however, it is a slower method due to physical contact between the inspection system and the part. The manual method typically involves a calliper, angle finder and/or gages to obtain the key dimensions of the part. The CMM, however, will measure spatial points on the part's surface with a contact stylus which, when contacting with the part, will trigger its sensor, thus obtaining the location of the point.

Non-contact: Here, the used methods do not engage in mechanical contact with the part. Instead, they acquire the surface of the part via light pattern projection, laser, x-ray, microwave. These methods offer higher acquisition speed despite having a lower accuracy when compared to the CMM. Non-contact methods can be further divided into active or passive, depending on how their acquisition process works [19], [20]. Active systems project energy on the part so it can be reflected from the part's surface, obtaining information about

its geometry and further allowing the reconstruction of its geometric elements. The active systems are more reliable than the passive systems, however, these are limited to the surface properties, having issues with specularity [19], [22]–[24]. In contrast to the active systems, the passive systems receive light instead of emitting it. Passive systems reconstruct the object through several photographs taken from different positions and angles [19], [23], [24].

Hybrid: These methods aim to implement two or more digitisation techniques to obtain better digitisation speed and accuracy. They are also flexible with the ability of being automated. One such method would be the application of a non-contact method onto a CMM for optimal path planning [19].

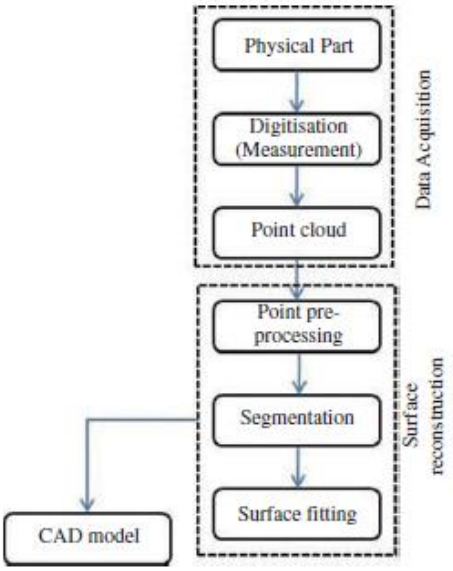

Figure 6 - Reverse Engineering basic steps [20]

Despite the possibilities of this technology, it does suffer from some problems. Namely, when digitizing black coloured surfaces, reflective surfaces, transparent surfaces and when the access to the surface is poor. In Figure 7 the behaviour of the reflected ray is presented for several cases of surface acquisition.

- **Black coloured surfaces:** The surface will tend to adsorb the optical energy without reflecting it, which means that the scanner's receiver will not receive any information, not being able to compute the location of the points;
- **Transparent surfaces:** In this case, the optical wave will simply pass through the surface, without allowing any information retrieval;

- **Reflective surfaces:** For these surfaces, two types of reflection are at play, diffuse and specular. Specular reflection is similar to the reflection in mirrors where the ray and the reflected ray have the same angle to the surface normal, while diffuse reflection will lead to the scattering of the ray. This behaviour allows for the receiver to capture the reflected ray. When specular reflection is the dominant type, however, only a fraction of the ray is reflected to the receiver which leads to lack of information of the surface;
- **Surface accessibility:** When the scanner is unable to scan near the surface normal, large angles to the surface normal are used. This promotes specular reflection, which hinders the acquisition of the geometry [25].

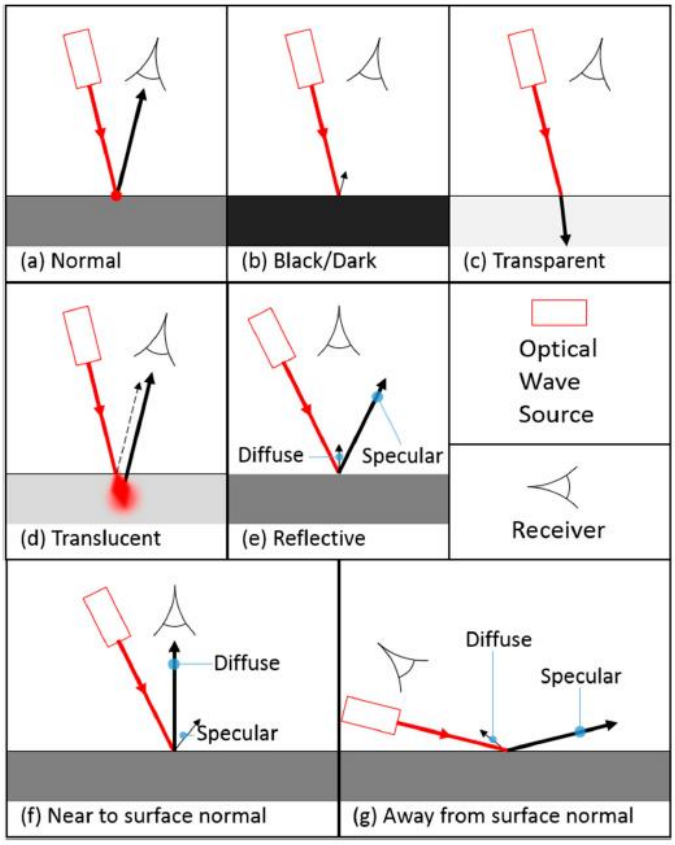

Figure 7 - Reflection behaviour for different surfaces [25]

Several systems and technologies exist for RE purposes. This section aims to identify the main ones and amongst the most suitable ones pick an appropriate solution for the inspection of metallic surfaces. Firstly, structured light is discussed, approaching two different methods, multiple exposures and adaptation of the fringe pattern intensity, following with laser scanning, photogrammetry and deflectometry. In the laser scanning

subsection, the effects of the orientation to produce outliers is explored. As for photogrammetry and deflectometry, a general overview is given.

2.3.1. Structured light

With the development of industrial processes and the continuous improvement of product quality, it becomes necessary to reduce the inspection time and therefore use other methods aside from contact. As such, optical methods appear as a suitable solution to today's demanding industry, having an ever-improved accuracy and offering fast inspection times for complex shapes and even volume assessment [26]–[28]. Nevertheless, they have their limitations related to the features being inspected, the environment where the inspection is done and the inspected surface when it comes to optical properties such as types of reflections and to its roughness [29]–[33]

Structured light is one of these systems, presenting an active approach [19]. A schematic for a Structured Light System (SLS) can be seen in Figure 8. This system is equipped with a projection unit and an acquisition system. The projection unit is responsible for the projection of encoded fringe patterns onto the inspected surfaces over short times to produce dense point clouds. This leads to the distortion of such patterns which, when captured by a camera, can be used to calculate the height information [30], [33]–[38]. In this step, through a phase-shifting algorithm the absolute phase map is obtained which enables the correspondence between points in the camera and points in the projector with the same codeword. The coordinates are then calculated from the absolute phase map through phase-height mapping which allows to obtain the 3D model and makes it possible to compare the model to the CAD model. Structured light systems find their use limited when it comes to shiny surfaces. Due to high reflectance, the captured images are degraded and the information from the patterns cannot be well retrieved from over- and under-exposed areas [33], [35], [36], [39]. In Figure 9, the application of an SLS to inspect a part can be seen. As for the effect of scanning on shiny surfaces, this can be seen in Figure 10. In Figure 10 b), the regions with strong reflection toward the camera are the ones which provide useful measurement information, while the ones where the light is much weaker cannot be properly measured. As for Figure 10 c), the exposure time is increased to 100 milliseconds (ms), the regions become very bright and have a much higher reflection, leading to the saturation of the camera. This makes it so the fringe patterns cannot be decoded and therefore not measurable [33].

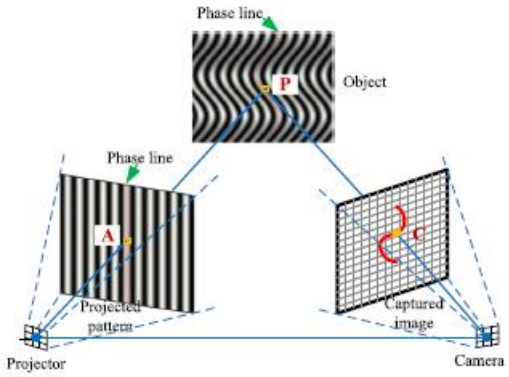

Figure 8 - Schematic of a structured light system [40]

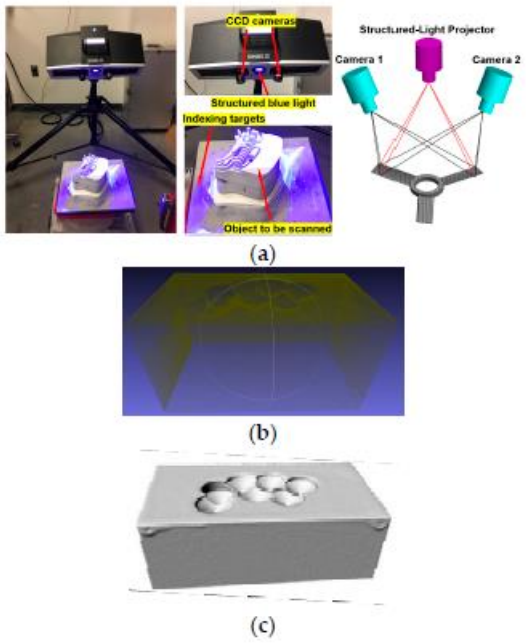

Figure 9 - Example of a structured light system being used to inspect a part a) System setup; b) Aligned point clouds; c) STL model of the part [37]

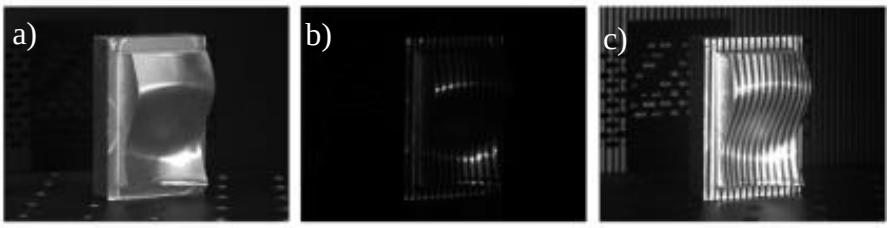

Figure 10 - Structured light scanning of a metallic part: a) The part; b) Reflected pattern with an exposure time of 16.7 ms; c) Reflected pattern with an exposure time of 100 ms [33]

Due to the mix of possible error factors being introduced into the measurement system, be it from the environment, internal equipment factors and/or the surface condition of the part, it becomes difficult to properly quantify the accuracy of such system. For the proper calibration, artefacts should be used to properly quantify the global error [34].

To avoid the use of spray paint on the part and risk adding more error to the measurement while polluting the production environment, high dynamic range (HDR) methods have been proposed for the scanning of shiny surfaces [39]. Among the studied methods are:

- Multiple exposures;
- Adjusting projected pattern intensities;

2.3.1.1. Multiple exposures

This method is based on obtaining a sequence of images under different exposures to then combine them into a set of HDR images. Phase-shifting is used for each pixel to select the brightest unsaturated intensities. This way, the method is able to gather information on regions with high reflectivity in the case of low exposure time as well as on low reflectivity cases for images at high exposure times [35], [36], [39].

In terms of exposure time, there is not an objective way to quantify the correct exposure time to use when faced with an unknown scenario. It must be noted that by requiring long exposure times, obtaining HDR images, can be time consuming [39].

Only if the group of images are subjected to different exposures under a determined light pattern can this method be applied. Due to the lighting of the images not being uniform, these captured images cannot be directly used for the 3D reconstruction. As such, the images with middle level of exposure are selected as the reference images for the fusion process.

In Figure 11, the scanning of the convex side of a stainless steel stamping part is shown. The brightness of the part is more notable in its sharp edges and curvature, while the remaining areas are dark. For short exposure times the models are incomplete and noisy while for long exposure time, the images become very bright and thus, due to the strong reflectance, the images are saturated which do not allow for the retrieval of useful data.

For validation, the part was scanned using the proposed method without spray, and then with spray. The results can be seen in Figure 12 a) for the scan without spray and Figure 12 b) with spray where the reconstructed surface is displayed and in Figure 12 c) the error map is shown. The main errors occur in the regions with sharp edges, reaching ±0.45 mm while the absolute mean error was calculated as 0.06 mm with a standard deviation of 0.08 mm [36]. Overall, not much changes from the original method, this proposed method requires more post-processing and the synchronization of the camera and the projector [39].

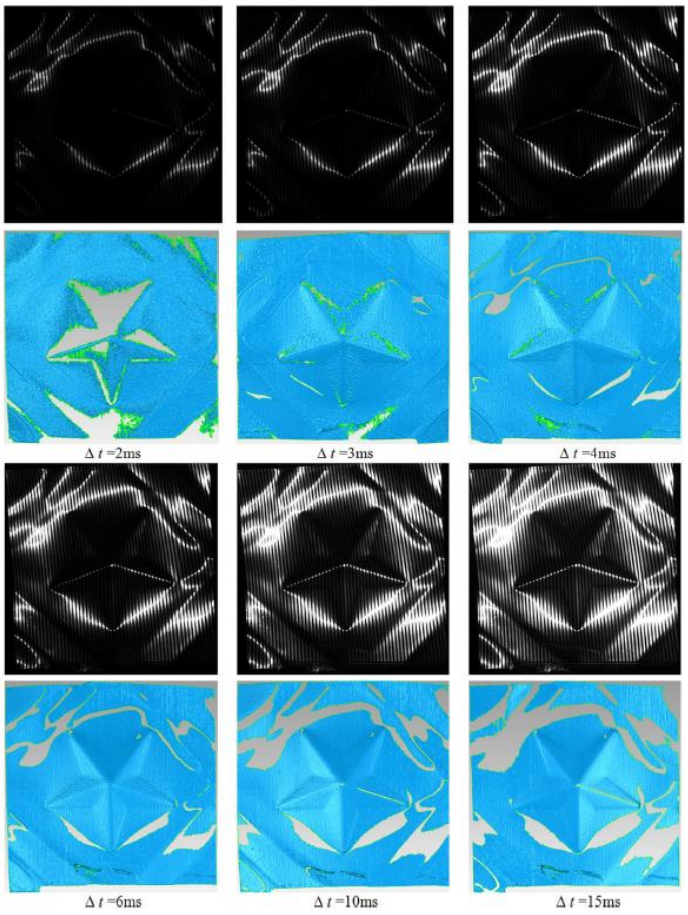

Figure 11 - Scan of the part with different exposure times [36]

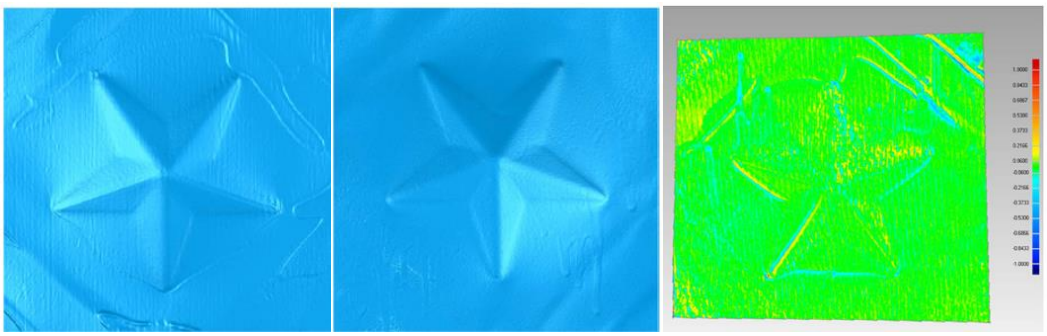

a) b) c)

Figure 12 - Comparison between scans: a) Without spray; b) With spray c) Error map with a nominal tolerance of +0.06/0.00 mm and a critical tolerance of ±1.00 mm, adapted from [36]

2.3.1.2. Adjusting projected pattern intensities

The adjusting projected pattern intensities method is proposed as a way to solve the scanning of shiny surfaces. It adapts the intensity of the pixel according to the camera response function which relates the scene's irradiance to the image intensities. This way, the intensity for each pixel in the projected pattern can be calculated. Consequentially, image saturation is avoided, and high signal-to-noise ratio (SNR) is maintained. Compared to the

multi-exposure method, where 207 images are necessary, this method only requires 31 images for the same situation [33], [35], [39].

Being proposed by the authors in [35], it aims to predict the optimal intensity for the projected pattern. For this to be possible, the optimal projection intensity and where it is located must be determined using the camera response function together with the coordinate mapping function. The camera response function aims to solve the optimal intensity being used, whereas for the location, the coordinate mapping function is used. With this function, contours outside the saturated zones are extracted and mapped to the projector image plane. Then, each contour point in the camera coordinate system is matched with the points in the projector coordinate system.

To compare the proposed method, an aluminium part is scanned with the conventional phase-shifting method as shown in Figure 13 and Figure 14. In Figure 13 b) and c) it can be seen that the middle of the part has high reflectivity, resulting in the production of discontinuities which can be seen from the absolute phase map in Figure 13 d). From the conventional method, most deviations fell in the range of [-0.3, 0.3] mm. As for the proposed method, the results can be seen in Figure 15 and Figure 16. From Figure 15 b) and c), the middle region no longer has such an intense reflectivity. This adds to the completeness of the overall reconstruction, as well as it improves the accuracy. Deviations from this method were in the [-0.15, 0.15] mm range. The surface comparison between both methods can be seen in Figure 17 [35].

This method appears as a more viable technique for the scanning of shiny surfaces as it requires less pattern images and can achieve a better accuracy than conventional phase-shifting. It should also be noted that the system does not require additional hardware costs [33], [35]. Depending on the projector, the range for intensity variation is limited. For this reason, the adjusting projection pattern intensity technique might not be suitable for surfaces with a very large variation of reflectivity. Ideally, a projector with high refresh rate and high dynamic range should be used to maintain appropriate inspection times [33].

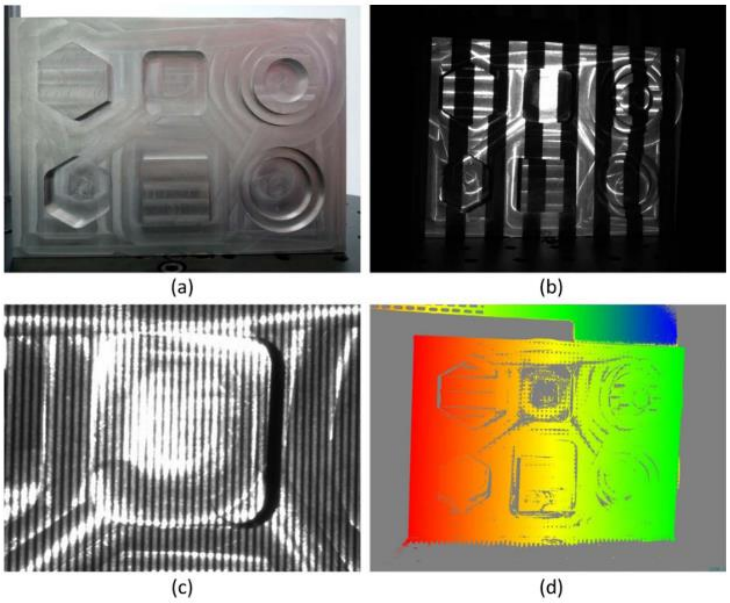

Figure 13 - Inspection of an aluminium part using conventional phase-shifting method; a) The part; b) Projection of stripes; c) High reflectivity regions; d) Absolute phase map [35]

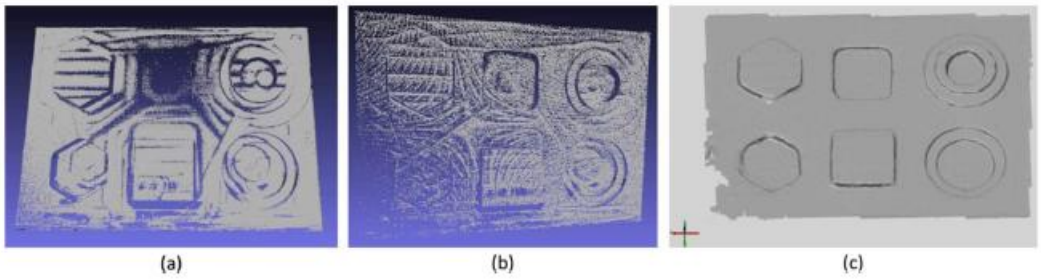

Figure 14 - Scanning results using phase-shifting method: a) Point cloud; b) Point cloud from a scan at a different angle; c) 3D reconstruction [35]

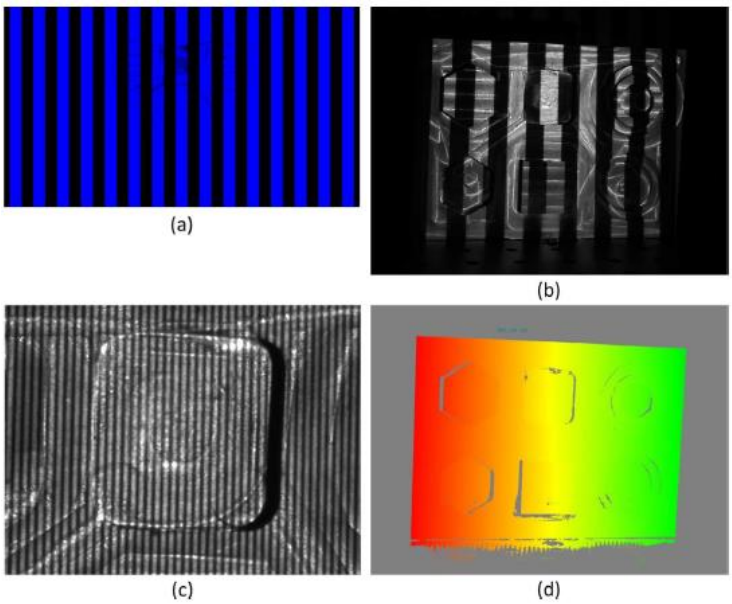

Figure 15 - Inspection of aluminium part using the proposed adjusting fringe pattern method; a) Adapted pattern; b) Projection of stripes; c) details under projection with high frequency adapted stripe pattern; d) Absolute phase map [35]

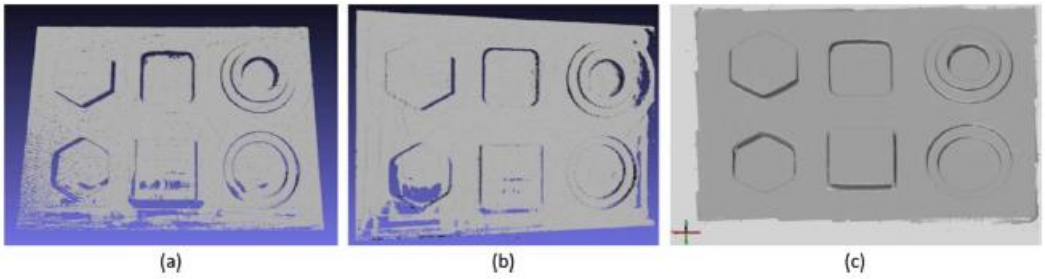

Figure 16 - Scanning results using the proposed method: a) Point cloud; b) Point cloud from a scan at a different angle; c) 3D reconstruction [35]

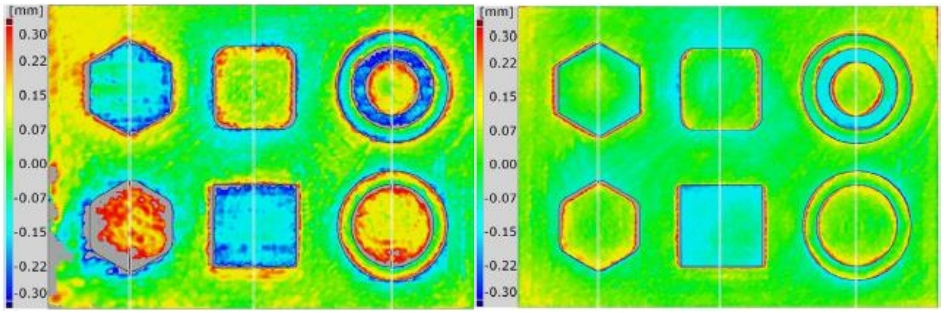

a) b)

Figure 17 - Surface comparison between both methods: a) Conventional phase-shifting; b) Proposed method, adapted from [35]

2.3.1.3. Challenges

Overall, there are still some limitations related to SLS. These are enunciated below:

- With the emphasis on high quality and high-resolution data acquisition, the file sizes of the acquired models can become quite large. It becomes necessary to have proper data storage to handle these file sizes;
- Despite having methods that can acquire the surfaces of transparent and shiny objects, it must be noted that the methods might not currently be ready to be used for industrial use where a fast and accurate acquisition is demanded for any object. The solution must guarantee robustness, efficiency and, at the same time, be cost-effective;
- It is very important to reduce the time cycle as much as possible, which is why the integration of automation in a method is important;
- The methods lack generality in the sense that one which performs well with a given surface is not guaranteed to work equally well with another. [40].

2.3.1.4. Overall method conclusions

Between the explored methods for the acquisition of specular surface inspection, it has been studied that the multiple exposures method will take much longer to obtain the full scanning part. In terms of accuracy they are similar, where multiple exposures has a root-mean-square (RMS) error reaching 0.016 mm for a measurement volume size of 100mm×40mm×31mm whereas adapting projected pattern intensities has an RMS of 0.012 mm for a measurement volume size of 320mm×30mm×150mm. Not only does it have a lower RMS for a bigger measurement volume, it also takes less time while being less complex [39].

2.3.2. Laser scanning

One of the most used and most well-developed optical inspection methods is laser scanning [26]. In this method, a laser striped pattern is projected onto the surface being inspected, requiring the pattern to be reflected back to a camera to receive and process the obtained information [24]. These characteristics makes laser scanning an active system. By obtaining dense point clouds with several millions of points, it becomes possible to retrieve geometric and volumetric information from the part through this technology [41]. Currently, blue LED (light-emitting diode) is used as light source as it improves accuracy and reduces need for more complex lighting setups [27], [41].

For laser scanning, the part placement should be done in a way that allows the maximum data capture of the part with the least scans. A proper planning on how the scan will be done will enable better results. While scanning, parts of the background will be picked up by the scanner, which should then be removed before obtaining the part mesh. A typical scanning flowchart can be seen in Figure 18. In [41], the authors compared laser scanning to photogrammetry for the scanning of a skull which can be seen in Figure 19. More detail can be seen from the laser scan than the photogrammetry one, showing laser has better scanning performance [41]. Photogrammetry is further explored in 2.3.3.

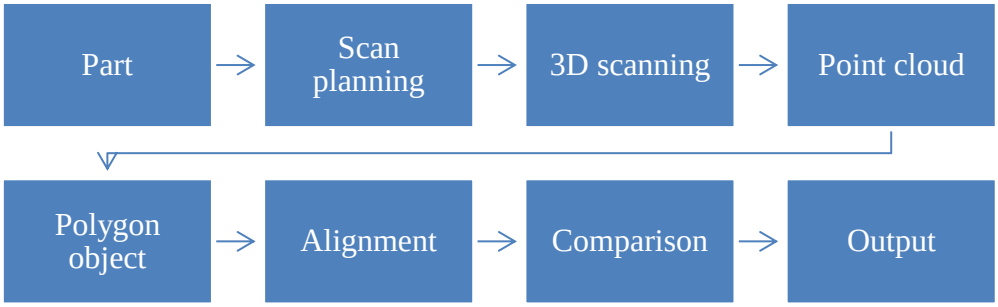

Figure 18 - 3D scanning flowchart, adapted from [42]

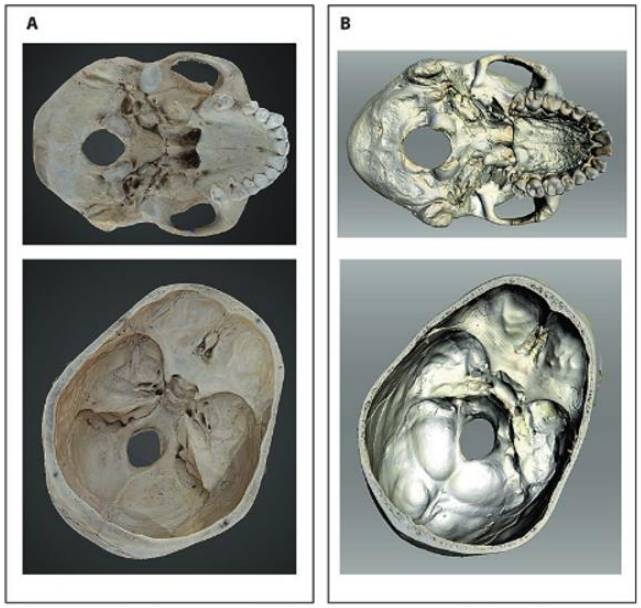

Figure 19 - a) 3D acquisition of a skull through photogrammetry; b) 3D surface scan with laser scanning [41]**.**

Laser scanning uses triangulation, requiring a source and a detector to process the collected data [19], [20], [43], [44]. Laser triangulation enables high data rate capture being usable in different configurations: point by point, stripe pattern projection or in a line. The incident laser line with a known width is projected onto the part and then the pattern is reflected to the charge-coupled device (CCD) sensor. The reflected data is then processed to obtain the 3D information of the part. [20], [43]–[45].

For applications where very high accuracy is not demanded, laser scanning can be used instead of the CMM. Laser scanning will be advantageous over the CMM as it can capture data of the full part at a very fast rate without being in contact with the part. However, it faces issues when scanning reflective surfaces. A schematic of the triangulation principle can be seen in Figure 20 [20], [43], [44].

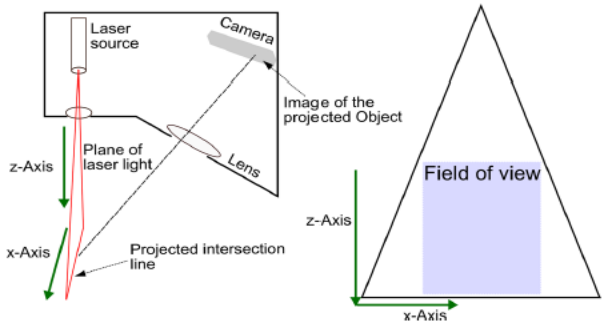

Figure 20 - Triangulation principle: a) Measurement principle; b) Resulting field of view [43]

2.3.2.1. Influencing factors for laser line scanning

There are some factors which influence the quality of the scanning, such as the scanner resolution, the object surface, the ambient lighting, and the scanning parameters. Ambient lighting can generate errors on the measurement of mobile laser scanners [44], [45]. As for the object surface itself, it becomes challenging for laser line scanning when in the presence of dark, glossy or translucent surfaces.

- For very shiny surfaces, a high amount of noise will be added to the point cloud, generating points that do not belong to the part's surface;
- For glossy surfaces, the light saturation captured by the CCD sensor is affected;
- Finally, when scanning dark surfaces, the light is absorbed which does not allow the CCD sensor to obtain the local data.

The scanning parameters, represented in Figure 21, can also affect the scanning quality:

- The scanning orientation should be done with the scanner normal to the surface as much as possible. In the case of freeform surfaces, it becomes necessary to properly plan the scan path [44];
- Field of view (FoV) is the 3D region where the system can capture data, being defined by the depth of field (DoF) and the scan width;
- Depth of field is related to the lens' focus. It is the distance between the laser source and the region from where data can be captured;
- Scan width is the width of the laser, which will only acquire points inside the FoV;
- Scan depth is the distance between the laser source and the reference surface. The lower this parameter is, the better the accuracy. It should be noted that by decreasing the scan depth, the scanning time is increased due to requiring a

greater number of scans, which itself can be a source of error as more error will be accumulated;

- Incident angle, θ, is the angle between the laser and the projected surface normal of the scanned point in the scanning plane. By increasing this parameter more uncertainty will be present. According to the authors in [44], the recommended range for the incident angle to achieve optimal performance is [-35°,35°];
- The projected angle, α, is the angle between the scanning plane and the surface normal at the scanning point. For the projected angle, it is recommended to use an angle in the range [-15°,15°] [44].

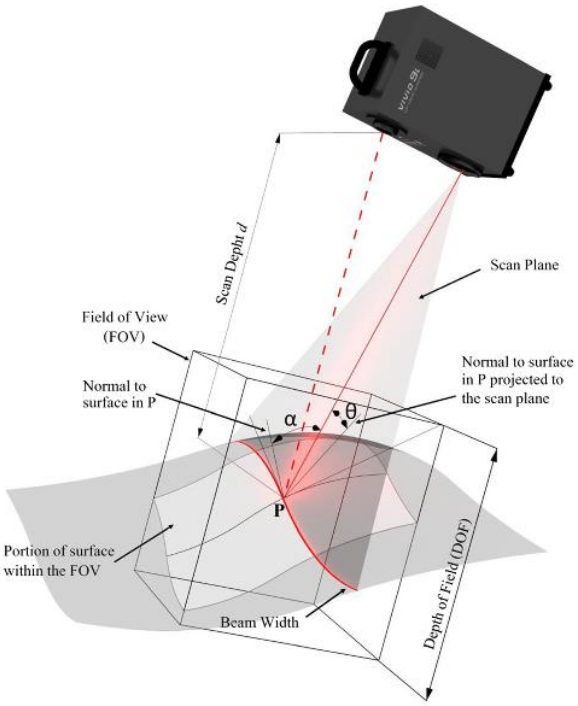

Figure 21 – Laser scanning parameters [44]

2.3.2.2. Outlier generation

During the acquisition process of laser scanning, the point clouds can become contaminated by outliers, especially when the surface is reflective. This can lead to the generation of points that do not belong to the actual surface. These outliers incur error upon the measurement, which can lead to false part rejection [46], [47].

Most outlier detection algorithms analyse the point cloud without knowing how they are generated and without considering the scanning setup. These algorithms will base themselves on assuming ideal conditions and randomness for outlier occurrence in the point

clouds, making them unsuitable for mechanical parts with reflective surfaces as these will produce complex outliers. There are two types of common outlier detection methods:

- Sparse outliers, which are detected locally, analysing each point's neighbourhood. Here, the proposed filter would be by threshold but this can be unsuitable due to the density of the points not always being uniform. Consequently, it can lead to sparsely sampled features being treated as outliers;
- Dense outliers are detected through global approaches, detecting the outliers as by-products by removing small clusters. However, these small clusters can be valid surface points as outliers can be very close to the surface and cannot be separated through this method [47].

In the most common applications, the part will not be perfectly smooth or completely rough. This means that when the light hits the surface of the part, there will be a mix of diffuse and specular reflections. In highly reflective surfaces, the specular reflection will be the predominant reflection type, which will generate multi-path reflections which in turn generate outliers. Outliers can be modelled in two ways: mixed reflections around convex edges leading to the acquisition of diffuse and specular reflection; and multi-path reflections which occur in concave geometry where the camera receives diffuse reflection directly and a secondary diffuse reflection.

In the mixed reflection scenario, the specular reflections produce false images. The direction of the reflected laser light is controlled by the incident angles between the scanned surface normal and the scanning plane. The orientation will then be responsible for the specularly reflected light to reach the camera. When scanning over edge features, due to the edge having a curvature, the normal of the surface will vary along the edge, which means the direction of the light being reflected will also vary around the edge. Due to this fact, some of the reflected light will reach the camera, producing two light stripes, thus introducing error into the scan.

In Figure 22, the scanning orientations considered by the authors in [46] to test the effect of varying the orientation angles on the production of outliers are presented. The appearance of outliers for each of these angles occurs in the following regions:

- For the in-plane incident angle (IIA), the outliers occur when there is a shift in the same direction along two scanned edges;

- For the out-plane incident angle (OIA), these occur when there is rotation around the scanned edge;
- As for the edge orientation angle (EOA), outliers appear when there is a “shift in the opposite direction along two scanned edges” [46].

Figure 23 shows the variation of the percentage of outliers with the variation for each of these angles. For each angle it can be seen:

- For an IIA above 10° the percentage of outliers is reduced to 0%. It can be seen from the graph that the evolution of the outliers will reduce with the increase of this angle;
- For OIA, the outliers are always present, reducing their amount with the increase of the angle. The outlier presence is the lowest at 45°;
- For EOA, the outlier presence is reduced to near 0% when this angle is above 25°, reaching its lowest presence value at an angle of 30°;

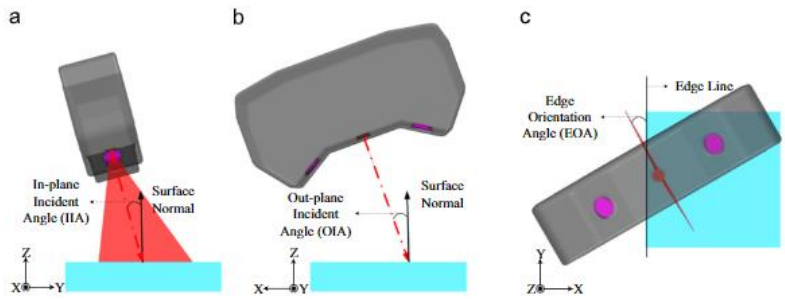

Figure 22 - Scanning orientations [46]

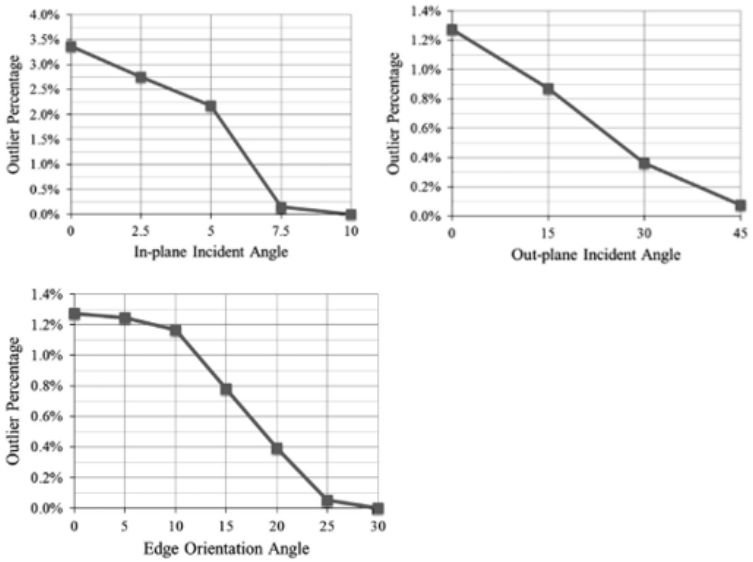

Figure 23 - Outlier percentage for variation in scanning orientations for the mixed reflections model [46]

For the multi-path reflection model, when scanning concave geometry with reflective surfaces, the laser light reflects specularly and hits another surface where scattered light is received by the camera. This leads to the camera receiving direct diffuse reflection and a secondary diffuse reflection which further leads to the appearance of outliers.

Just as the previous model, the three scanning orientations affect the presence of outliers. In this case, outliers will always be present due to the secondary reflection being diffuse, which makes it insensitive to the surface normal. The presence of outliers for each angle occur in the following ways:

- For the IIA, outliers appear when there is a shift along the concave edge;
- For the OIA, the rotation around the concave edge will produce outliers;
- For the EOA, just like what happens for the OIA, outliers appear when there is rotation around the concave edge.

In Figure 24 the graphs of the variation of outliers with the variation of the angles are once again presented. The evolution for each angle can be summarised as follows:

- For the IIA, the percentage of outliers decreases drastically when the angle increases to 15° with a percentage of around 0.2%, decreasing slowly until just below 0.2% at 30°;
- For the OIA, the percentage is much larger, having a presence of 0.5% for 30°, reaching its lowest value of around 0.45% at 45°;
- Finally, for the EOA, the outlier presence appears to be null at 45°, increasing again for higher angle values [46].

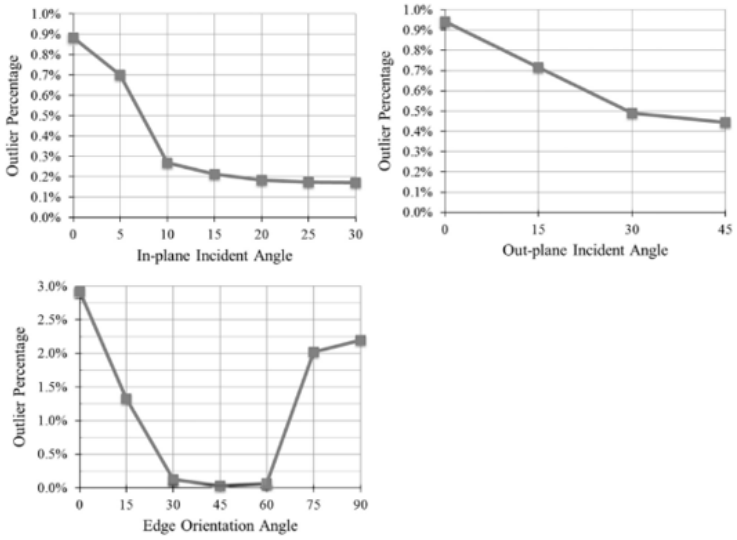

Figure 24 - Outlier percentage for variation in scanning orientations for the multi-path reflections model [46]

Reduction of outliers is an important task for laser scanning. This can be done with careful scanning path planning combined with an algorithm to automatically remove outliers. To do this, it is necessary to properly distinguish a valid surface point from an outlier [46], [47]. As such, the authors in [47], based on the view-dependency properties of the outliers, propose three criteria to filter outliers: overlap ratio, point spacing and surface variation.

- **Overlap ratio:** By obtaining several point clouds from the same region in different orientations and by aligning these point clouds properly, there will be overlap, especially for the valid surface points. In the case of outliers, even with scans in different orientations, due to the view-dependency seen above, the actual shared orientations will be low and as such have low overlap. This enables the possibility to use the overlap ratio as a filter. Nevertheless, in the case of being in the presence of multi-path reflections around concave geometry, the outliers will be complex and will occur for any orientation and as a consequence, might have a higher overlap. For these cases it is necessary to find more filters to remove outliers;
- **Point spacing:** Outliers formed by multi-path reflections are somewhat sparse, while good surface points will be dense and with good overlap. This enables the application of a local point spacing threshold to filter the outliers. Outliers will have high point spacing as they are not as dense as good surface points, which allows the use of a point spacing threshold as a filter;

- **Surface variation:** In multi-path reflection, outliers will generate planar surface patches around concave planar geometry. For curved geometry, the distribution of these will be irregular and not planar, allowing the assessment in terms of surface variation. A good surface patch will have high curvature or sharpness, depending on the feature, with a small neighbourhood radius (has high overlap) while outliers will produce points in several directions, leading to a higher neighbourhood radius and low overlap.

The goal of the scanning path planning is to take advantage of the view-dependency of outlier formation and plan accordingly. As such, to reduce their formation, rotating scans are proposed where the scan orientation will rotate according to a given angle interval to guarantee view-dependency of the outliers. The EOA is the angle used for the variation in orientation as it can change outlier occurrence regions and even lead to their full reduction.

Another aspect that should be considered is the number of scans. With fewer scans, there might not be enough overlap, whereas with many scans, more orientations will be used, more overlap will be achieved, but more data will be present, and the scanning time will be longer.

The scheme of this proposed method can be seen in Figure 25. Scans are done with 45° IIA and an EOA which will vary in 360/n, where n is the number of scans. After scanning, outliers are removed by applying the above discussed filters. In Figure 26 an application of this scheme, together with a comparison with a poorly planned scan path is shown. Due to this method relying on view dependent properties of outliers, small concave features such as holes or inner features will have some points removed falsely because of lack of overlap [47].

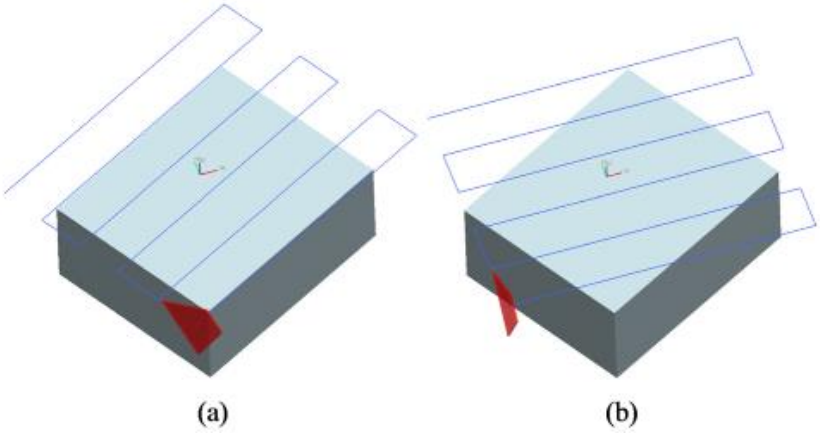

Figure 25 - Scanning of an object with the proposed method: a) 45° IIA and 0° EOA; b) 45° IIA and 30° EOA [47]

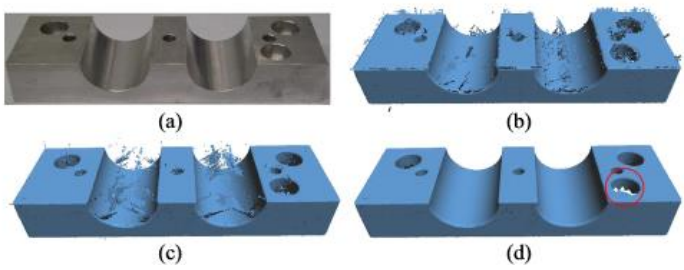

Figure 26 - Scanning of an aluminium part with concave cylindrical surfaces a) The part; b) Scan from a poorly planned path; c) Scan obtained from rotating scans; d) Point cloud after applying outlier filters [47]

2.3.3. Photogrammetry

Photogrammetry is a passive system; it receives light without having any influence upon the scene lighting. The geometry of the surface under inspection is obtained from the integration of photos taken simultaneously by different cameras in different points of view. At its base, it shares the same principle as triangulation. It can be a rather cheap and simple solution to some RE applications due to only requiring cameras, and camera equipment. It finds some use in the automotive, aircraft, railway ship building and building industries.

The quality of the obtained model will be dependent on the camera resolution, the lighting and the sharpness of the surface's texture which in turn is affected by the surface reflection. It is important to take several pictures in different angles and to guarantee enough overlap to have reference points present to properly join the pictures together and form the model. For photos without enough lighting, or with too much exposure, out of focus or even those which are redundant should be removed. This carries the downside of part of the surface being covered by those photos possibly not being present after the reconstruction [19], [23], [24], [41], [48]–[50].

When taking pictures, coded points should be placed around the part to be measured, or even on the part itself if it is big enough. Ideally, at least 5 marks should be in common between images These marks, as seen in Figure 27, can further help the automation and robustness of value generation and the orientation of the cameras, enabling the calibration of the cameras and a greater precision. The 3D coordinates of the part are calculated based on these marks. A scale bar with the same length as the part itself should also be added to the scenery [51], [52]. There are some main parameters to take into consideration for this method:

- The camera must be able to get sharp and precise shots of the part, ideally with the background out of focus;
- The lighting should also be consistent with the reduction of shadows, otherwise more error will be introduced into the reconstruction;
- The setup of the specimen should allow to obtain the maximum amount of the part. During the process, the part will need to be flipped to obtain the full model [41];
- The number of cameras is also of interest as it will allow for different points of view from where it becomes possible to take pictures in different angles. This increases the method's repeatability while also improving the triangulation at the cost of more processing time [49], [52];
- Proper contrast and surface triangulation should be maximized, which requires the avoidance of high angular views [52].

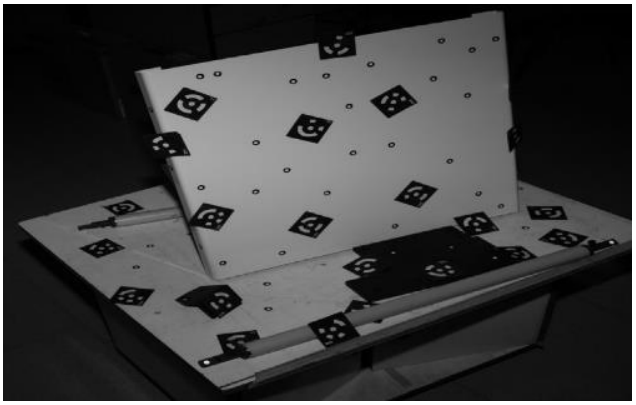

Figure 27 - Layout of marked points on part, together with scale rulers [51]

The bottleneck of photogrammetry is its software, requiring post-processing to obtain the final model. In Figure 28, the creation of the digital model is shown. This post-processing phase has several steps such as:

- **Photo-masking:** In this step, the background is removed, performing manual and automatic adjustments;
- **Alignment:** A rough alignment is performed according to the reference points present, producing a point cloud;
- **Evaluation:** During the point cloud generation, it might be necessary for a user to evaluate the cloud;
- **Mesh generation:** The point clouds are aligned and then merged;
- **Texture:** Colour and shading is added to the model [41].

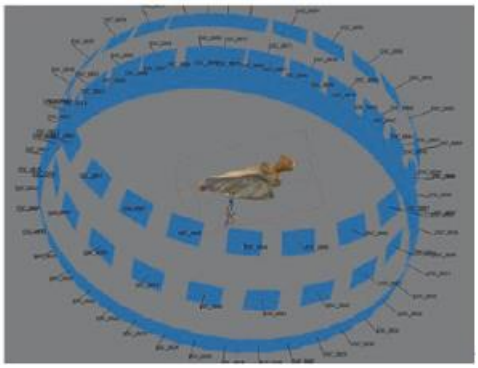

Figure 28 - Creation of digital model through photogrammetry [41]

Photogrammetry's challenges are mainly related to the part's material. For highly specular and reflective parts the point clouds become distorted due to the reflected light on the surface, which adds inaccuracy and hinders the full model acquisition, as can be seen in Figure 29 [24], [50]. Nevertheless, some approaches can be done to improve the model's reconstruction. The application of a polarizing filter lens will reduce the glare of the reflected light, but it has the downside of also reducing the exposure of the camera which will introduce noise into the pictures. A longer shutter speed will improve the exposure, but also increase the time cycle of the system. By applying some trade-offs, it becomes possible to improve the model reconstruction [50].

Figure 29 - Scanning of a dental tooth key [50]

2.3.4. Deflectometry

Some products can have specular surfaces, posing a challenge to conventional optical methods due to the reflectance of the surface. The typical way to solve this problem would be to spray the part with a matte coating, but this incurs in inaccuracy. To solve the issue of inspecting specular surfaces, another method can be used, deflectometry [53]–[57].

In deflectometry, the three-dimensional information of the surface is modulated into a phase of sinusoidal pattern [55]. Deflectometry is popular for specular surface inspection due to its large dynamic range, high accuracy, automatic data processing and not having to be in contact with the part to inspect it [56], [57].

Deflectometry is a technique based on the specularity of the specimen and whose main working principle is according to the law of reflection, where the reflected angle is double the angle to the ray [58]–[60]. A known sinusoidal pattern, which is shifted several times by a fraction of its period, is projected by a diffuse screen, usually a Liquid Crystal Display (LCD). This projected fringe pattern is then reflected from the specular surface and captured by a CCD camera. Deviations from the flat surfaces will result in the distortion of the fringes of the pattern. The phase information is obtained from the reflected fringe patterns which is then used to obtain the slope data of the specular surface, allowing the reconstruction of the three-dimensional data by integrating the local slope data [53], [55]–[61]. In Figure 30, a schematic of the process is shown.

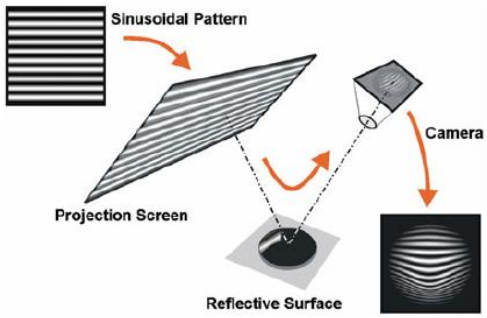

Figure 30 - Deflectometry schematic [61]

By knowing the orientation between the camera and the display projector, it is possible to calculate the normal vector at each surface point and obtain the gradient data of the surface curvature. From here, the surface can be obtained from integrating its gradient data. During this process, the local height information is lost. This issue can be solved by using two cameras and phase-shift deflectometry, where a series of phase-shifted fringe patterns are projected and the image for each pattern is recorded. This method can achieve high height accuracy, being able to reach the nanometre range [61], [62].

According to the authors in [59], phase measuring deflectometry (PMD) follows some main steps:

- Camera and monitor setup: The FOV must cover the measuring volume, requiring the proper object placement with the necessary adjustments to the camera so it can observe the reflected fringe patterns;
- Capture of the fringe images from the reflected pattern;

- Obtain the 2D phase information, X-direction and Y-direction slope values from the fringe pattern analysis;
- Height information reconstruction based on the slope values.

The goal of PMD will be to acquire the geometric information of the part by phase-shifting and phase wrapping which will entail retrieving the phase information and matching its absolute value to the corresponding pixel. By obtaining the absolute phase values and knowing the period of the fringe pattern, it becomes possible to locate these values on the screen. Next, the slope values can be calculated and then use the gradient data to conduct the reconstruction of the geometry data [55], [59], [60].

In terms of applications, PMD can be used for the following purposes:

- Through PMD, it is possible to study the influence of misalignment on the part;
- PMD is well-suited for flaw detection, being able to observe defects, flaws and cracks on specular surfaces based on the retrieved phase information. Due to this ability, it is used in the automobile industry for side glass and car body inspection. The system will measure the curvature of the surface and then compare it to the reference which will then allow for the defect evaluation [55], [59], [62], [63];
- Used for the defect assessment of free-form telescope mirrors [59], [63].

Despite its benefits and abilities, it has some limitations which are summarised below:

- Calibration: It is necessary to conduct screen calibration and geometry calibration. In geometric calibration, the geometric relations between the display screen and the camera rays are obtained. The camera must also be corrected for distortion while the screen should be calibrated for uniformity and linearity [59], [60], [62];
- Camera distortion: To avoid projection error, the mapping of the captured images should be corrected. Low order aberrations such as defocus and astigmatism should be taken into consideration during mapping correction [60];
- Specular surfaces are affected by ambient light, which affect the measurements by PMD;
- The PMD method for rough metal surfaces is limited because visible light alone cannot apply enough specular reflection to the part. Methods applying infrared to deflectometry have been presented to solve this problem [56].

3. Product development

This chapter relates to the product development phase. Firstly, the customer needs will be shown and analysed to set the main path for the development. After establishing the needs and setting the roadmap, a simplified case of a bottle is analysed to have an estimate of the necessary accuracy for the project. Next, the equipment used for the technology studies is discussed. This will involve the use of a CMM, a laser scanner and a structured light system. Finally, the development of the project, thus far, is exposed by discussing the script development that has been done inside the Geomagic Control environment. The goal of the developed scripts is to conduct the operations necessary to obtain the volume of the moulds from point clouds, inspect their surface and guide the user during the preparation phase.

3.1. Design methodology

Before beginning the development of the project, it is necessary to know what the client wants, what he needs and what he would hope for. The first type of needs can be gathered by interviewing the client and discussing what is lacking and the main requirements to solve his problem statement. As a first step, discussions with Intermolde were done to obtain this data and their main necessities can be seen in Table 2. To analyse further decision making and improve the satisfaction of the client, a Kano analysis is done based on the features that the product will have and on the client's needs. This is summarized in Table 3. This analysis highlights the basic needs of the customer and what can be done to improve his satisfaction such as implementing a deviation report together with the volume so the mould production process can be improved, instead of solely focusing on the volume calculation.

Table 2 - Voice of the customer

Features	Physical Properties	Product Quality
I want it to automatically get the volume of the mould	I want it to scan different mould materials	I want it to reduce volume inspection time
I want it to generate surface inspection	I want it to get the surface data of the mould without spray	I want it with a precision in the order of 0.01 mm
I want it to guide the user on necessary steps	I want it to be able to acquire differences between polishing	I want it with good repeatability

Table 3 - Product features using a Kano analysis

Customer need statements	Kano Analysis
User guidance	Delighter
Process improvement	Delighter
Automated surface acquisition	Must be
Automatic volume calculation	Must be
Surface acquisition without spray	Must be
Fast result treatment time	Must be
Surface deviation reporting	Satisfier
Acquisition of different mould materials	Satisfier

3.1.1. Design constraints

There are some main design points that must be respected. One of the most important to respect will be the necessary accuracy to properly gauge the volume deviation, as well as the surface deviation. In Table 4, the required volume tolerances related to the volume of the mould are shown. Based on this, and by simplifying the problem considering the bottle a normal cylinder, an estimate of the accuracy can be obtained.

Figure 31 shows the dimensions for the simplified model. These are selected for the volume to be slightly lower than 500 cm^3 and consider the tightest tolerance. To figure the required accuracy, the surface deviation is considered equal around the cylinder in this model. The volume of the cylinder will be given by Equation 1, where t corresponds to the volumetric tolerance.

$$v = v_{CIL} + t \qquad \text{Equation 1}$$

By expanding the equation:

$$(\delta + r)^2 \pi h = \pi r^2 h + t \qquad \text{Equation 2}$$

In Equation 2, δ is the term for the surface deviation. By simplifying this equation:

$$\delta = \sqrt{\frac{\pi r^2 h + t}{\pi h}} - r \qquad \text{Equation 3}$$

Equation 3 enables the calculation of the surface deviation for the simplified cylinder model. By applying the dimensions from Figure 31 this deviation will be 0.0151 mm. Even though the calculation is being done for the case where wear and the surface deviation are uniform, an order of magnitude estimate for the level of accuracy required by the system is obtained.

Table 4 - Volume tolerance table for the moulds

Volume (cm^3)	Tolerance (cm^3)
Up to 500	±0,5
501-800	±0,8
801-1300	±1,0
>1300	±1,5

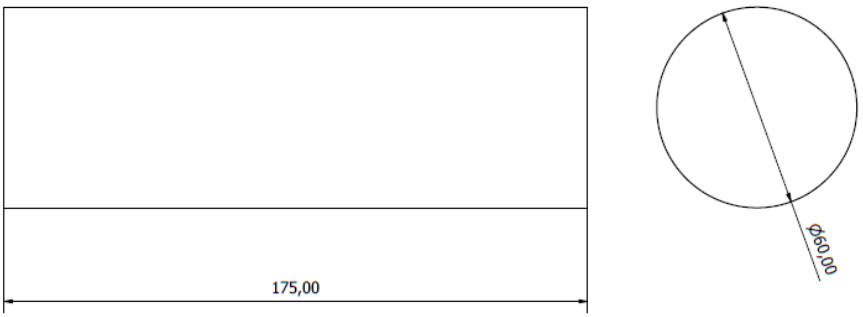

Figure 31 - Dimensions of simplified case in millimetres

As for other constraints:

- According to Intermolde, the maximum area of the mould would be 400mm×200mm. Since it is a rather small area, light systems, such as a laser scanner and a SLS can be used as they can cover this area with ease;
- Their maximum deviation allowance for diameters is 0.1 mm. The accuracy requirement for this constraint is fulfilled since a precise system is needed to inspect the surface deviations;
- Spray cannot be used, not only does it influence the results, but it also pollutes the working environment and makes the automation of the system more complex;
- Their goal is also to pick random moulds from the series and subject them to testing. This means that a system using conveyors and a working line does not make sense for their purposes, but instead a single station to load the moulds and conduct the inspection. This can further be done with laser system or a SLS, both with a rotating table as the mould's area makes it possible to acquire the whole surface in few scans with these systems.

3.1.2. Roadmap

With the main requirements and constraints identified, the path to develop the project can be set. This project will follow two main paths: software development and technology studies. The defined roadmap can be seen in Figure 32.

The software development is done to achieve the necessary client demands and fulfil latent needs, such as user guidance. Two scripts will be developed, one which will be used as a preparation step and will guide the user accordingly; and another, dedicated to the result treatment which will deliver the calculated volume and a report of the surface deviations.

The technology studies are done to determine which light system is more applicable by studying the limitations and benefits of each. This will involve using the light systems in different conditions such as acquiring the surface of polished and unpolished moulds. Scanning different materials also allows to check the systems' surface acquisition ability. Validation of these systems is a must, to ensure they are performing correctly and within the requirements.

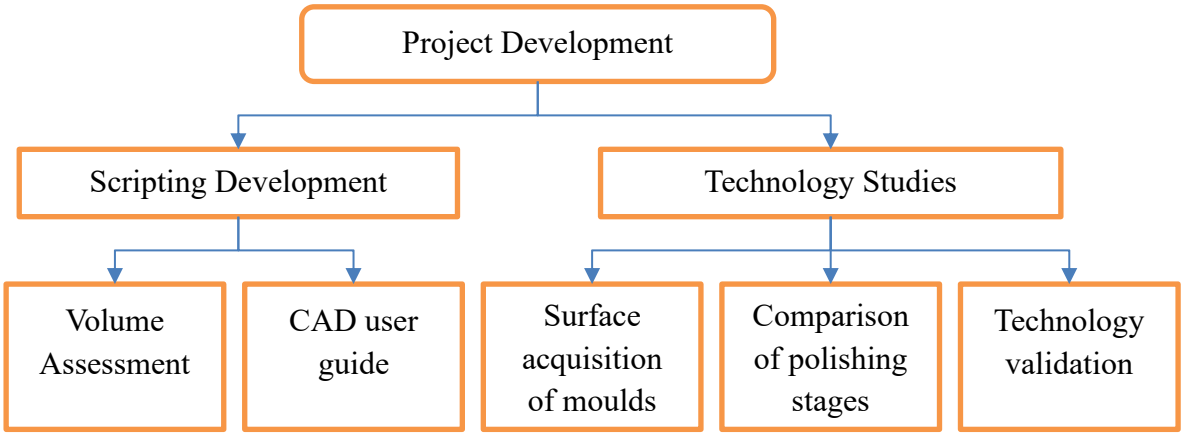

Figure 32 - Project development roadmap

3.2. Technology

In this section, the hardware and software that were used for the development of the project will be explored. The systems used for the case studies were a CMM, a laser scanner and a structured light system. For the software development, Geomagic Control 2015 was used. This software is used for metrological applications and can manipulate point clouds and STLs. Geomagic also has a rich API (application programming interface) which allows the development of scripts to automate tasks. The scripting language used to control Geomagic's API was Python 2.7.

For precise measurements and to guarantee that the surface can be acquired, a CMM using contact measuring is used to provide ground truth measurements. The used CMM was the X-Orbit 55-7 from Wenzel, shown in Figure 33 a). This machine has a listed measurement uncertainty of 2.2 μm, which will enable a precise inspection when conducting the validation of the light systems. To make inspections, the system uses Quartis, a software owned by Wenzel [64].

As for the light systems, the FARO blue scanner attached to the Quantum M FARO arm and the Cronos 3D Dual from Open Technologies were used. The FARO laser scanner is a blue light scanner, seen in Figure 33 b), which has a listed inaccuracy of 0.025 mm and when attached to the FARO arm can have a measuring uncertainty of 0.055 mm. By calibrating the scanner, it is possible to compensate for this uncertainty and obtain more trustworthy results. This scanner enables a point acquisition rate of up to 1.20 million points per second which, together with the blue laser technology, will enable it to acquire the surfaces of the moulds. This scanner can scan directly to Geomagic's environment to obtain point clouds, providing the installation of the correct drivers [65]. Now regarding the SLS, the basis of the Cronos 3D Dual is the use of white structured light, as shown in Figure 33 c). The system itself has a measuring uncertainty of up to 0.06 mm with an acquisition time of 4 seconds per frame. The system is used together with a rotating table to acquire the whole surface of the part. The RevEng software is used for the scanning, which allows the user to check if the pixels of the camera are underexposed or overexposed to adjust accordingly [66].

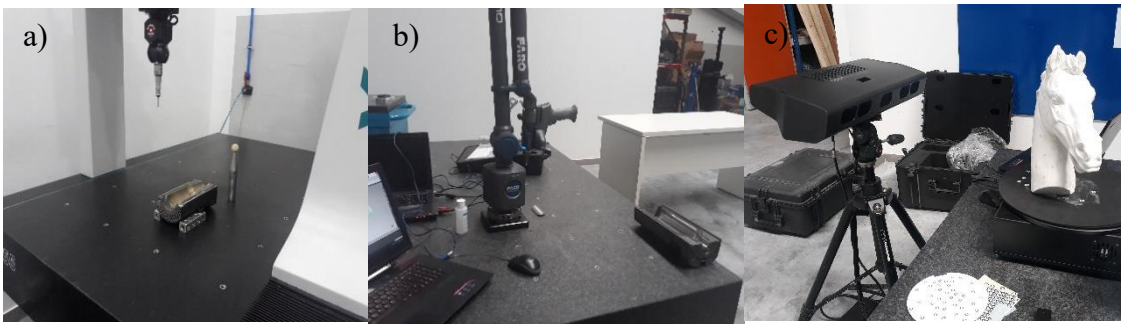

Figure 33 - Equipment used: a) X-Orbit 55-7 b) FARO Quantum M with the blue scanner attached c) Cronos 3D Dual

3.3.Script development

To automate the volume calculation, two scripts were developed. The first will be related to the preparation stage of the CAD file used for inspection and volume assessment. This script will guide the user throughout the process to standardize it as much as possible. As for

the second script, it is dedicated to volume assessment and surface inspection, will be responsible for the calculation of the volume and deviation comparisons. A general overview of the process is shown in Figure 34. In Appendix A and B, the manuals for the programmer and the user, respectively are shown.

For the development of these scripts, Python 2.7 is used since it is the most recent version of Python that Geomagic Control 2015 can use. This section will delve into the development of both these scripts, highlighting their purposes, the reasoning behind them and the challenges faced during their development.

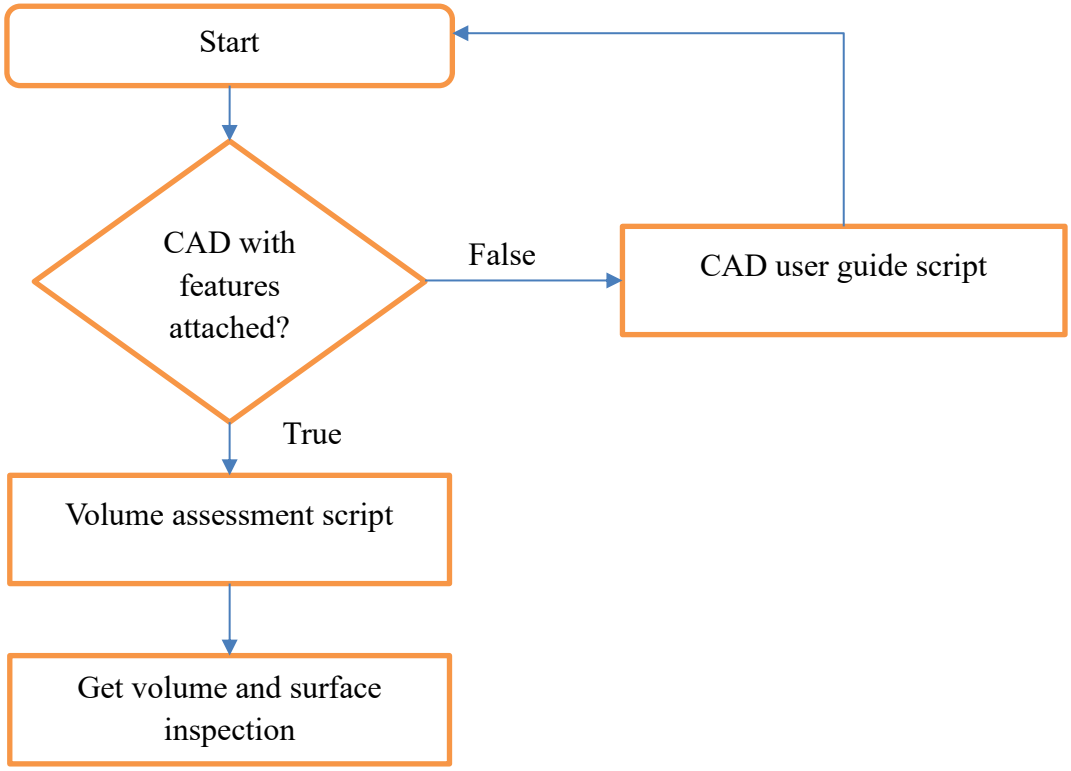

Figure 34 - Overview of script workflow

3.3.1. User CAD guide

Before engaging on the volume assessment side, some preparation must be done to enable part evaluation. For this reason, a guiding script was developed to help guide the user throughout the whole process. This script must generate a simple interface and give the user enough clues to properly execute the process. There are four main parts to this script: the presented dialogue, the feature creation, the cancel button and the delete feature button. A simplified diagram of the current iteration of this script can be seen in Figure 35. For further information, the input/output function block can be seen in Appendix C

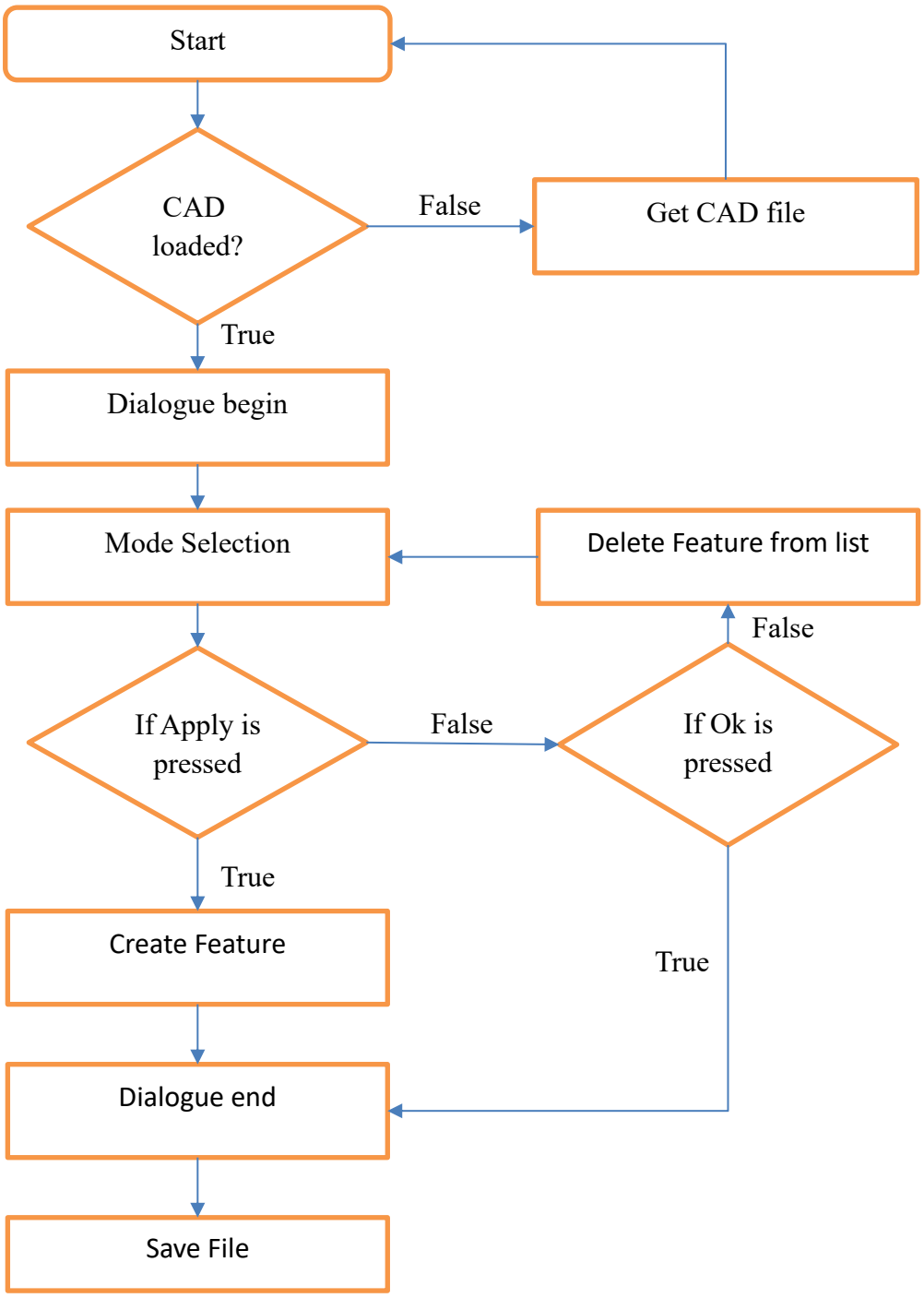

Figure 35 - CAD guide script diagram

Firstly, it is the in the best interest to check if a CAD model is currently loaded into the environment, in case there is no cad model, the user will be asked to import one, otherwise the dialogue for the CAD feature creation is called. The dialogue interface, originally, had a dropdown and three buttons, apply, ok and cancel, shown in Figure 36 a). To make this interface more user friendly, the cancel button was disabled from the starting dialogue because it had the same use as the ok button. A delete feature button and the display of the features attached to the model was implemented, as seen in Figure 36 b).

The dropdown is used to select the feature creation mode. If the user wishes to create features with the selected mode, he can then press the apply button. A message on the dialogue interface will inform the user to click on the CAD faces to create features. During this stage, only the cancel button is enabled so the user can cancel the selection at any time. In the previous iteration of this script, the user would have to press the cancel button twice in a row to delete the features he created during this instance. This, of course, is very cumbersome and not clear, so, to improve the clarity, the delete feature button can be used. The feature creation is done based on the face ID and the primitive feature of the CAD itself. When the user clicks a face, the ID of this face is obtained, then, based on the primitive feature of the CAD the resulting feature is created and added to the model with the mode name attached. An example of feature creation can be seen in Figure 37. As for the feature deletion, in Figure 38 the deletion of the previously created plane is done. Once the feature creation is completed, the user will cancel the selection and press the ok button to save the features to the model. After pressing the ok button, a dialogue asking if the user wishes to save the file will be presented as shown in Figure 39. This will be the final stage of the script.

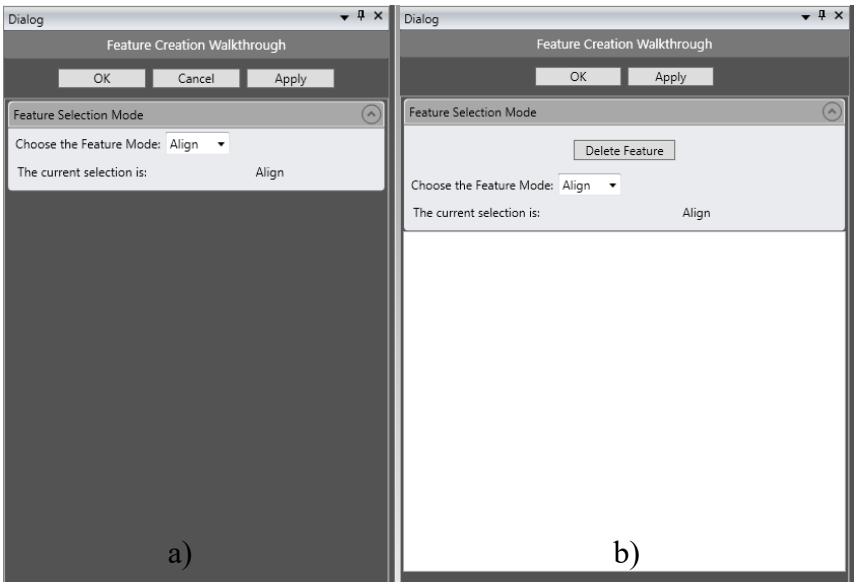

Figure 36 - Initiation of the dialogue: a) First version; b) Second version

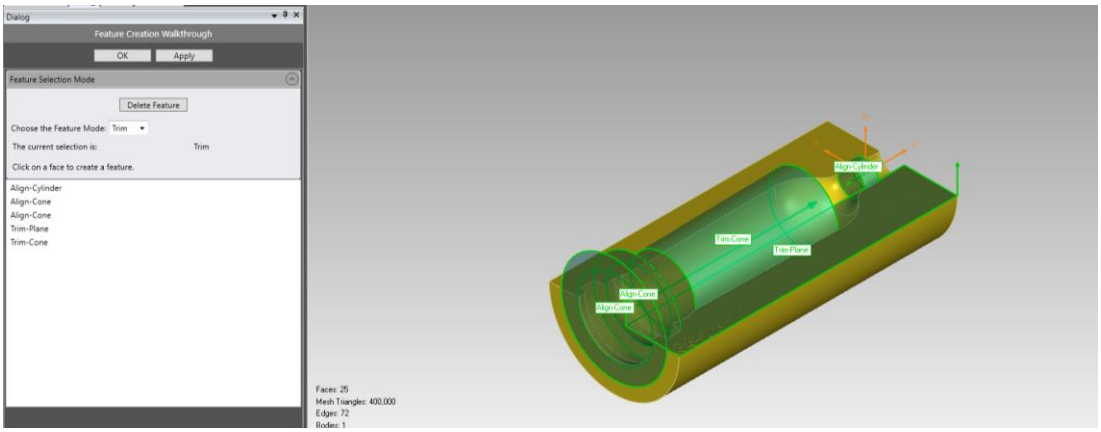

Figure 37 - Feature creation example

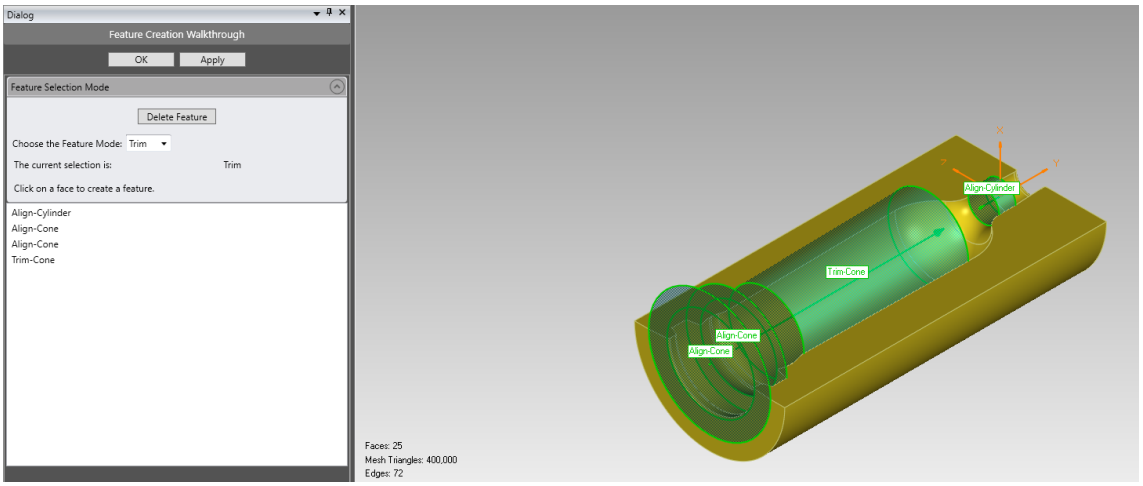

Figure 38 - Feature deletion example

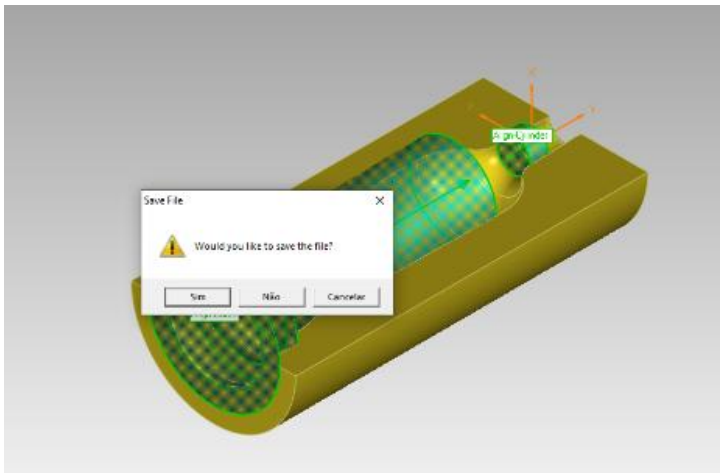

Figure 39 - Prompt for file saving

To build this program, a class was created for everything related to the dialogue presentation and overall interface. In this class there are several methods: for the display of the dialog, for the creation of the dropdown, a method for each button and for the face picking with the consequential feature creation. The methods vary between the buttons:

- The ok button, once pressed will exit the dialogue any time it is pressed;
- When the apply button is pressed, the dropdown, the delete feature button, the ok and apply buttons are disabled, toggling on the visibility for the cancel button. It also becomes possible for the user to begin picking the CAD faces;
- If the cancel button is pressed, the feature picking is stopped. Then, the previous buttons become visible and the dropdown becomes enabled. Finally, the cancel button is set to being invisible, once again;
- By selecting a feature inside the displayed list and then pressing the delete feature button, the feature will be deleted from the model and its name erased from the array where the face ID and the feature's mode are stored.

The class is the main part behind this program. Besides the class, the program will start with a condition, to check whether a CAD model is present or not. Based on this check, the user can be asked to import the desired file. The user will be asked to import a CAD model until there is one in the environment. It will be assumed that the user will not want to import different CAD models to the same environment.

With this script, some benefits can be achieved, such as:

- User guidance, enabling a lower entry knowledge into the process;
- Allows the user to delete features in the case of mistakes;
- Asks to save after each run;
- Does not allow duplicate feature creation;
- Simple and clear interface;
- Further standardizes the process.

During the development of this script there were some issues:

- The creation of the correct feature when clicking on a CAD face. The challenge here would be related to the creation of the feature and then further attachment of the feature to the model. To solve this issue, when clicking on a face, the face ID is stored for that face and then the primitive feature for that face ID is evaluated. Based on the result of that evaluation, a feature is created with the parameters of this primitive feature with the further attachment to the model;
- The disabling of duplicate features. The creation of duplicates should not be permitted as it can add further confusion to the process while adding no value.

To solve this problem, a two-dimensional array is applied, carrying the ID of the feature and its mode. It becomes possible to guarantee unique features by introducing a condition which checks if an ID-mode pair is already present in this array;

- Exiting the dialog and stopping the feature creation. During the initial development, the prompt to continue to create features was still active after leaving the dialogue. This was due to a lack of a condition inside the cancel button;
- Reducing the possibility of mistakes done by the user. Given the importance of this stage, it is necessary to stop the user from committing mistakes, this is why some buttons become disabled and messages are prompted given the actions of the user;
- Creating a button to run the script. For better user interface, it is valuable to being able to press a button and initiate the script. The issue here was related to properly creating a button inside the Geomagic Control environment for this effect. Through the customer support, it was possible to manipulate a file to present a button inside the environment.

3.3.2. Volume Assessment Script

To further automate the process of the volume acquisition, a script must be developed to treat the data retrieved from the mould scanning to then produce results related to the volume of the mould and its deviations. For this purpose, the script should lower the necessary Geomagic operation skill level needed by the operator, as well as helping in taking less time to obtain the volume when compared to the manual process. Through scripting, it also becomes possible to increase repeatability while reducing human error. Furthermore, by calculating the volume automatically inside Geomagic's environment, the 3D comparison of the surface to the CAD model can be obtained. This will allow to inspect the surface condition of the part and enable the improvement of the production process. A diagram of this script can be seen in Appendix D with the respective function blocks shown in Appendix E.

As such, the script will contain the following main steps: point cloud treatment, mesh trimming, 3D comparison, alignment of all the parts and the volume calculation. Before

initiating the point treatment step, the user will be asked how many parts he wishes to analyse.

The acquired point clouds are in a raw state, as shown in Figure 40 a) and, as such it is necessary to treat them. In this step the process starting from the acquired point clouds to their conversion to an STL mesh is described. Firstly, the global registration of the clouds is done, where the similar areas between the clouds become coincidental and thus will share overlap, as shown in Figure 40 b). The normal direction of the points is also adjusted so that they become properly oriented, avoiding points oriented in the wrong direction. Next, the point cloud objects are merged to form a single point cloud object, enabling an easier manipulation, and allowing for the alignment to the respective CAD object via a best-fit alignment. This type of alignment will give the same weight to every point of the cloud; thus, the error of the points will be distributed along the clouds. Once the alignment is done, the point cloud object is converted into an STL mesh. Then, the features which will be used for trimming and alignment are created based on the CAD through a best fit on the surface, as can be seen in Figure 41. Only the top plane for the mould halves is created separately by prompting the user to select which areas of the surface will count towards the plane's creation. This is done due to a lack of an accurately representative CAD model of the mould and because this area of the mould halves can have a curvature which, if the entire surface is selected, will affect the plane's height and thus the final volume value.

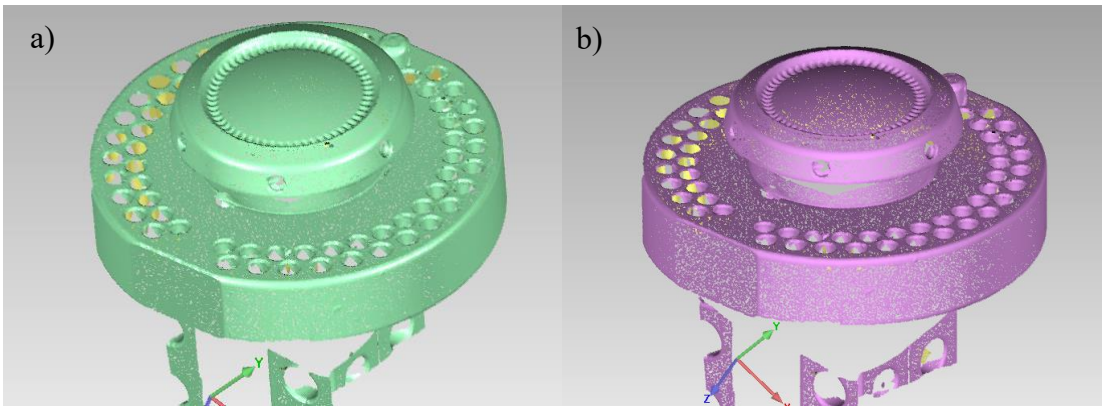

Figure 40 Scanned point clouds: a) Points clouds; b) Global registration of the points

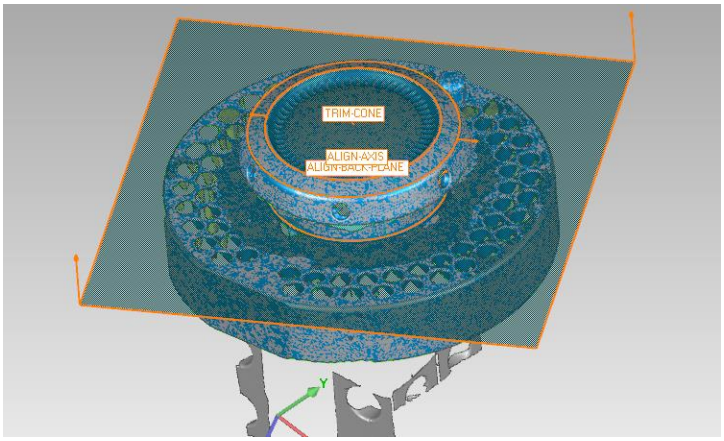

Figure 41 - Resulting mesh with the created features

With the STL of the part, it is necessary to isolate the areas of interest. As such, the aim will be to isolate the moulding surface of the mould part. With the use of the previously created features, namely those with the purpose of trimming the mesh, the mesh can be successfully trimmed, shown in Figure 42 a). Depending on whether the part is a bottom or half of the mould, different features are used. For the mould halves, planes are used for the trimming. Here, offset planes are created in the order of 0.01 mm to cut deeper into the mesh and produce a clean trim. However, for the bottom part, two cylinder objects are created from the master cone feature. One, using the radius of the smaller cone base, and the other created by multiplying this radius by a factor of 5. The smaller cylinder is then subtracted from the larger one. Next, this surface is converted into an STL to subtract this new object from the bottom mesh, resulting in the region of interest.

After the features are used for the trimming, the user is prompted to select any further areas he wishes to delete from the environment, as can be seen in Figure 42 b). This will serve as a safeguard for the times where the features are not enough to properly trim the parts of the moulds. In the end, the result can be seen in Figure 43.

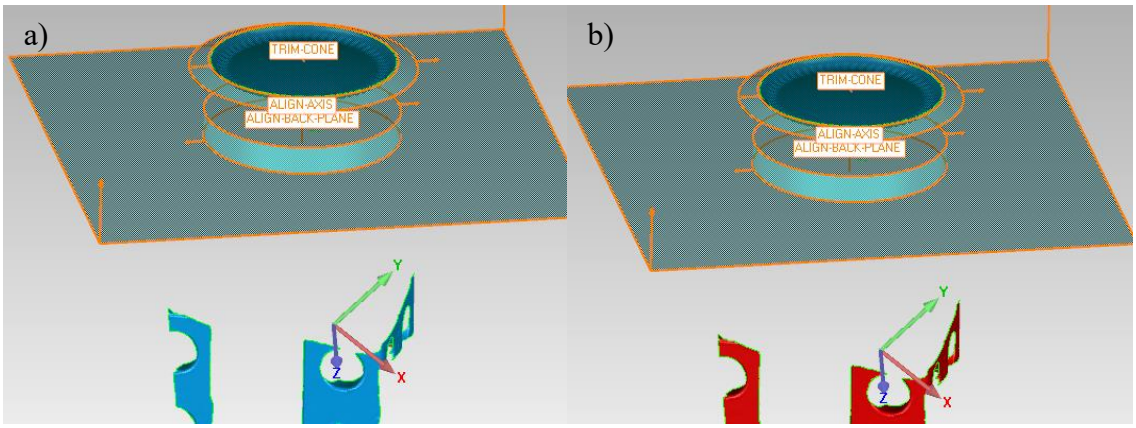

Figure 42 – STL mesh: a) Trimmed mesh; b) User selecting extra geometry to be trimmed

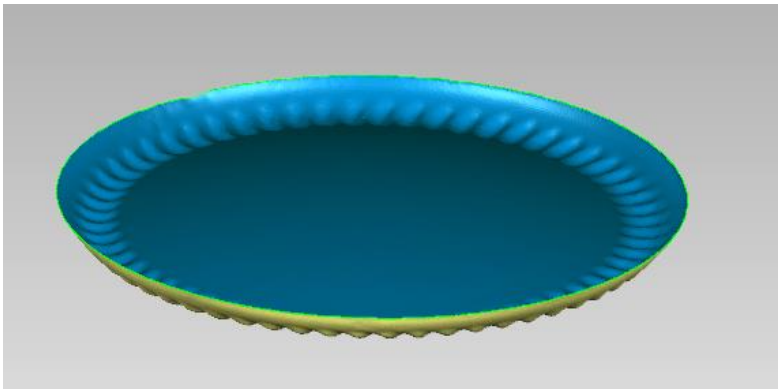

Figure 43 – Final trimmed mesh

With the trimming step complete, the part is aligned through a feature-based alignment and the evaluation of the mould's surface is done next. In this stage, two choices are presented to the user:

- Automatically generate inspection points around the mesh. Picking this method will generate 100 random inspection points around the mesh. This method has the advantage of not requiring any pre-planning and will deliver a general inspection of the part. However, it has the limitation of generating points outside of the region of interest on some parts;
- Load a predefined file containing the location and the tolerance of the specific points to be inspected. Despite requiring the creation of a file containing this information, it is more robust for part inspection. By specifying the point locations, the inspection is certain to be done in the region of interest. For future iterations of the part, the point location file can be reused or even modified.

After choosing the surface inspection method, a deviation map, as seen in Figure 44, is created over the model to show the overall surface state of the part. Then, once the

comparison is processed, a report containing the 3D comparison of the part to the CAD and the deviations of the inspection points is generated. Finally, the file is saved, and the user is prompted to select the next part to be analysed. This process is repeated until the full mould set is analysed.

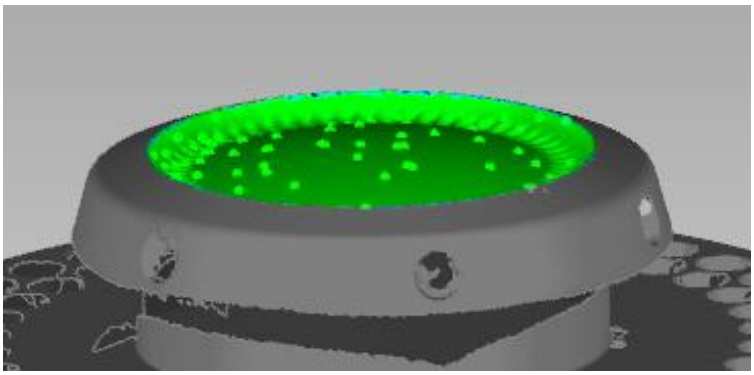

Figure 44 - Deviation map with the point cover over the mesh

Once every part of the mould set has its STL treated and analysed, the meshes of the parts are automatically loaded into the environment. With the meshes loaded, the alignment is done via feature pairs based on the features that were created during the point treatment step with the alignment mode tag attached. This will take the misaligned meshes, as seen in Figure 45, and place them appropriately to one and another. As for the top plane, a condition is set to check if the plane of the reference object and of the test object are facing the same direction. This condition is done by checking whether the dot product of the normal vectors is positive. If not, the normal of the test object is multiplied by -1 to rotate it. After the alignment, the meshes are merged, generating a single mesh. The generated mesh is created from partial meshes, which will not have overlap, thus producing holes in it. The final bottle mesh, shown in Figure 46, is obtained by having these holes automatically filled up to a given diameter. After closing the holes, any open geometry is also deleted so that only the volume of the mesh of the bottle is accounted for. It must also be noted that the normal direction of the triangles will be in the opposite direction since the scanning is done to the moulding surface and not to the bottle directly. For this reason, the normal direction of the triangles must be flipped to present the volume properly, otherwise it will appear as being negative.

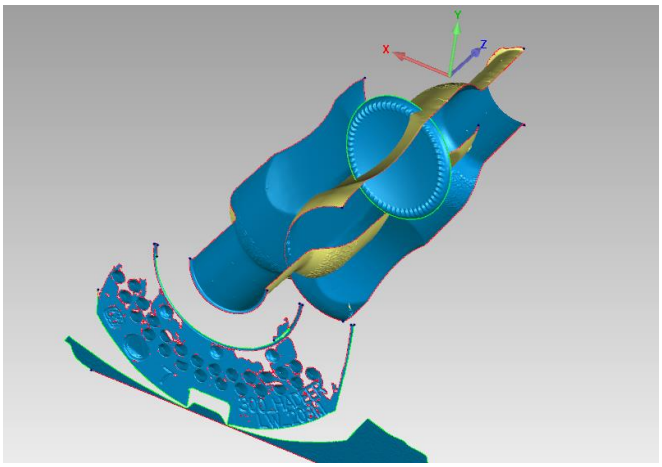

Figure 45 - Misaligned meshes

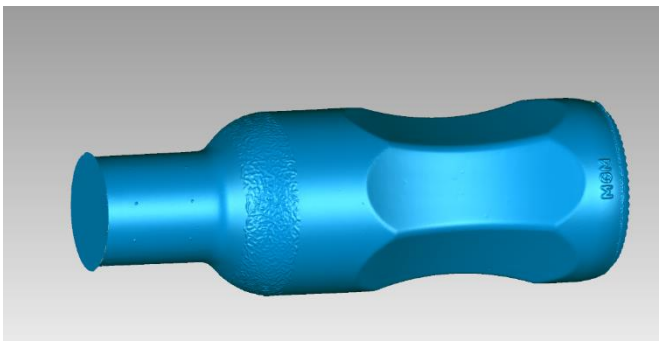

Figure 46 - Final bottle mesh

The use of this script offers advantages to the overall process:

- The volume of the scanned parts can be obtained automatically with repeatability and reduced user error;
- The processing time is below the time needed to do the operation manually, up to 6 minutes compared to 15 to 20 minutes manually;
- Generates information about the surface of the cavities;

During the development of this script some challenges were faced, namely:

- The alignment process of the parts. It is important for the parts to be aligned properly to achieve a valid volume value. There are situations where the base is planar and others where it is conic. When the base is planar, the normal of the plane of the base part of the mould must face the same direction as the base plane in the half part of the mould. The correct alignment pairs must be used;

- Trimming the meshes correctly to obtain the region of interest. Trimming the meshes is necessary to obtain the regions of interest. As such, features are used as references for the trimming;
- Trimming while accounting for variation of the geometry. The interface of the moulds can vary. As such, conditions for different variations are set in place, namely for conic and planar interfaces between the bottle halves and the bottle bottom moulds;
- How to properly treat the points. This issue relates more to the planning of the whole task structure on how it should be done to minimize error and produce a reliable dataset. It was possible to overcome this obstacle through the process described above for point treatment.
- The creation of the top plane is difficult because the area selected in the CAD program for the definition of this feature will be used for its creation in the STL model. This means that if the CAD model is simplified with a straight plane extending from the front face to the back face, the same area will be selected on the STL, which will have the refrigeration markings and the valleys/castles selected to count for the plane creation. This will lead to an unfaithful definition of the plane. To solve this issue, an accurate CAD model, representing the real mould models should be made available. Currently, another solution was developed by prompting the user to define the top plane through the selection of triangles on the STL and generate this plane via a best fit algorithm;
- Feature creation: The presence of outliers or ghost surfaces in the valid surfaces used for the feature creation will lead to the incorrect creation of these features. To solve this problem, the correct scanning of the surface must be ensured. It is also necessary to have an accurate representative CAD model for correct feature creation.

4. Validation and results

This chapter is where the case studies to determine the viability of the light systems will be explored. The simplified flow of the study process can be seen in Figure 47. The goal will be to study the ability to acquire the surface and to be able to produce comparative studies. It will begin with the analysis of the surface acquisition of the used cast iron moulds and the scanning of unpolished bronze moulds. This will allow to verify the systems' ability to acquire reflective surfaces and the ability to obtain the volume of the mould sets. Next, a study of the difference between the unpolished and polished condition is done. This has the objective of checking if the light systems were able to fulfil the customer need to identify differences between the polishing stages. Following, the results from the technology validation are analysed in terms of surface acquisition ability and measurement using a standardized ring gauge and a bronze mould. In the end of the chapter, conclusions from the tests are drawn and a comparison between both light systems is presented.

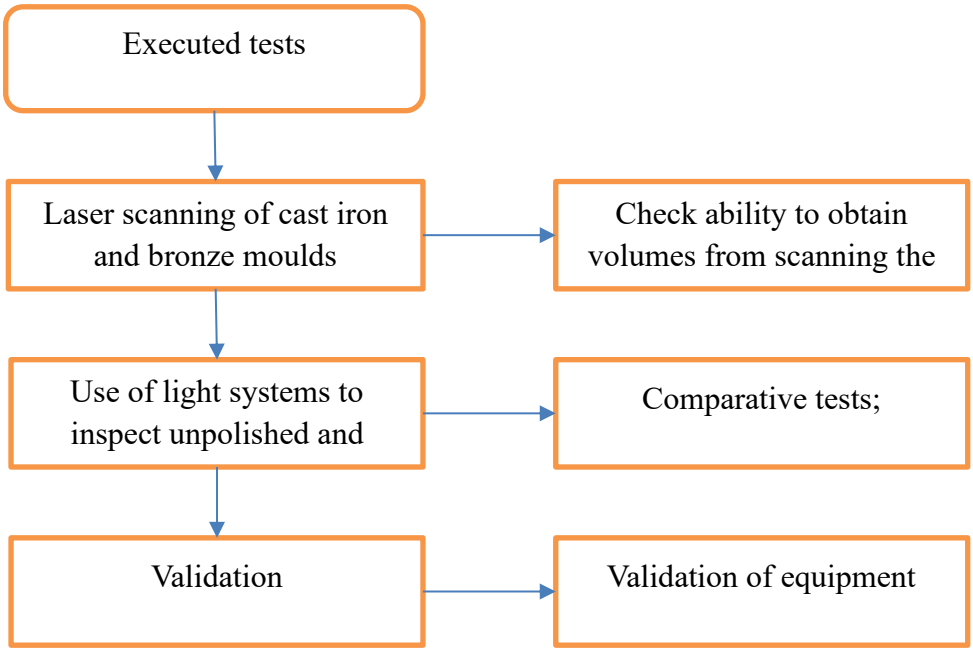

Figure 47 - Overall test methodology

4.1.Surface acquisition of moulds using light systems

To begin testing the data acquisition ability of the equipment and figure further concerns, constraints and needs, sets of moulds were requested from Intermolde. The goal was to scan these moulds, analyse their volume from the scanning and compare them to the volume obtained from Intermolde's water testing procedure. These water tests are used as the ground

truth for this study. The scanning of different material types using different light systems will allow the verification of the ability for surface acquisition and thus the viability of using these systems for the desired application. This study will begin with the analysis of the scanning of cast iron moulds using a laser scanner, then the scanning of an unpolished set of bronze moulds using a laser scanner and an SLS.

4.1.1. Cast iron mould surface acquisition using laser scanner

Three sets of cast iron moulds were obtained from Intermolde, as shown in Figure 48. To prove the ability of using a light system for the volume acquisition and due to industrial time constraints, the FARO blue laser scanner attached to the FARO Quantum M arm is used. The scanning of the mould halves does not require any sort of fixture, unlike the bottom where the assembled fixture can be seen in Figure 48 b). This way, the cylindrical area can be accessed more easily by the laser scanner. Since the surface that will be scanned is not very detailed, a point spacing of 0.15 mm and an edge length of 1.5 mm are used. This allows the correct definition of the surface while maintaining the file size at a reasonable size. This is because the point spacing is more related to the resolution of the scan and responsible for capturing detail. Geomagic Control is used as the scanning software to produce the point clouds and manipulate the resulting meshes. A schematic of the procedure for this study can be seen in Figure 49

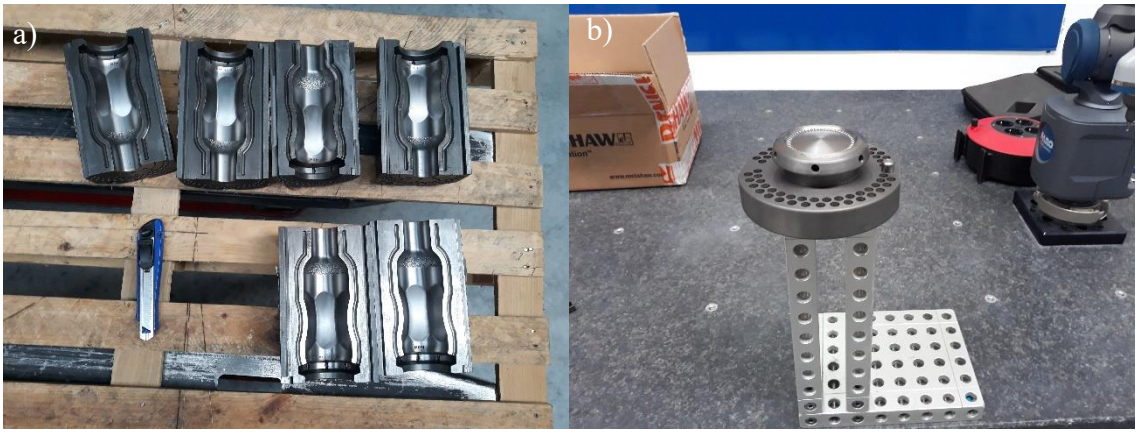

Figure 48 – Set of cast iron moulds: a) Cast iron mould halves; b) Cast iron mould bottom

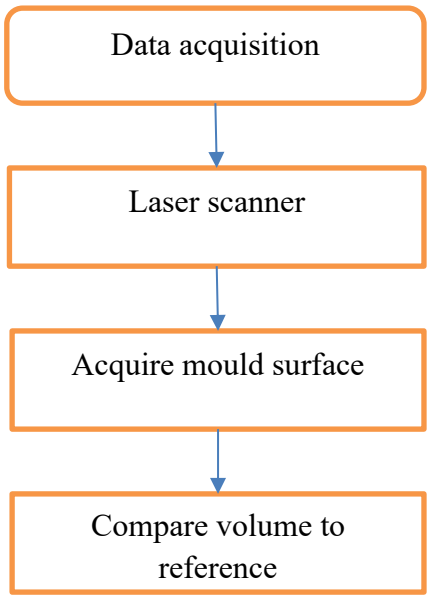

Figure 49 - Diagram for the cast iron mould acquisition test

The scanning is done considering the angular position of the scanner to acquire the highest number of points, while also decreasing the appearance of outliers. During the scanning, some areas proved more problematic due to the reflectivity of the surface, namely in the shoulder area, near the bottleneck and the engravings on the bottom mould. From these scans it can also be seen that the surface itself is well-defined and overall smooth. The production of outliers in the regions of interest was negligible, which further aids for a well-defined surface production.

With the scans, the volume assessment script is executed to obtain the volume for each set of moulds. During this step, some adjustments had to be done to the script to ensure that the calculation of the volume is correct. The most critical feature definition is the top plane, due to a slight curve existing on the top surface of the female half of the mould. This, of course, means that the whole top surface should not be considered for a definition of a plane as it will result from the average height of the set of points and lead to a shorter volume, especially in larger moulds where this effect is highly noticeable. To mitigate this effect, the points being selected to generate the plane should be in the extremities of the curve. Another factor that contributes to the volume calculation accuracy is the weight of each feature pair which itself can lead to inaccurate results. The feature pairs used in this case, in order of weight, were a top plane pair, a bottom plane pair and an axis pair. The top plane pair is the one with the most weight because it will be responsible for a higher volume deviation and to emulate the real-life condition of the closing of the mould. With the alignment processed, the STLs can be merged to produce a closed bottle model, and thus obtain its volume.

The surface acquisition of the cast iron moulds resulted in a well-defined STL without noticeable outliers. In Figure 50, it can be seen that the markings are also obtained with good definition. Given this was the first attempt at acquiring the data from a mould using a light system, some challenges arose due to the definition of features and alignment pairs. For better visualization, a diagram of the plane names used is shown in Figure 51. The first set of results is shown in Table 5. The differences between the calculated values and the water test volumes was due to larger weights attributed to the back-plane pair of the mould instead of the top plane. By correcting the priority of alignment pairs, the volumes tended to resemble more closely to the ground truth, as shown in Table 6. This will be related to the top plane covering a larger area and thus be more in control of volume deviations. With this correction, the deviations between the Intermolde's volume values and the ones obtained with the laser scanner are much closer, being inside, in this case, their own rate of repeatability of 0.15 cm^3. It must also be noted that the values themselves are in the same order from lowest to highest volume. This promotes the viability of the laser scanner for these applications.

This first case shows the importance of setting the correct priority for the alignment pairs for volume acquisition and the laser scanner's ability to deliver a well-defined surface with similar volume results as the ground truth. It also highlights the laser's ability to achieve a calculated volume of similar range as to the reference test. This study shows the viability of using light systems for the volume acquisition of cast iron moulds.

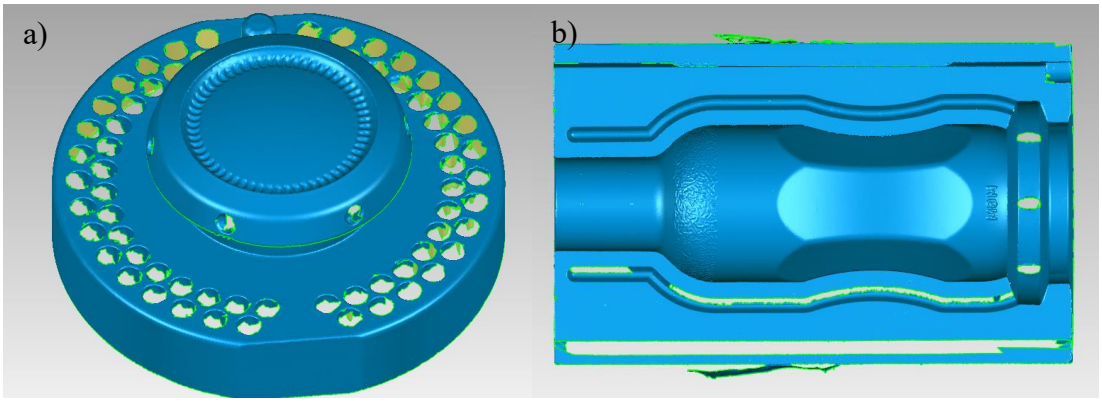

Figure 50 - Cast iron mould STL obtained from laser scanning: a) Mould bottom; b) Mould half

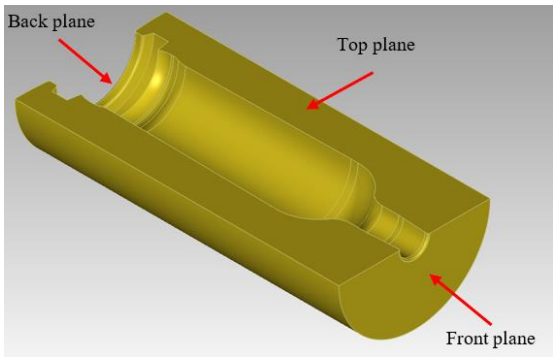

Figure 51 - Plane nomenclature for the moulds

Table 5 – Initial volumes obtained from laser scanning and water testing of the initial cast iron moulds

	Water tests volume [cm^3]	Laser volume [cm^3]	Deviation [cm^3]
Cav 7	375,71	374,84	0,87
Cav 12	375,46	374,83	0,63
Cav 14	375,23	374,97	0,26

Table 6 - Corrected volume values

	Water tests volume [cm^3]	Laser volume [cm^3]	Deviation [cm^3]
Cav 7	375,71	375,82	0,11
Cav 12	375,46	375,44	0,02
Cav 14	375,23	375,28	0,05

4.1.2. Acquisition of unpolished bronze moulds using laser and structured light

For the next study, using the unpolished bronze moulds shown in Figure 52, the ability of the light systems to acquire the desired surfaces and their respective volume is tested. A schematic for how this test will be done can be seen in Figure 53. It will involve the use of a laser scanner and an SLS for the surface acquisition of the moulds to then compare these results. Unfortunately, only an unpolished version of the bronze moulds was available for the study. Despite not being able to test in the least favourable condition, with polished bronze moulds, the test will still allow to see if the light systems are limited in the acquisition of this type of material.

Figure 52 - Unpolished bronze mould set

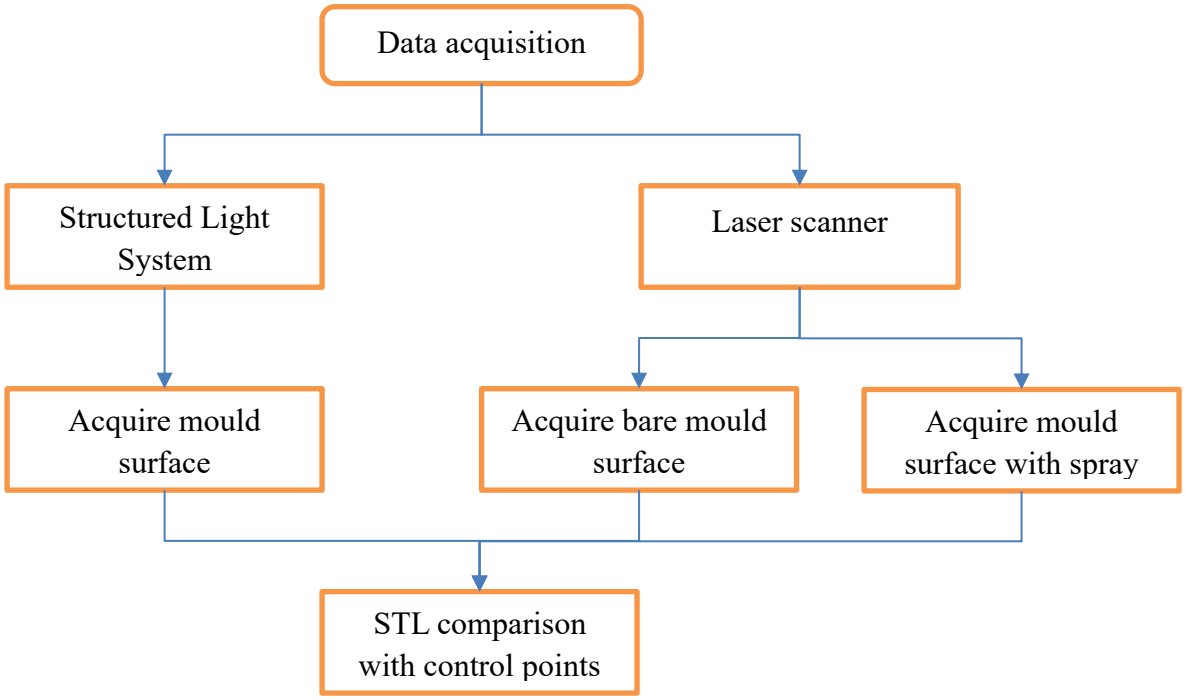

Figure 53 - Test plan for the scanning of the unpolished bronze moulds

The scanned moulds were for bottles with a nominal volume of 330 cm^3. The water test results were not shared and as such, in terms of comparison, it is only possible to use this nominal value as the reference value. Just like in the previous case, the FARO blue scanner is used with a point spacing of 0.15 mm and an edge length of 1.5 mm for the laser scanning. Now, an SLS will also be used to compare the surface acquisition of both systems in terms of the surface itself and the volumes obtained from their acquisition. For the SLS, the main parameters to account for are:

- The exposure, to guarantee the camera's pixels are not in overexposure nor in underexposure. With the current system, checking and adjusting the exposure is necessary;
- The orientation of the part will also influence the scanning if the pixels become out of adequate scanning range, due to reflections;
- External lighting can influence the camera's exposure and the acquired data. For this reason, the system must be used in a dark room.

In Table 7, the values obtained from the light systems and their respective deviation to the nominal value are presented. The laser scanner presents values in a closer range to the nominal value; however, it would be necessary to have access to the water test results to retrieve the most correct conclusions. In this case, the focus will be the difference in obtained volumes from both systems and their ability to acquire the surface.

Table 7 - Volumes obtained from the bronze mould scanning using the light systems

	Laser		**Laser with spray**		**SLS**	
	Volume [cm^3]	Deviation [cm^3]	Volume [cm^3]	Deviation [cm^3]	Volume [cm^3]	Deviation [cm^3]
Cav 11	330,57	0,57	330,42	0,42	329,11	0,89
Cav 24	330,50	0,50	330,48	0,48	329,10	0,90

The used SLS struggled with producing a valid surface of the mould, leaving several holes in the region of interest. When scanning with this system, these bronze moulds required a thin layer of white coating to obtain a complete surface. This, however, was not the case for the laser scanner. The laser scanner was able to properly obtain the surfaces without the use of spray. Nevertheless, outliers were still produced, such as small clusters near the edges. For this reason, the difference in the volumes from both systems can be explained by the application of coating to the mould in the SLS's case as it will decrease the obtainable volume by adding more material to the surface.

As an experiment, to inspect the influence on the coating to the laser scanning, a thin layer of coating was applied for another scan using the laser. The results of this experiment can be seen in the volume results shown in Table 7 and the differences between scans shown in Figure 54 and Figure 55. As expected, the surface acquisition was more complete, eliminating any noticeable outliers. The necessary scanning time also decreased by requiring fewer scans. The comparison between the point clouds of these scans can be seen in Figure 54. In Figure 55 b) the improved detail acquisition of the engraving of the bottle symbol can

be seen, as well as an overall cleaner surface definition compared to Figure 55 a). The volume values are similar, which can be explained by having applied a thin coat and the laser's inaccuracy being in the same range as the thickness of this coating.

These tests confirm that light systems can acquire the surfaces of materials used for bottle moulds. The need to align the parts of the mould set properly to obtain the volume is also highlighted. The next step of the studies will be the analysis of the difference between polishing stages. This will be done by scanning sets of unpolished moulds and then scanning again the same sets after polishing.

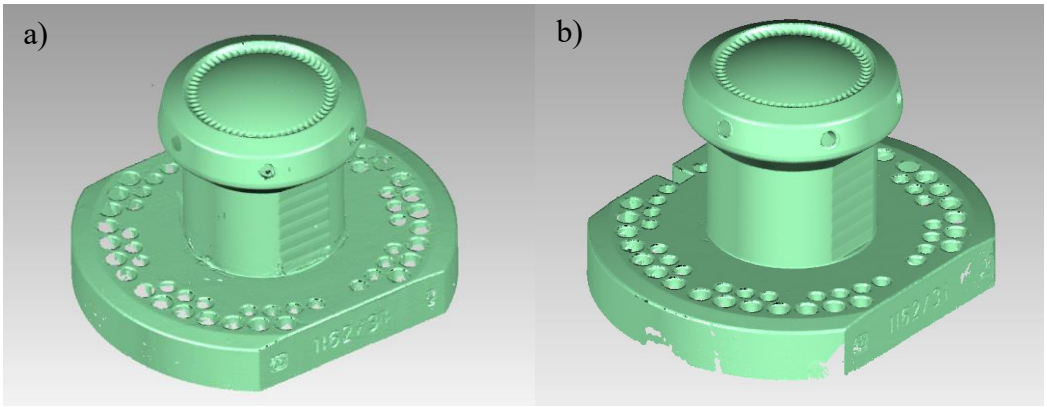

Figure 54 - Point clouds of the bottom mould part: a) Scan without spray; b) Scan with spray

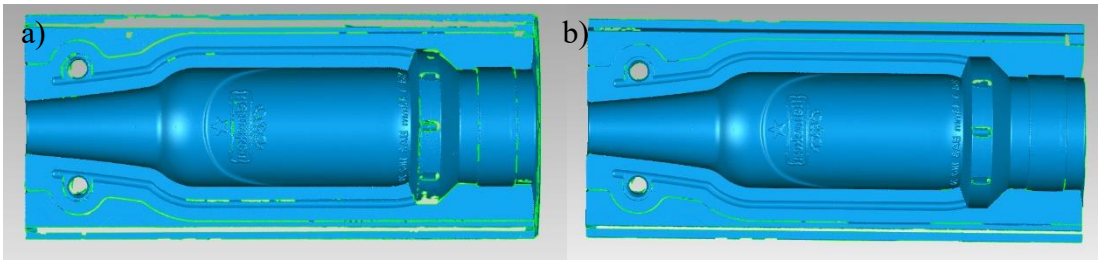

Figure 55 - STL of the mould halves: a) Without spray; b) With spray

4.2.Differences in the acquisition of unpolished and polished moulds

In this next case study, four sets of cast iron moulds will be inspected twice to test condition differences, once when they are unpolished and again after polishing. These studies will set constraints to the system and point to possible solutions, depending on the differences that will be seen from the polishing operation. The deviations of the surface, in the polished condition, could eventually be the result of the uncertainty of the equipment which would mean the solution would be better suited for volume acquisition than for defect inspection. It is important to validate the technology's accuracy and surface acquisition to be certain whether this is the case.

To execute this study, the FARO arm with the FARO blue scanner attached and the white light SLS from Open Technologies with a rotary table are used for the testing of both material conditions. By conducting the inspection with these systems, the main datapoints that will be retrieved are: the time for data acquisition, the ability to spot differences between the unpolished moulds and the polished moulds, the scanning ability of both light systems and the volume of the moulds.

4.2.1. Procedure

To begin this study, a procedure, shown in Figure 56 was developed to guide the process more clearly. The goal will be to study each equipment's performance in the scanning of these moulds.

Given that an important parameter of the laser scanner is the point spacing, four different spacings will be analysed: 0.40 mm, 0.25 mm, 0.15 mm and 0.05 mm. This will allow to check the effects this parameter will have on the resulting volume and the overall surface acquisition of the moulds. It is expected that the higher point spacings will result in a less detailed scan with a shorter file size. However, one must take notice to the fact that the moulds for glass bottles do not present very detailed geometry when compared to a plastic part. In terms of differences of the resulting volume, it is expected the difference to be negligible. The scanning of the moulds with each equipment shall also be timed to compare the acquisition time.

In the end, these tests will allow for comparative studies between the laser scanner and the SLS in terms of scanning ability, volume differences and acquisition time. Scanning ability will be classified on the overall acquired surface quality. The variation of this parameter is expected to be more noticeable when scanning the polished cast iron moulds due to a more reflective surface.

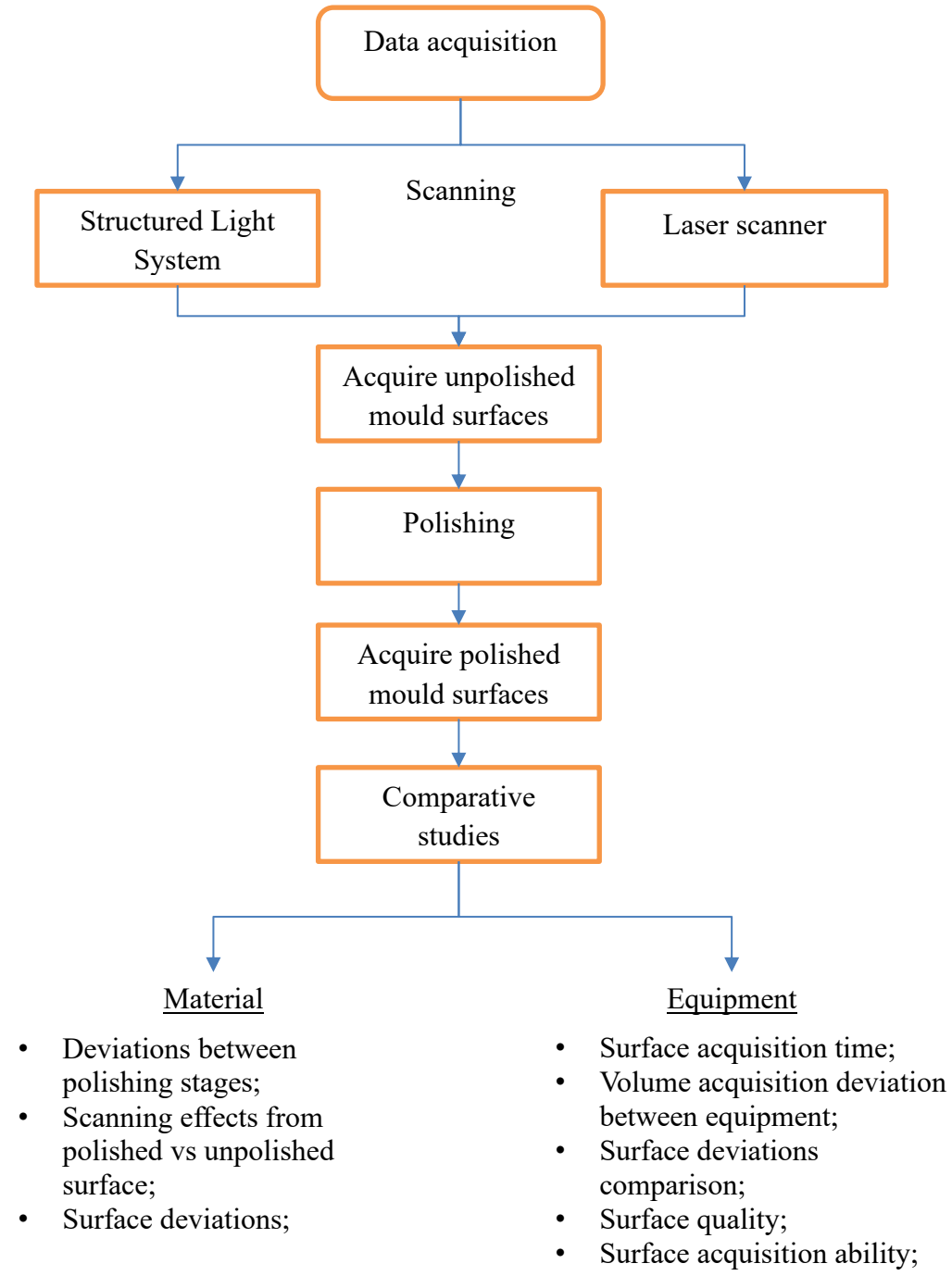

Figure 56 - Polished and unpolished scanning study flow chart

4.2.2. Unpolished moulds

This case study begins with the scanning of the unpolished moulds, Figure 57. For the first step, the moulds are scanned using the FARO laser scanner. During this stage, one of the four sets of cast iron moulds was selected for scanning and the point spacing test was done. This test is related to the difference between volume and surface acquisition when using different point spacings. It starts with a high point spacing, 0.4 mm, and then lower values, as low as 0.05 mm. In terms of acquisition time, the difference was negligible where

the scanning of the mould halves would take on average 1 minute 50 s, whereas the bottom would take around 2 minutes. However, the post-processing time was very noticeable being just seconds for the highest point spacing value and up to 10 minutes for the lowest one. By using the blue laser scanner, it was possible to obtain the full surface of the moulds without spray.

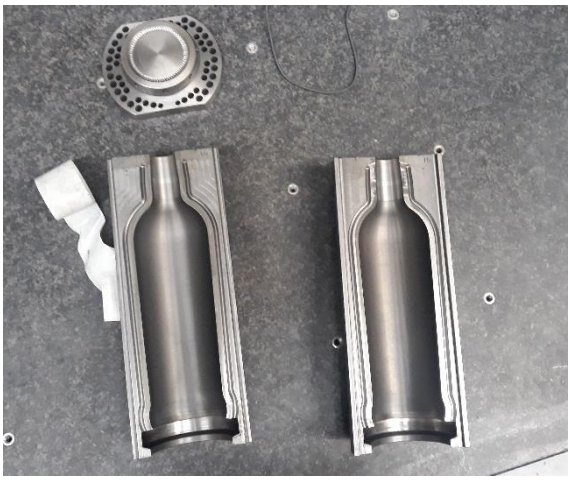

Figure 57 - Unpolished cast iron mould set

Next, the unpolished moulds are scanned using the SLS, as shown in Figure 58. During these scans, it was necessary to first find a proper positioning to acquire the surface in one go. Then, the adequate exposure to acquire the surface must be set. This step required varying the exposure values until a proper one could be found. Despite varying the exposure values and the part orientation, it was not possible to produce the whole surface, missing patches on account of the overexposure of the camera's pixels. As such, to be able to scan these moulds, a white matte coating had to be applied. This will allow the acquisition of the surface; however, it will decrease the possible obtainable volume by covering the moulding surface.

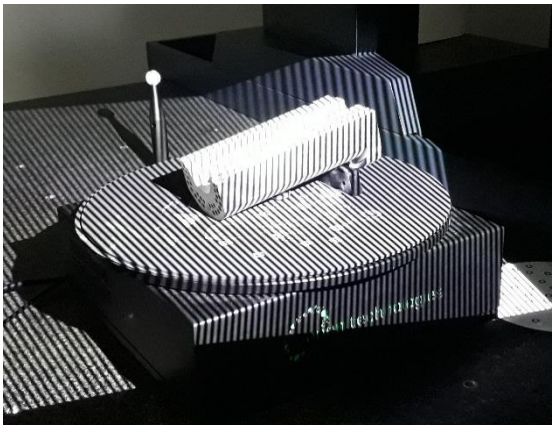

Figure 58 - Unpolished cast iron mould being scanned by structured light

4.2.3. Polished moulds

For this test, the same set of moulds was used, after a polishing operation done by Intermolde. After polishing, the surfaces are, once again, acquired. The moulds, shown in Figure 59, are now more reflective. It is expected that the resulting scans show that there are, indeed, differences between the polishing phases.

Figure 59 - Polished cast iron moulds

Just as before, the moulds' surfaces are acquired using the blue laser scanner. The surface acquisition of these moulds was more challenging, requiring more scans to obtain the surface. This is due to the reflectivity increasing the difficulty of point cloud capture. In the regions where there are holes in the mould, small clusters of outliers were also present. Despite these challenges, the surfaces were acquired successfully.

For the final step of this study, the moulds are scanned with the SLS, as seen in Figure 60. Just as what happened with the unpolished version of these cast iron moulds, this system was unable of acquiring the surface without any matte coating. After covering the moulds with a thin layer of white powder, their scanning became possible and the surface was acquirable.

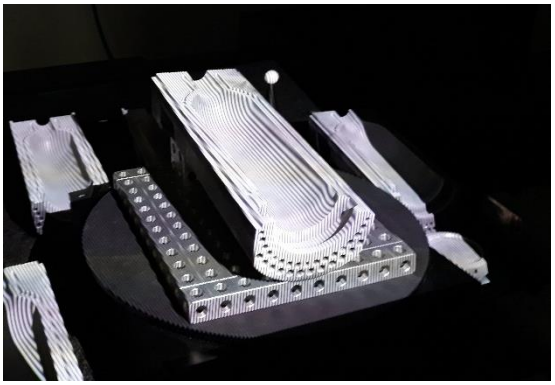

Figure 60 - Polished cast iron mould being scanned by structured light

4.2.4. Results

The ability to inspect the differences between polishing phases is an important factor for this project as it requires the systems to acquire the surfaces in a more reflective state. The results to discuss, in this section, will be in terms of both conditions: unpolished and polished. Firstly, the surface acquisition performance will be discussed and then the volume values and their differences are analysed.

The surface acquisition of the unpolished moulds with the laser scanner was done without any problems. It required up to 10 scans to obtain the whole surface of each mould part, taking up to 6 minutes for the scanning of the set. The obtained point clouds were well defined and did not present any outliers. However, when using the SLS, despite the number of scans and time to scan being similar, the surface had missing information and some outliers. This made the acquired STL unsuitable to be used for inspection and volume calculation. For this reason, it was necessary to apply a thin coat. As was seen before, this will lead to a lower volume value, however, with the unpolished mould requiring spray, the polished moulds will as well. Nevertheless, the focus in this case will mainly be in terms of differences between the polishing phases, so the deviation between volumes for the unpolished and polished mould will be the key analysis point rather than the absolute values of both.

As for the scanning of the polished moulds, the laser scanner still performed well to obtain the surface of the mould parts, requiring 16 scans and around 8 minutes for each mould set. This increase in time and number of scans is explained by the more reflective surface causing more limitations in the amount of information retrieved from the scanner. Nonetheless, the appearance of outliers was still negligible. With the scanner, by having done both conditions without spray, it is possible to compare the absolute values to the ground truth. Next, the moulds must have a coating applied to them to decrease the reflection and make it possible to be scanned by the SLS. With the coating, the surfaces were acquired with success and took 8 scans and 2 minutes to produce the entire surface of each mould part.

From the point spacing test, it was seen that the obtained volumes were similar as seen in Table 8. This shows that the selected point spacing does not necessarily affect the resulting volume of the moulds. Rather, it is responsible for the detail obtained from the scan, which means markings and other detailed geometry would be better defined at a lower point

spacing. The selected value should allow to obtain enough detail without overloading the file and taking too much time in the post-processing.

Table 8 - Results from the point spacing test

Point Spacing [mm]	Volume [cm^3]
0.4	1174,87
0.25	1174,84
0.15	1174,84
0.05	1174,80
Standard Deviation	0,0287

Regarding the differences found in the surface between the unpolished and the polished moulds, to have an idea of the effects the polishing has, surface comparisons are done. To represent the differences more accurately, the unpolished version of the mould part is used as the reference part to which the comparison will be made. This will show, clearly, the areas that were polished which can help ascertain any abnormality done during this process. By being able to distinguish the differences between the unpolished and the polished mould part, the polishing process can be studied and its consistency improved.

Both light systems were able to obtain credible surface comparison results, the surfaces of the polished mould had noticeable material removal. In Figure 61 and Figure 62 the comparisons made between the mould parts of the cavity 16 mould retrieved by the laser and the SLS, respectively, are shown. From these comparisons, for both light systems the areas that indicate loss of material are in accordance to each other. This also highlights the areas that were polished, namely the middle section of the mould surface, where the middle of the bottle would be shaped, in the transition zone to the bottleneck and at the end of this middle section. In the bottom mould part, the polishing was light, not having much material removed. The scanning defects on the surface can also be seen, which are noticeable on the SLS's case due to possible point cloud overlap errors and more spray in a given area. From these results, it is shown that light systems are able to distinguish the surface deviations when a mould has been polished. This means the system can be used not only for regular mould inspection but also to study the differences in polishing, which can aid the polishing process to become more consistent and predictable. It is also a path to improving the production process by knowing how the wear of the mould will progress with its use.

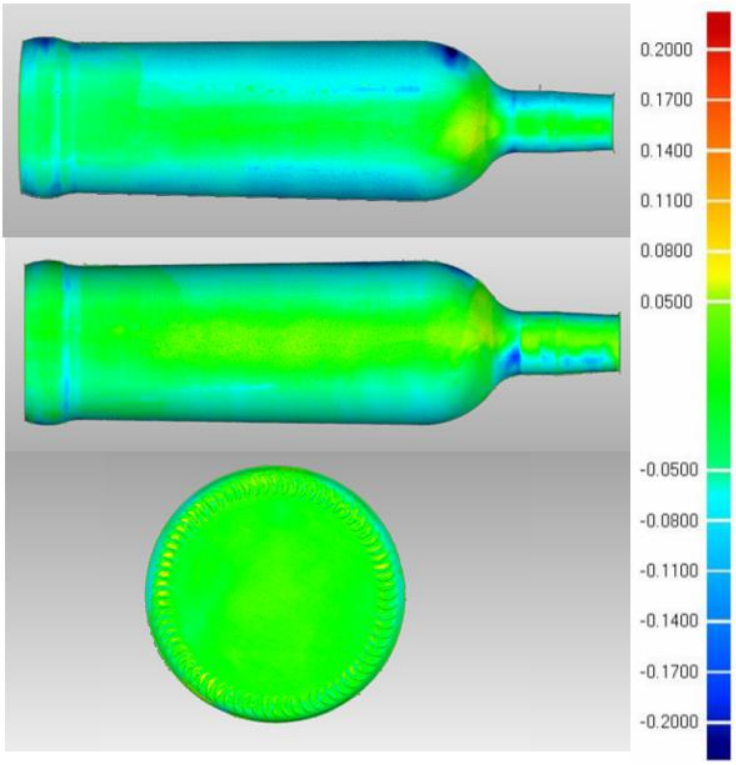

Figure 61 - Surface comparisons of mould cavity 16 from the laser scans

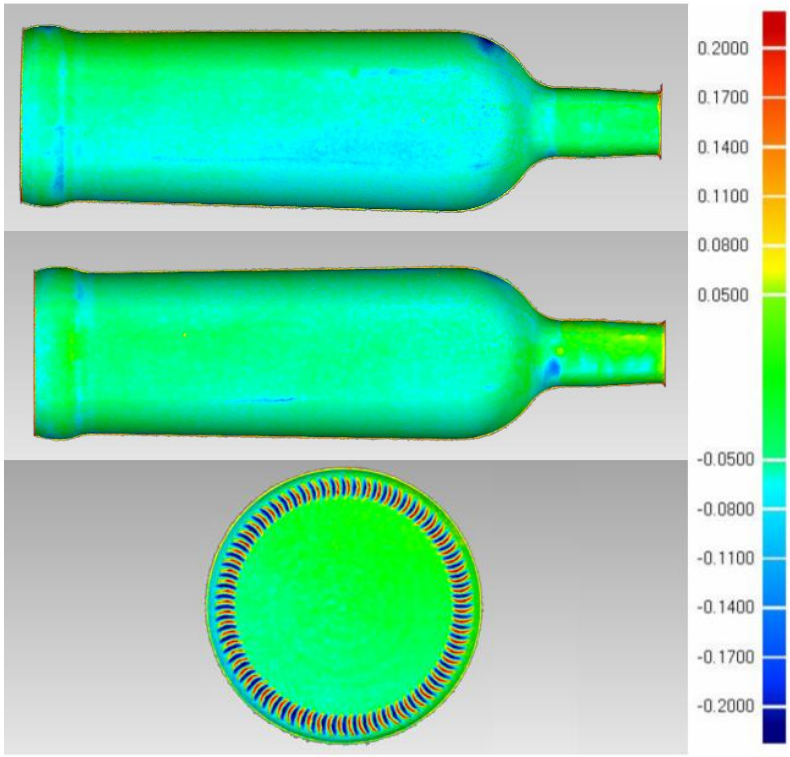

Figure 62 - Surface comparisons of mould cavity 16 from the SLS scans

Finally, the volumes obtained with both systems and between polishing conditions will be analysed. First the absolute values will be discussed, following with the deviations between the unpolished and polished condition, shown in Table 9 and Table 10, respectively.

In the case of the laser scanning, the absolute values are somewhat similar, the greatest difference showing up in the case of the mould from the cavity 16 in the unpolished condition with a difference of 0.42 cm^3 when compared with the tests done by Intermolde. This difference can be explained by incorrect feature creation which can indicate an area to have been incorrectly acquired. As for the remaining values, in the case of the polished condition, they are in overall accordance with the results obtained from the water tests. This does not occur for the SLS though. The absolute values for these moulds was much lower than the ones obtained from the water tests, with a difference of around 2.50 cm^3. One of the reasons behind this will be due to the application of coating to the mould, where it would be more concentrated in the moulding surface, thus reducing drastically the volume, given it is a much larger volume than the bronze ones. Another reason is the fact that the amount of information captured by the system resulted in a very rounded STL, which means the edges would be more curved and simplified, introducing more error into the results.

In the case of the volume deviations, the laser scanner performed similarly to the water tests, with the case of the mould of cavity 16 being the one which most deviated due to the reasons stated before. However, in the SLS's case, these deviated more, with the cavity 1 mould being the closest one to the reference value. As for possible reasons, the amount of coating applied could be different as well as due to the inaccuracy of the system itself.

From this study, the performance of the used equipment is shown. The study allowed to obtain several comparison terms, such as surface acquisition performance, volume deviations and time to compare between the equipment. This test confirms the viability of using a laser system with the purpose of obtaining proper comparative results. As for the SLS, the one which was used performed poorly, failing at surface acquisition. Nevertheless, the technology is quite automatable.

Table 9 - Volumes obtained from each method in the unpolished and polished condition

	Water tests volume [cm^3]		**Laser volume [cm^3]**		**SLS volume [cm^3]**	
	Unpolished	Polished	Unpolished	Polished	Unpolished	Polished
Cav 1	1174,81	1176,53	1174,70	1176,41	1172,48	1174,25
Cav 15	1174,98	1175,81	1174,87	1175,87	1172,91	1174,57
Cav 16	1175,26	1176,50	1174,84	1176,59	1172,49	1174,40
Cav 17	1174,80	1176,43	1174,86	1176,29	1172,72	1174,71

Table 10 - Volume deviation between the unpolished and polished condition from each method

	ΔWater tests volume [cm³]	ΔLaser volume [cm³]	ΔSLS volume [cm³]
Cav 1	1,72	1,71	1,77
Cav 15	0,83	1,00	1,66
Cav 16	1,27	1,75	1,91
Cav 17	1,63	1,43	1,99

4.3. Validation of equipment – Ring gauge and bronze mould

The validation of the used technologies is a necessary step to guarantee the validity of the results and if the technology itself is capable of being used for the desired application. To compare and validate the laser scanner and the structured light system, it is necessary to compare both to a ground truth. A CMM measurement will be used as the reference to then compare the technologies and verify if there is validation in the results achieved by either. For this reason, this case study will be dedicated to the validation of the technologies by using a ring gauge and a bronze mould.

4.3.1. Validation using ring gauge

This study should be done based on Intermolde's moulds, however, due to industrial constraints, it was not possible to obtain further sets of moulds to validate the technologies. As such, an alternate solution was found by using a standardized part, a 50 mm diameter ring gauge, shown in Figure 63. Since it is a standardized part and used for calibrations, its inner diameter will have a high level of precision, allowing the inspection of the differences of the technologies to the micrometer range. This feature is useful to quantify more clearly the possible deviations that can be encountered during the actual application of the mould scanning. The ring is also as shiny as the cast iron moulds from Intermolde, which is a favourable characteristic for this test because it can further emulate the actual application of scanning a polished cast iron mould. There are three main steps in this test and as such a test plan, shown in Figure 64, was developed to execute it accordingly and obtain the necessary data.

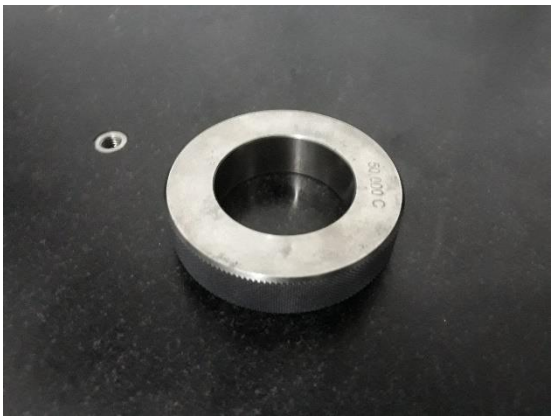

Figure 63 – Ring gauge

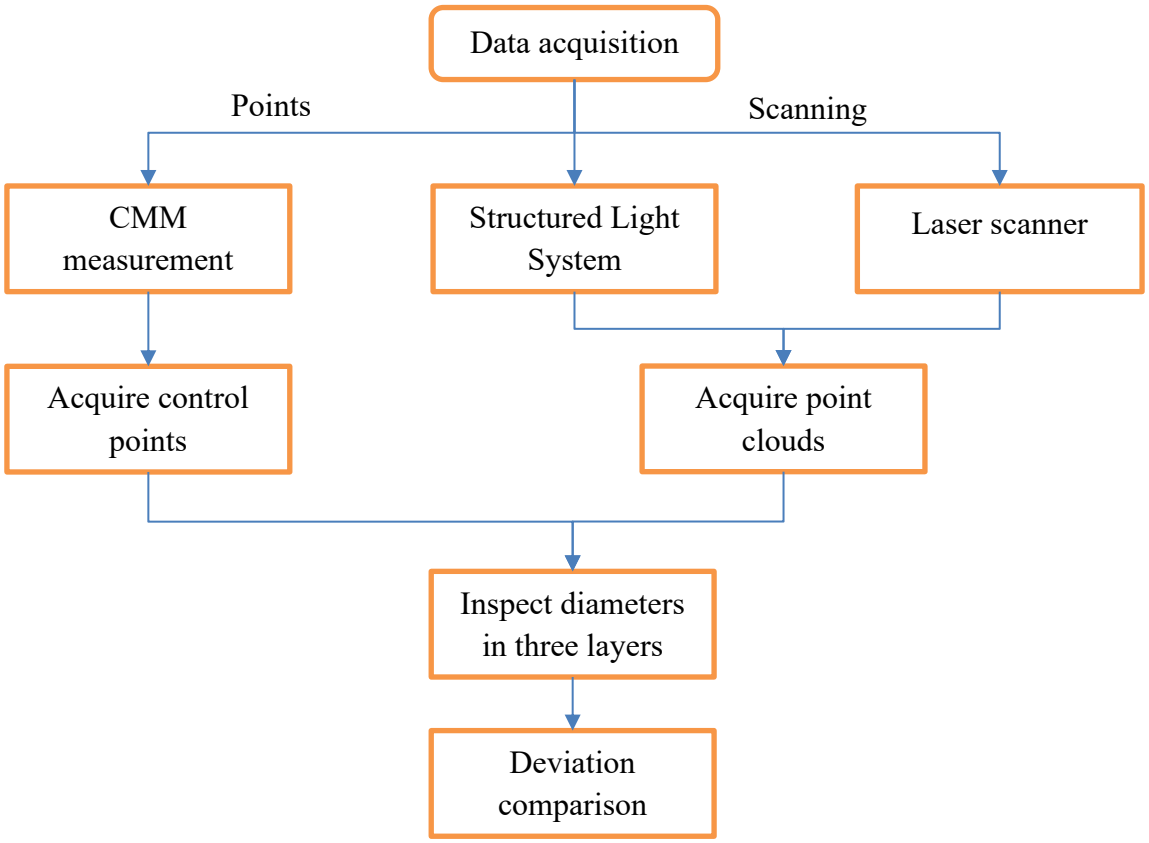

Figure 64 - Flow diagram for the validation test

To perform this study, the X-Orbit 55-7 CMM, the FARO blue laser scanner and the Cronos 3D Dual SLS are used. Fixing blocks are employed to fix the ring gauge and position it for adequate surface acquisition. Since the internal diameter is a known parameter, 50 mm, the surface acquisition will focus on this feature for further inspection.

Firstly, the ring is inspected by the CMM. Here, since the goal is to check the diameter along the internal cylinder, a series of points will be inspected at different heights to check this parameter. To use the CMM for this purpose, an alignment of the part is defined, picking the top plane and the internal cylinder's axis as the reference features for the coordinate

system of the part. Next, once the alignment is done, ten points around the cylinder are inspected by using a 2 mm diameter probe with a length of 30 mm before moving to a new height. The heights used were -3 mm, -5 mm and -10 mm in relation to the top plane. In total, 30 points were inspected, allowing to properly define the internal cylinder while also obtaining data to compare the diameters at these different heights. In Figure 65, a schematic of the inspected points using the CMM is shown.

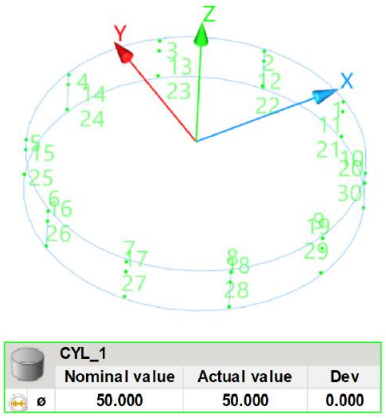

Figure 65 - Results from the CMM measurement

Next, the ring was scanned using the FARO blue laser scanner. A point spacing of 0.15 mm was chosen as this part does not have any detail in the regions of interest. Only 8 clouds were necessary to acquire the ring's surface. The obtained STL can be seen in Figure 66 a). With the surface obtained, sections can be taken according to the heights that were used during the CMM inspection to then inspect the inner diameter for comparison.

Finally, the SLS is used to inspect the ring gauge. This was the area where the most challenges were found. In the first attempt of the scan, due to the shininess of the ring, the obtained surface was poorly defined due to the overexposure of the camera. This resulted in some areas not having points and in the production of outliers. Despite varying the exposure level, the surface was always poorly defined. For this reason, to produce a good surface, the ring's surface was covered in a thin layer of white powder. After this step, it was still necessary to adjust the exposure level to obtain point clouds with as many valid points and as much of the surface as possible. With this, an STL of the part is obtained, shown in Figure 66 b), where the same process of inspecting the diameter is done to then compare the results.

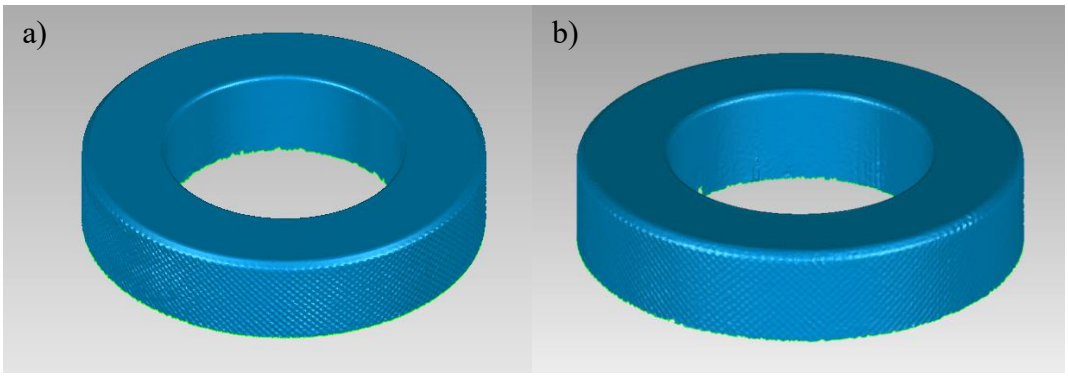

Figure 66 – Ring gauge STL mesh: a) Obtained from laser scanning; b) Obtained from SLS scanning

Having measured the diameters at three separate depths, these can be compared between the systems. Table 11 shows the diameters for each depth and for each system, while also highlighting the deviation between the ring gauge's nominal diameter value of 50.000 mm and the actual value. These diameters, in the case of the light systems will be dependent on the system's inherent inaccuracy and its ability to obtain the surface. With the CMM, the deviations are very low, up to only 0.001 mm, showing its high precision for the diameter inspection. However, moving onto the light systems, these show much higher deviations, with the laser having a deviation of up to 0.038 mm and the SLS of 0.057 mm. In the laser's case, these deviations can be attributed to the measurement uncertainty of the FARO arm, 0.03 mm, and to the reflective nature of the surface, making it a challenging surface to acquire. As for the SLS, it required spray once more, due to the reflectivity of the part. By applying spray, the surface will have an extra layer which will also decrease the possible diameter from the scanning, this explains the higher deviation from this light system.

This test shows some of the limitations when acquiring shiny surfaces via light systems. Next, the scanning of a bronze mould is done for further validation results.

Table 11 - Comparison of the ring gauge inspection

	CMM		**Laser**		**SLS**	
Depth [mm]	Diameter [mm]	Deviation [mm]	Diameter [mm]	Deviation [mm]	Diameter [mm]	Deviation [mm]
-3	50,001	0,001	49,966	0,034	49,943	0,057
-5	50,001	0,001	49,969	0,031	49,948	0,052
-10	50,000	0,000	49,962	0,038	49,951	0,049

4.3.2. Bronze mould acquisition

Due to a lack of suitable samples, a demo mould, shown in Figure 67, is used for this test. This is a bronze demo mould, with similar geometry to the moulds used by Intermolde.

However, this mould does not have any available CAD model, requiring RE to obtain it. This step can, however, lead to unreliable deviations from the systems due to simplifications during the process, such as surface adjustment which can involve the flattening of some surfaces or disrespecting the curves of others. For this reason, to make a more accurate comparison, the deviations obtained using the light systems will be compared to each other, using the CMM as the reference.

Figure 67 - Demo bronze mould

This case will involve the scanning of the mould with the laser scanner and the SLS to then produce a CAD model. With the CAD obtained from the RE, control points can be defined for the CMM inspection. After the CMM measurement, the deviations and the coordinates of the measured points are exported and are used for the light systems' comparisons. The coordinates are used to inspect the very same points in the model and thus enable the deviation comparison. In Figure 68, a flow chart for this procedure is shown.

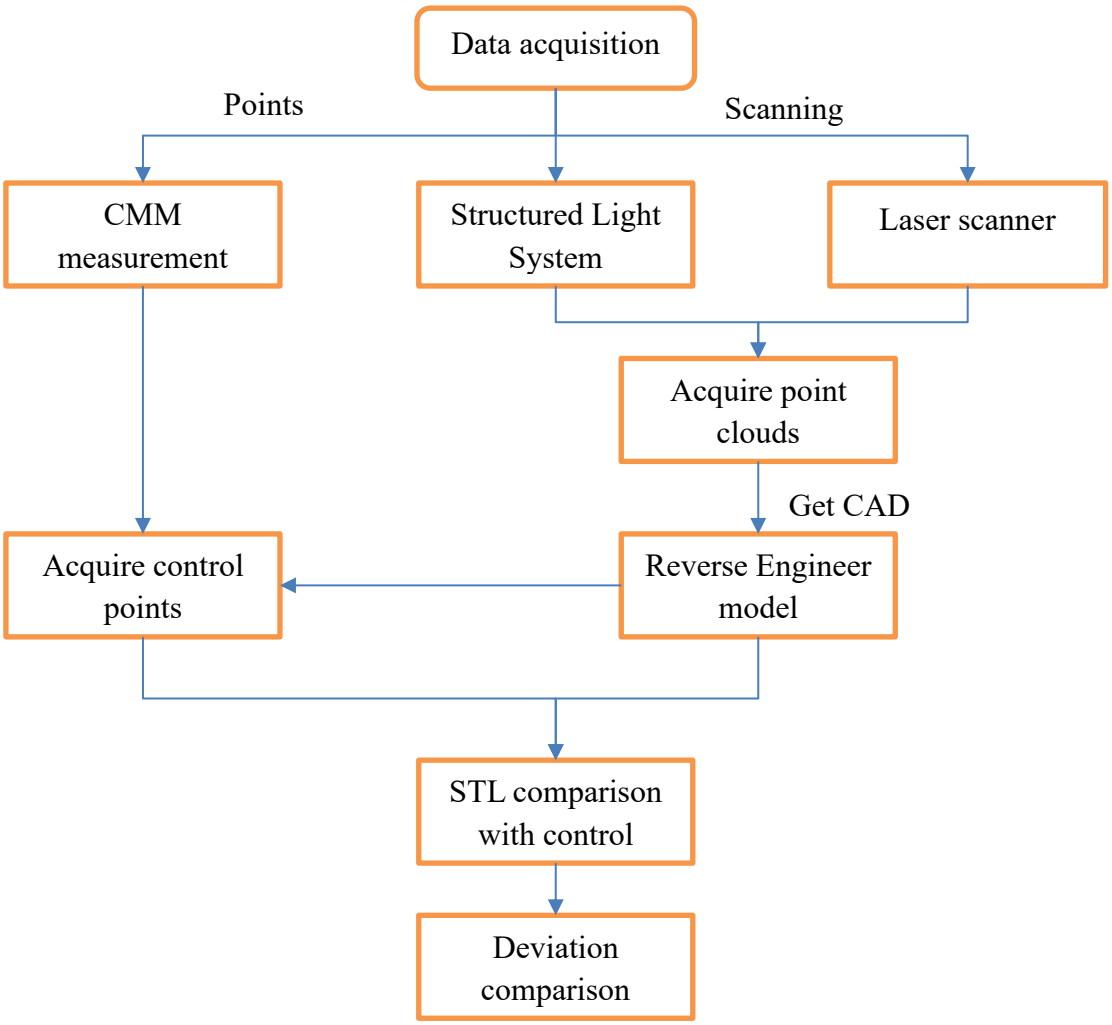

Figure 68 - Flow chart of the case study procedure

Firstly, a virtual model of the mould must be acquired before doing the CMM measurement. As such, the mould is scanned using the FARO arm blue laser scanner and then again using the SLS. Since this part does not have too much detail, the laser scanning was done with a 0.15 mm point spacing. The surface of the mould was successfully acquired with 6 clouds and without noticeable outliers present on the surface. Next, the mould is scanned using the SLS as seen in Figure 69. For this system, the initial attempt resulted in a poorly defined surface with missing areas and with overall poor surface quality. This was due to the mould still having too much glare, resulting in the overexposure of the moulding surface in the areas closer to the edges of the top plane. Reducing the exposure of the camera resulted in areas such as the top plane, the back plane and areas in the moulding surface to become underexposed. Anti-glare spray was used to apply a thin coat to allow the proper scanning of this part. This way, it was possible to obtain the whole surface of the mould.

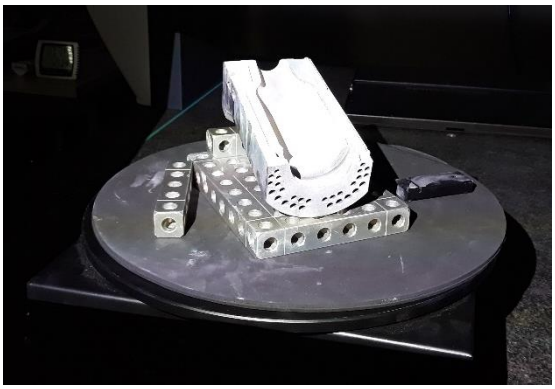

Figure 69 - Bronze mould being scanned by structured light

With the scan model, it becomes possible to move onto obtaining the CAD of this mould via RE and conduct the CMM measurement. Due to the application of spray in the SLS scanning, the reverse engineering was done using the model obtained from the laser scanning, because the spray will lead to further inaccuracies in the reconstruction of the surface. For the CMM inspection, the mould part is fixed on the CMM as shown in Figure 70. Next, inspection points are defined, as well as the strategy to measure them. During this procedure, a 2 mm diameter probe with a 30 mm extension was used, allowing for good retrieval of data in terms of precision and depth. By measuring the given inspection points, the deviations from the model and the coordinates of these points are exported to later be used for the analysis of the scan data.

Figure 70 - Mould fixed on the CMM

To make the comparison between the SLS and the laser, the Mean Absolute Error (MAE) is used which is defined by Equation 4, where y_i represents the reference value, x_i the actual value and n the number of datapoints in use. This will help quantify more clearly the validity of the systems. The deviations of the CMM will be used as the reference value, while the deviations obtained by the light systems will be considered the actual value for each case. The results of this measurement can be seen in Table 12. These results show that the laser

scanner finds itself within the claimed uncertainty, even for more reflective surfaces. Whereas in the SLS's case, despite presenting an uncertainty within its specifications, the value is for a matte coated surface. Which means it was not possible to verify the effects of a reflective surface scan on the uncertainty of this particular system.

$$MAE = \frac{\sum_{i=1}^{n} |y_i - x_i|}{n}$$ **Equation 4**

Table 12 - Mean Absolute Error for the light systems

Light system	MAE
Laser scanner	0,03552
SLS	0,04684

4.4. Study conclusions

These studies have demonstrated the abilities of light systems to acquire the moulding surfaces in different conditions and of different materials. With the equipment that was available, the laser scanner was the system which performed the best, being able to acquire the surfaces in all tests without having to apply a coating to the parts. It was also possible to obtain similar results to Intermolde's water tests and verify the differences between the polishing of the sets of cast iron moulds. The SLS, however, required coating in all the tests it was used. Due to using the spray, the volume values obtained from SLS were quite below the ones from the water tests. Nevertheless, the difference between unpolished and polished moulds was observable.

To explore the effects of a applying a matte coating when using the laser scanner, a thin coating was applied on the unpolished bronze moulds. From this test it was possible to conclude that a thin coating does not have a noticeable effect on the volume of the mould. Nevertheless, it improves the surface acquisition. The study of the effect of the point spacing in volume was also found to be negligible. Its effect is related to the amount of detail achieved in the point cloud. From the validation tests, the systems performed according to specification which demonstrates the viability of using light systems to solve the problem statement.

A comparison between the used laser scanner and the SLS is presented in Table 13. The data that was obtained during the case studies is used for this comparison. This table highlights the better performance of the FARO laser scanner compared to the Cronos Dual system. The time to scan for the laser can be up to 8 minutes when scanning a more reflective

surface, like the polished cast iron mould sets. The SLS, however only requires 6 minutes for this purpose. For the laser, this parameter can be dependent on the user's expertise at scanning, where the more experience the person operating the scanner, the better the acquisition of the point clouds and the quicker the part is scanned. For the SLS, the time is only dependent on the number of scans that will be done to acquire the surface. This SLS only performs better than the laser scanner in the number of scans necessary to generate the surface. It would be necessary to use a state-of-the-art SLS to truly compare both technologies in terms of their limitations to the desired application.

Table 13 - Comparison between the used systems

Parameter	FARO Laser Scanner	SLS Cronos Duo
Precision [mm]	0,03552	0,04684
Number of scans needed	Up to 10	8
Surface acquisition	Can scan polished cast iron moulds without spray	Needs spray for mould scanning
Comparative results	Able	Able
Time to scan a mould set	Up to 8 minutes	6 minutes

With these case studies, a benchmark table, in Table 14, is done to compare the technology of each light system, with the CMM as the baseline, where ↓ means worse in that parameter and ↑ means better. In this table it is important to consider the automatability, cost and ability to acquire the surface, which can change depending on the material's reflectivity for the light systems. The laser scanner and the SLS are considered to have a similar automatability, while being worse than the CMM. This is because the CMM has in place several automated mechanisms and several degrees of freedom, while these light systems would require the addition of more mechanisms to become automated for the requirements of this project. The CMM is the most precise and most able to acquire surfaces because as a contact method it is not dependent on other factors, such as reflectivity. Nevertheless, it is a slow process which will not allow to obtain proper comparative results and will be challenging to obtain the volume of the part. The light systems are, in fact, able to produce adequate comparative results, thus showing the deviations of the whole surface, and are quicker to obtain the data. The SLS is considered to be better in speed than the laser by requiring less movements and the speed of the full scan only being dependant on the number of point clouds that will be acquired. In terms of data capture, the SLS is more capable than the laser by having a broader field of view, while the laser requires more path planning to obtain the whole surface of the part. The SLS does have the disadvantage of requiring to be placed in a dark area to avoid the effect of exterior lighting on the results.

By adding the scores of the systems, the technology that would be best suited for the desired application would be the SLS. However, to be certain, tests using a state-of-the-art SLS should be done and to verify if it indeed matches the laser in terms of surface scanning and data acquisition.

Table 14 - Benchmark comparison between the equipment

Parameter	CMM	Laser Scanner	SLS
Precision		↓	↓
Speed		↑	↑↑
Surface acquisition		↓	↓
Automatable		↓	↓
Comparative results		↑	↑
Volume acquisition		↑↑	↑↑
Cost		↑↑	↑↑
Working conditions		=	↓
Data capture		↑	↑↑
Cost to automate		↓	↓
Final Score	0	3	4

A summary of the benefits and limitations of the product can now be done based on the results from the case studies and application of the scripts to these same case studies. Furthermore, a table summarising these characteristics is shown in Table 15. This product has several main benefits, such as:

- It has been shown through scripting, that the product is able to deliver both the volume and surface inspection automatically, which further allows to quantify part inspection;
- Based on the case study in 4.1.1, the automatic volume calculation falls inside the repeatability range of the reference values from the water tests;
- This product allows to trace the results obtained from the volume calculation and surface inspection, being able to show the client how the process was done and its results. It further associates these results to a given version;
- Despite the scanning times to obtain a mould set being somewhat high and the data processing time being around 7 minutes, this whole process is still faster than the conventional method while also delivering more data;
- The data obtained from this product can then be used to study the process and improve it. It should also be noted the possibility of integrating such system not only for mould inspection but also for part series inspection, like plastic parts.

Nevertheless, there are some drawbacks associated to this product:

- The sensitivity to the part geometry, where the CAD model must be an accurate representation of the real part for the volume assessment script to work properly;
- The initial investment will also be quite high due to requiring the acquisition of the software, light systems and their respective automation. An estimate between 75000 and 150000€ is believed to be accurate approximation of the cost of the final product;
- Finally, the whole process will generate large file sizes, requiring an adequate computer to be able to process the data.

Table 15 - Benefits and limitations of the project

Benefits	Limitations
Acquires volume and delivers surface inspection	Sensitive to part geometry
Applicable to part series inspection	Initial cost: 75 000 – 150 000€
Enables quantifiable part inspection	Generates large file sizes
Enables result tracing	Takes up to 7 minutes to process data
Achieves volume values in the repeatability range of the reference value	
Scanning and data processing time below the time needed through the conventional method	

Finally, a comparison between the conventional method and the one that has been developed can be done, which is shown in Table 16. The one that has been developed will require a higher investment, however it becomes worthwhile when compared to the conventional method for the following:

- The processing time of the developed product is less than the conventional method, taking up to 15 minutes when compared to the 20 minutes on average of the conventional method;
- More data can be acquired by obtaining the surface of the moulds/parts. By retrieving the surface, surface inspection and volume calculation can be done. This further allows to study the processing of the parts and the wear of the moulds, such as figuring where the most deformation happens, the influence of the operator during mould polishing and possible effects the polishing can have in a given area;

- The knowledge required to use the scripts is rather basic, whereas through the conventional method, specialized training is necessary;
- The light systems have enough sensitivity to pick up on the differences from a polishing operation which allows to conduct comparative studies between parts;
- Finally, the product that has been developed can be used for more than just inspecting glass blow moulds. It can be applied for situations where a series of parts is needed to be inspected, which is common in the plastics industry.

Table 16 - Comparison between the conventional and the developed method

Parameter	Conventional method	Developed method
Investment	Low	High
Time consumption	20 minutes	Up to 15 minutes
Type of acquired data	Volume	Volume, surface inspection, mould wear study
Knowledge to perform	Specialized training	Basic
Comparative results	Only between volumes	Can check differences between polishing stages
Applications	Limited	Versatile

5. Conclusions and Future Work

The use of reverse engineering methods and their continuous development allows to obtain more data about parts which aids in improving the production process. Inside the reverse engineering systems available, light systems like laser scanners and structured light systems are employed to inspect parts due to their acquisition speed and versatility in surface scanning. Production processes are evermore growing to become automated and inspection is an important step to ensure quality. With this project, the aim has been to combine both these subjects and develop a product capable of fulfilling these needs for the automatic volume assessment and surface inspection of moulds used to make glass bottles. Thus far, the ability of processing the scan data to automatically obtain the volume and the surface inspection has been completed. Technology studies have been conducted to verify which would be the best suited light system technology.

During this project, software was developed to solve the automatic calculation of the volume and deliver a surface inspection report based on scan data from the surface acquisition of the moulds. This enables the improvement of the production process by studying the effects of the process on the surface of the moulds. To function, the script requires the CAD model to have the features which will be used for alignment and mesh trimming. For this reason, a second script was developed to assist the user in the CAD preparation. It was found that the script is sensitive to how accurately the CAD resembles the STL mesh and if the mesh has any noticeable outliers on the surfaces used for feature creation.

To assess which system would be best suited for the client's needs, three studies were done. These served to verify the systems' ability to acquire the moulds' surface, to see if they can distinguish differences after the moulds are polished and to validate the used technologies. It was found that the light systems can be used to check the differences after polishing the moulds. As for the used systems, the blue light laser scanner was able to acquire the surfaces of polished cast iron moulds and unpolished bronze moulds, whereas the white light structured light system required white spray to apply a matte coating on the moulds to acquire their surfaces.

By using these scripts and a reverse engineering system, it could take up to 15 minutes, or less, depending on the computer, to obtain the volume and the surface inspection of the mould set. The time to inspect each mould set can, therefore, be reduced while benefitting from obtaining more data. This type of system, by delivering surface information, has the added benefit of allowing to not only verify the mould, but also to study several mould sets to assess the production process and lead to their improvement. Furthermore, this type of product can be applicable to other industries where series part inspection is required.

Finally, a benchmark comparison between the technologies based on the client needs was done. From this comparison it was seen that a state-of-the-art structured light system would be more viable to use as the reverse engineering system for this application. However, it would be necessary to conduct tests on this system to validate it and compare it to the results obtained from the laser scanning before proceeding with its use.

Overall, there are issues that must be addressed for future work:

- A test on the surface acquisition between an unpolished bronze mould and then after polishing should be done using the laser scanner and a state-of-the-art structured light system to test them under the most difficult condition and understand the limitations of the systems;
- The development of the product with the most viable light system. This will entail the programming and setting up the system to scan the part correctly;
- Implementation of more user tips on the CAD guide script, such as displaying a diagram of the features to be created to further standardize the process;
- Addition of more conditions to the volume assessment script to account for possible geometry variations of the moulds;
- More validation tests should be done regarding the surface acquisition;
- The repeatability of the systems should be studied;
- Streamline the volume assessment script by finding the most time-consuming functions and reduce the time needed to analyse a full mould set;
- To improve the mould production process, tests regarding the wear of these moulds over the time they are used should be done.

Bibliographic References

[1] R. Coles, D. McDowell, and M. J. Kirwan, *Food Packaging Technology*, 1st ed. Blackwell Publishing Ltd and CRC Press, 2003.

[2] N. Kovacec, Miroslav; Pilipovic, Ana; Stefanic, "Improving the quality of glass containers production with plunger process control," *CIRP J. Manuf. Sci. Technol.*, vol. 3, pp. 304–310, 2011.

[3] M. Testa, O. Malandrino, M. R. Sessa, S. Supino, and D. Sica, "Long-Term Sustainability from the Perspective of Cullet Recycling in the Container Glass Industry : Evidence from Italy," *Sustainability*, pp. 1–19, 2017.

[4] B. M. Scalet, M. Garcia Muñoz, Q. Sissa Aivi, S. Roudier, and D. S. Luis, "Best Available Techniques (BAT) Reference Document for the Manufacture of Glass," Brussels, 2013.

[5] H. Vasudev, L. Thakur, and A. Bansal, "A review on performance of glass mould coated with different coating techniques," in *Proceedings of 4th International Conference on Production and Industrial Engineering.*, 2016, p. 12.

[6] The European Glass Container Federation, "Container glass production under the EU-ETS reform post-2020: an asset for Europe's low-carbon economy," Brussels, 2016.

[7] Glass Alliance Europe, "Glass Production," 2019. [Online]. Available: https://www.glassallianceeurope.eu/images/cont/gae-glass-production-eu28_file.pdf. [Accessed: 15-Nov-2019].

[8] C. Giannopapa, "Development of a Computer Simulation Model for Blowing Glass Containers," in *ASME 2006 Pressure Vessels and Piping/ICPVT-11 Conference*, 2006, pp. 165–172.

[9] M. Sarwar and A. W. Armitage, "Tooling requirements for glass container production for the narrow neck press and blow process," *J. Mater. Process. Technol.*, vol. 139, no. 1–3, pp. 160–163, 2003.

[10] R. Penlington, M. Sarwar, and D. H. Lewis, “Application of advanced coatings to narrow neck press and blow plungers in the glass container industry,” *Surf. Coat. Technol.*, vol. 76–77, pp. 81–85, 1995.

[11] S. Grégoire, J. M. A. C. de Sá, P. Moreau, and D. Lochegnies, “Modelling of heat transfer at glass / mould interface in press and blow forming processes,” *Comput. Struct.*, vol. 85, no. 15–16, pp. 1194–1205, 2007.

[12] P. Manns, W. Döll, and K. Günter, “Glass in contact with mould materials for container production,” *Glas. Sci. Technol. Glas. Berichte*, vol. 68, no. 12, pp. 389–399, 1995.

[13] W. L. Guesser, L. Kluge, and D. C. Jr., “Moldes de ferro fundido para a produção de peças em vidro,” *Fundição e Serviços*, p. 78, 2012.

[14] V. Hitesh, T. Lalit, and S. Harmeet, “A REVIEW ON TRIBO-CORROSION OF COATINGS IN GLASS MANUFACTURING INDUSTRY AND PERFORMANCE OF COATING TECHNIQUES AGAINST HIGH TEMPERATURE CORROSION AND WEAR,” *i-manager’s J. Mater. Sci.*, vol. 5, no. 3, p. 38, 2017.

[15] K. M. Mashloosh, “Wear resistance of different types of cast iron used in glass blow mould,” *Diyala J. Eng. Sci.*, vol. 8, no. 3, pp. 1–21, 2015.

[16] D. Filipe and S. Pereira, “Análise e Seleção de Materiais para Moldes de Vidro de Mesa Análise e Seleção de Materiais para Moldes de Vidro de Mesa,” Instituto Politécnico de Leiria - ESTG, 2014.

[17] E. Henriques, P. Peças, and B. Silva, “Application of Quick Change-over Method (SMED) in the Production of Moulds to the Glass Industry,” in *RPD 2008 – Rapid Product Development*, 2008, p. 5.

[18] P. Moreau, D. Lochegnies, S. Gregoire, and J. M. A. César de Sá, “Analysis of lubrication in glass blowing: Heat transfer measurements and impact on forming,” *Glas. Technol. - Eur. J. Glas. Sci. Technol. Part A*, vol. 49, no. 1, p. 23, 2008.

[19] Z. Geng and B. Bidanda, “Review of reverse engineering systems–current state of the art,” *Virtual Phys. Prototyp.*, vol. 12, no. 2, pp. 161–172, 2017.

[20] S. H. Mian, M. A. Mannan, and A. Al-Ahmari, “Accuracy of a reverse-engineered mould using contact and non-contact measurement techniques,” *Int. J. Comput. Integr. Manuf.*, vol. 28, no. 5, pp. 419–436, 2015.

[21] M. Irshad, M. Azam, M. Sarfraz, and M. Z. Hussain, “Reverse Engineering of Generic Shapes Using Quadratic Spline and Genetic Algorithm,” in *Advances in Intelligent Systems and Computing*, K. Arai and S. Kapoor, Eds. 2020, pp. 678–686.

[22] O. Aubreton, A. Bajard, B. Verney, and F. Truchetet, “Infrared system for 3D scanning of metallic surfaces,” *Mach. Vis. Appl.*, vol. 24, no. 7, pp. 1513–1524, 2013.

[23] I. Reljić and I. Dunder, “Application of photogrammetry in 3D scanning of physical objects,” *TEM J.*, vol. 8, no. 1, pp. 94–101, 2019.

[24] I. Ihrke, K. N. Kutulakos, H. P. A. Lensch, M. Magnor, and W. Heidrich, “Transparent and specular object reconstruction,” *Comput. Graph. Forum*, vol. 29, no. 8, pp. 2400–2426, 2010.

[25] W. L. K. Nguyen, A. Aprilia, A. Khairyanto, W. C. Pang, G. G. L. Seet, and S. B. Tor, “Morphological Box Classification Framework for supporting 3D scanner selection,” *Virtual Phys. Prototyp.*, vol. 13, no. 3, pp. 211–221, 2018.

[26] J. R. M. Pereira, I. de Lima e Silva Penz, and F. Pinto da Silva, “Effects of different coating materials on three-dimensional optical scanning accuracy,” *Adv. Mech. Eng.*, vol. 11, no. 4, pp. 1–6, 2019.

[27] M. Hawryluk, J. Ziemba, and Ł. Dworzak, “Development of a method for tool wear analysis using 3D scanning,” *Metrol. Meas. Syst.*, vol. 24, no. 4, pp. 739–757, 2017.

[28] X. Zhao, M. Tootkaboni, and B. W. Schafer, “Laser-based cross-section measurement of cold-formed steel members: Model reconstruction and application,” *Thin-Walled Struct.*, vol. 120, no. September, pp. 70–80, 2017.

[29] S. Matthias *et al.*, “Metrological solutions for an adapted inspection of parts and tools of a sheet-bulk metal forming process,” *Prod. Eng.*, vol. 10, no. 1, pp. 51–61, 2016.

[30] J. Wang and Y. Yang, “High-speed three-dimensional measurement technique for

object surface with a large range of reflectivity variations," *Appl. Opt.*, vol. 57, no. 30, pp. 9172–9182, 2018.

[31] T. Koutecký, D. Paloušek, and J. Brandejs, "Sensor planning system for fringe projection scanning of sheet metal parts," *Meas. J. Int. Meas. Confed.*, vol. 94, pp. 60–70, 2016.

[32] H. Du, X. Chen, J. Xi, C. Yu, and B. Zhao, "Development and verification of a novel robot-integrated fringe projection 3D scanning system for large-scale metrology," *Sensors*, vol. 17, no. 12, pp. 2886–2898, 2017.

[33] H. Lin, J. Gao, Q. Mei, Y. He, J. Liu, and X. Wang, "Adaptive digital fringe projection technique for high dynamic range three-dimensional shape measurement," *Opt. Express*, vol. 24, no. 7, p. 7703, 2016.

[34] S. Martínez-Pellitero, E. Cuesta, S. Giganto, and J. Barreiro, "New procedure for qualification of structured light 3D scanners using an optical feature-based gauge," *Opt. Lasers Eng.*, vol. 110, pp. 193–206, 2018.

[35] H. Lin, J. Gao, Q. Mei, G. Zhang, Y. He, and X. Chen, "Three-dimensional shape measurement technique for shiny surfaces by adaptive pixel-wise projection intensity adjustment," *Opt. Lasers Eng.*, vol. 91, pp. 206–215, 2017.

[36] Z. Song, H. Jiang, H. Lin, and S. Tang, "A high dynamic range structured light means for the 3D measurement of specular surface," *Opt. Lasers Eng.*, vol. 95, no. September 2016, pp. 8–16, 2017.

[37] X. Zhang, W. Cui, W. Li, and F. Liou, "A hybrid process integrating reverse engineering, pre-repair processing, additive manufacturing, and material testing for component remanufacturing," *Materials (Basel).*, vol. 12, no. 12, 2019.

[38] J. B. Krolczyk, G. Pihan, and S. Legutko, "Application of optical scanning system to determine the machining allowances," *MATEC Web Conf.*, vol. 112, Jul. 2017.

[39] H. Lin, J. Gao, G. Zhang, X. Chen, Y. He, and Y. Liu, "Review and comparison of high-dynamic range three-dimensional shape measurement techniques," *J. Sensors*, vol. 2017, p. 11, 2017.

[40] S. Zhang, "High-speed 3D shape measurement with structured light methods: A

review," *Opt. Lasers Eng.*, vol. 106, pp. 119–131, 2018.

[41] I. Dixit, S. Kennedy, J. Piemontesi, B. Kennedy, and C. Krebs, "Which tool is best: 3D scanning or photogrammetry – It depends on the task," in *Biomedical Visualisation : Volume 1*, vol. 1120, P. M. Rea, Ed. Springer International Publishing, 2019, pp. 107–119.

[42] H. Wang, J. Zhou, T. Zhao, and Y. Tao, "Springback compensation of automotive panel based on three-dimensional scanning and reverse engineering," *Int. J. Adv. Manuf. Technol.*, vol. 85, no. 5–8, pp. 1187–1193, 2016.

[43] M. M. Auerswald, A. von Freyberg, and A. Fischer, "Laser line triangulation for fast 3D measurements on large gears," *Int. J. Adv. Manuf. Technol.*, vol. 100, no. 9–12, pp. 2423–2433, 2019.

[44] S. Gerbino, D. M. Del Giudice, G. Staiano, A. Lanzotti, and M. Martorelli, "On the influence of scanning factors on the laser scanner-based 3D inspection process," *Int. J. Adv. Manuf. Technol.*, vol. 84, no. 9–12, pp. 1787–1799, 2016.

[45] Y. M. Amir and B. Thörnberg, "High Precision Laser Scanning of Metallic Surfaces," *Int. J. Opt.*, vol. 2017, 2017.

[46] Y. Wang and H. Y. Feng, "Effects of scanning orientation on outlier formation in 3D laser scanning of reflective surfaces," *Opt. Lasers Eng.*, vol. 81, pp. 35–45, 2016.

[47] Y. Wang and H. Y. Feng, "A rotating scan scheme for automatic outlier removal in laser scanning of reflective surfaces," *Int. J. Adv. Manuf. Technol.*, vol. 81, no. 1–4, pp. 705–716, 2015.

[48] K. Zaba, S. Nowak, M. Kwiatkowski, M. Nowosielski, P. Kita, and A. Sioma, "Application of non-destructive methods to quality assessment of pattern assembly and ceramic mould in the investment casting elements of aircraft engines," *Arch. Metall. Mater.*, vol. 59, no. 4, pp. 1517–1525, 2014.

[49] D. B. Gajic, S. Mihic, D. Dragan, V. Petrovic, and Z. Anisic, "Simulation of photogrammetry-based 3D data acquisition," *Int. J. Simul. Model.*, vol. 18, no. 1, pp. 59–71, 2019.

[50] K. Earley, D. Livingstone, and P. M. Rea, “Digital curation and online resources: digital scanning of surgical tools at the royal college of physicians and surgeons of Glasgow for an open university learning resource,” *J. Vis. Commun. Med.*, vol. 40, no. 1, pp. 2–12, 2017.

[51] D. Zhang, Y. Li, J. Liu, G. Xie, and E. Su, “A novel 3D optical method for measuring and evaluating springback in sheet metal forming process,” *Meas. J. Int. Meas. Confed.*, vol. 92, pp. 303–317, 2016.

[52] G. Kortaberria, U. Mutilba, E. Gomez-Acedo, A. Tellaeche, and R. Minguez, “Accuracy evaluation of dense matching techniques for casting part dimensional verification,” *Sensors*, vol. 18, no. 9, pp. 1–22, 2018.

[53] S. Werling, J. Balzer, and J. Beyerer, “A new approach for specular surface reconstruction using deflectometric methods,” in *Informatik 2007 – Informatik trifft Logistik – Band 1*, 2007, pp. 44–48.

[54] R. D. Wedowski, G. A. Atkinson, M. L. Smith, and L. N. Smith, “Dynamic deflectometry: A novel approach for the on-line reconstruction of specular freeform surfaces,” *Opt. Lasers Eng.*, vol. 50, no. 12, pp. 1765–1778, 2012.

[55] H. Han, S. Wu, Z. Song, and J. Zhao, “An Accurate Phase Measuring Deflectometry Method for 3D Reconstruction of Mirror-Like Specular Surface,” in *Proceedings - 2019 2nd International Conference on Intelligent Autonomous Systems, ICoIAS 2019*, 2019, pp. 20–24.

[56] C. Chang, Z. Zhang, N. Gao, and Z. Meng, “Measurement of the three-dimensional shape of discontinuous specular objects using infrared phase-measuring deflectometry,” *Sensors*, vol. 19, no. 21, 2019.

[57] P. Zhao, N. Gao, Z. Zhang, F. Gao, and X. Jiang, “Performance analysis and evaluation of direct phase measuring deflectometry,” *Opt. Lasers Eng.*, vol. 103, pp. 24–33, 2018.

[58] P. Kiefel and P. Nitz, “Quality control of Fresnel lens molds using deflectometry,” in *AIP Conference Proceedings*, 2016, vol. 1766, p. 050004.

[59] L. Huang, M. Idir, C. Zuo, and A. Asundi, “Review of phase measuring

deflectometry," *Opt. Lasers Eng.*, vol. 107, pp. 247–257, 2018.

[60] C.-H. Tseng, "Simulation of Phase Measuring Deflectometry of Freeform Surfaces," The University of Arizona, 2019.

[61] M. Quinten, *A Practical Guide to Surface Metrology*, 1st ed. Cham: Springer International Publishing, 2019.

[62] G. P. Butel, "Analysis and new developments towards reliable and portable measurements in deflectometry," The University of Arizona, 2013.

[63] Z. Zhang *et al.*, "Three-dimensional shape measurements of specular objects using phase-measuring deflectometry," *Sensors*, vol. 17, no. 12, 2017.

[64] Wenzel, "Xo 55-7," 2018. [Online]. Available: https://www.wenzel-group.com/pdf/used-machine/15985/. [Accessed: 10-Nov-2020].

[65] Faro, "[TECHSHEET] FARO 8-Axis Quantum S FaroArm / ScanArm V2," 2019. [Online]. Available: https://insights.faro.com/techsheets/techsheet-faro-8-axis-quantum-s-faroarm-scanarm-v2. [Accessed: 10-Nov-2020].

[66] P. Volonghi, G. Baronio, and A. Signoroni, "3D scanning and geometry processing techniques for customised hand orthotics: an experimental assessment," *Virtual Phys. Prototyp.*, vol. 13, no. 2, pp. 105–116, 2018.

Appendix A – Programmer's manual: function descriptions

Here, the code descriptions for each function used in the volume assessment script is done. This will include a description of the function's purpose, its arguments and its outputs.

point_treatment:

Function: Responsible for treating point clouds. Takes empty list, populates it with the point models by iterating over a list filled with the loaded models and filtering the ones that are point objects. Then, executes global registration for similar areas to coincide with each other, repairs the normal direction of the points and merges the point objects into a single point object with the name of the CAD model's name. Returns the point object and the CAD model.

Arguments:

point_list – Empty list to be filled with the point objects

model_list – List populated by the models loaded in the environment

bestfit:

Function: Aligns the point object to the CAD model through a bestfit algorithm, error distributed evenly.

Arguments:

mesh_points – Point object to be aligned to the CAD model

cad_model – Reference CAD model object

bestfit_fine:

Function: Aligns the point object to the CAD model through the bestfit algorithm, but only making fine adjustments to the point object's alignment.

Arguments:

mesh_points – Point object to be aligned to the CAD model

cad_model – Reference CAD model object

wrap_points:

Function: Converts the point object into an STL mesh. The original point object is deleted to free up memory and the new STL object is added to the environment. This

STL model is then defined as the “Test” model for future operations concerning alignment and feature creation in relation to the CAD model which is set as the “Reference” model. Small triangle clusters that may have formed are eliminated via a manifold operation. This function returns the STL object and the “Test” model object.

Arguments:

pts_model – Model representation of the point object

pts – Model of type Points

CAD_obj – Model of type CAD

fill_holes:

Function: Fills holes of up to a diameter of 50 mm.

Arguments:

mesh – Model of type mesh

section:

Function: Takes the mesh model, reads the features associated to it from the autocreation operation, filters the plane features and stores them in a list. Offset planes are created in relation to the original planes to make a clean cut. Offsets should be small, like 0.03 mm. These planes then intersect the mesh and delete the selection above them, thus trimming the mesh. Next, the cone features are read. In the case of the model having a cone and being a mould half, an offset plane is generated based on this cone’s bottom plane. After trimming, the trimmed mesh object is returned.

Arguments:

mesh_model – Model representation of the mesh object

mesh_conversion:

Function: Reads a list containing cylinder surfaces and converts them to an STL. This function is part of the process to trim the bottom mould. Returns a list populated by the mesh objects of the cylinders

Arguments:

cyl_list – List containing cylinders created based on the bottom mould’s cone

mesh_union:

Function: Makes a Boolean addition of the cylinder mesh objects to create a target and a tool for the mould bottom trimming. Returns the resulting object.

Arguments:

mesh_list – List containing the mesh objects of the cylinders created through the mesh_conversion function.

mesh_subtract:

Function: Makes a Boolean subtraction of the tool to the target. This results in an object that can be used for the mould bottom trimming.

Arguments:

target – Cylinder mesh object that is used as the reference object for the subtraction

tool - Cylinder mesh object that is subtracted

align_comp:

Function: This function will execute a feature-based alignment between the CAD and the STL objects. Firstly, the plane features and the cylinder features are read for each case and stored in list, accordingly. Then, the feature alignment pairs are defined. It was seen that the priority should be top plane pair→bottom plane pair→axis pair. Then, the alignment is executed and the STL object is subjected to the resulting 3D transformation.

Arguments:

cad_model – Model representation of the CAD object

stl_model – Model representation of the mesh object

stl – Model of type mesh

file_save:

Function: Saves the .wrp file of the trimmed mesh with its features associated to a designated location. Will delete the remaining objects in the environment before saving to ensure only the mesh is saved for future loading. Returns the file path to then be able to load this file.

Arguments:

mesh_model – Model representation of the mesh object

path – Designated path to where the file will be saved

model_list – List of the models loaded in the environment

mesh_align:

Function: With the mesh objects loaded into the environment, this function aims to align them to then enable their merging and obtain the bottle model. A list containing the models in the application is iterated and the number of triangles for each of them is stored in another list to then select the model with the highest number of triangles as the reference. This will ensure only the bottle halves will become the reference object. Then, just as in align_comp, the feature pairs are created and set. In this case, having to execute two alignments, a list which will contain the feature pairs for the "Test" models is created.

Arguments:

model_list – List of the models loaded in the environment

fill_top:

Function: Fills the front hole, in the bottleneck area.

Arguments:

mesh – Model of type mesh

Appendix B – User manual

To aid the user, the following procedure is presented to ensure the correct use of the application is done.

1. Start CAD guide

Firstly, to begin, Geomagic Control must be running. Then, by going to the Bottle Mould analysis tab, buttons to execute either the CAD feature creation or the volume assessment are present. To start the CAD feature guide, this button, highlighted in red, must be pressed.

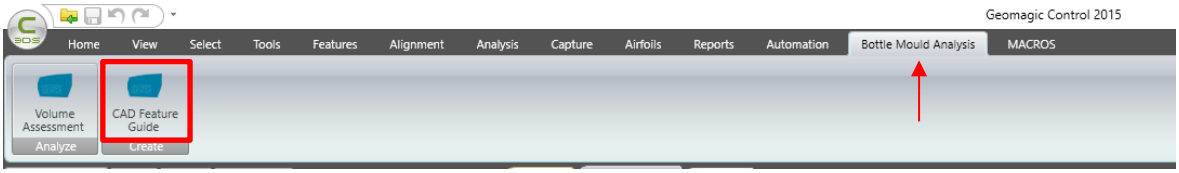

2. Load CAD

Pressing the button will lead to asking the user the CAD he wishes to load and thus begin the program.

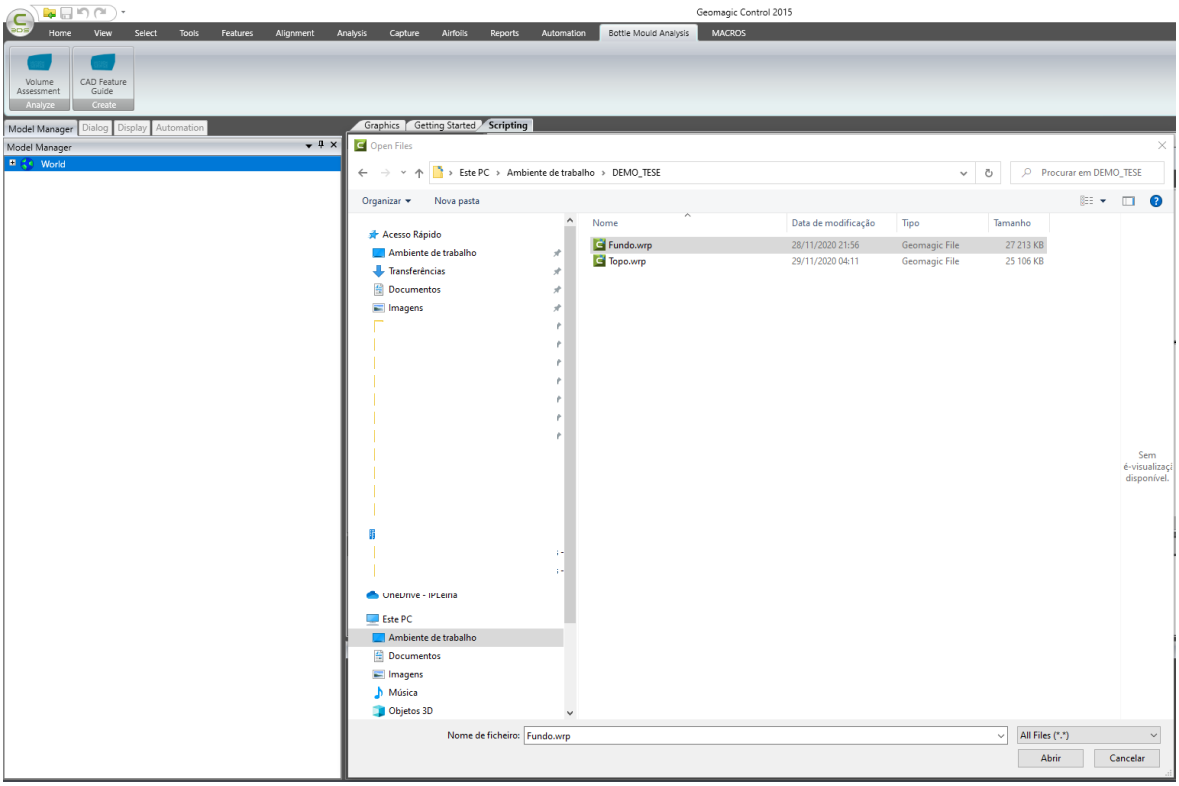

3. Select creation mode

With the CAD loaded, the user defines which mode the created features will be associated with. The modes are accessed via a dropdown as shown in the below figures. The selectable modes are: Align, Trim and Top.

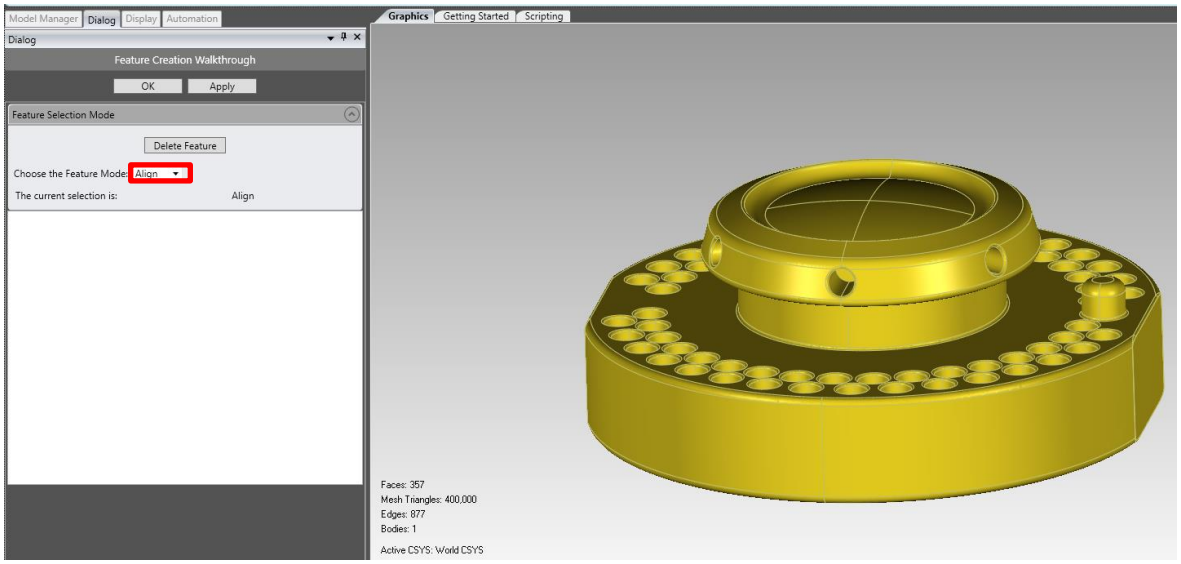

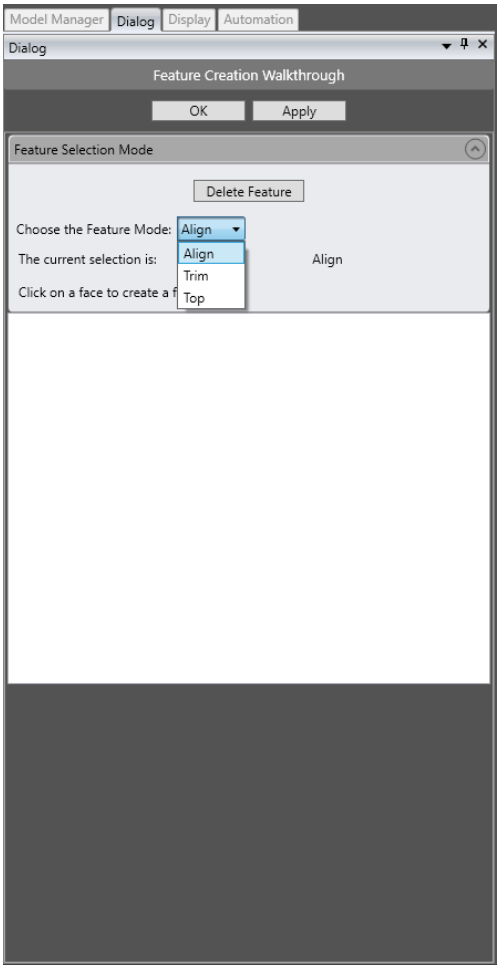

4. Create features

Having the mode selected, the features can start being created by pressing the apply button and then clicking on the desired face of the CAD model to generate the corresponding feature. To stop creating features, the cancel button must be pressed.

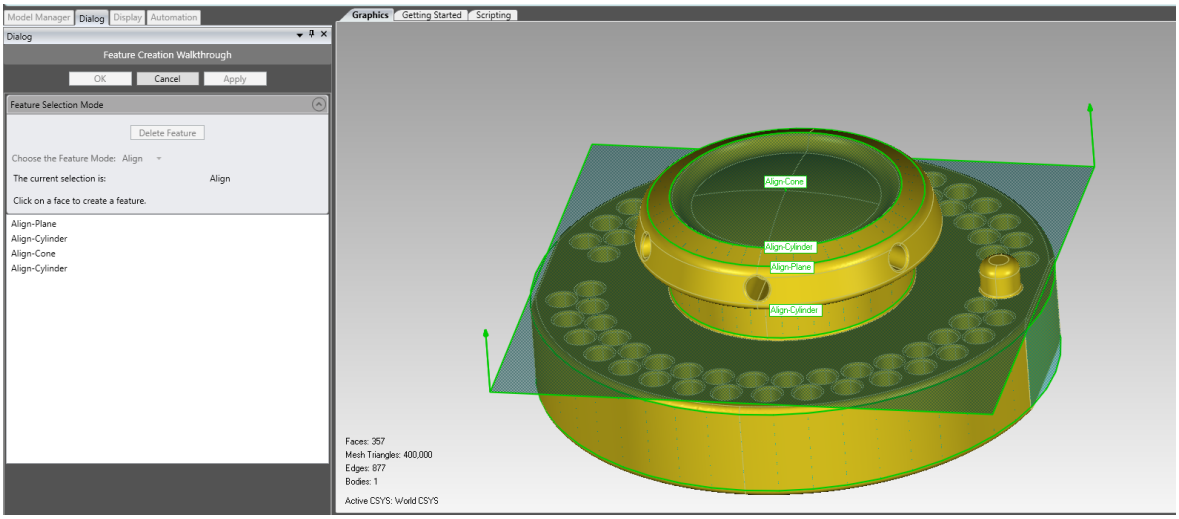

5. Delete features

If a feature is created by mistake, it can be deleted by selecting it from the dropdown and then pressing the delete feature button. To end the dialogue, the OK button must be pressed.

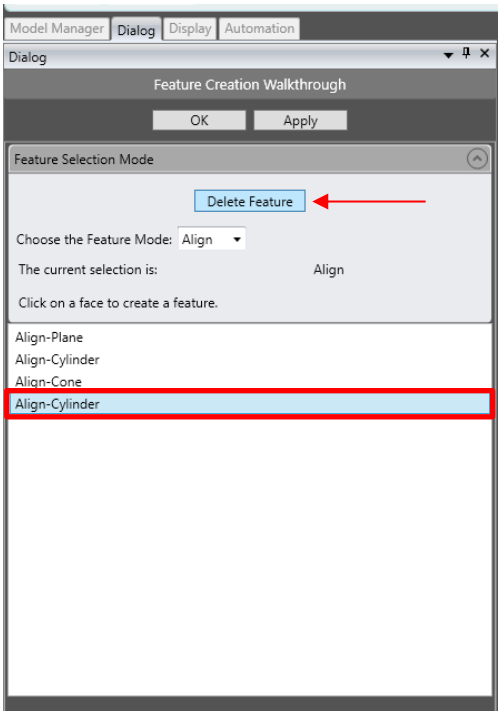

6. Save file

By pressing the OK button and exiting the dialogue, a prompt to save the file is called.

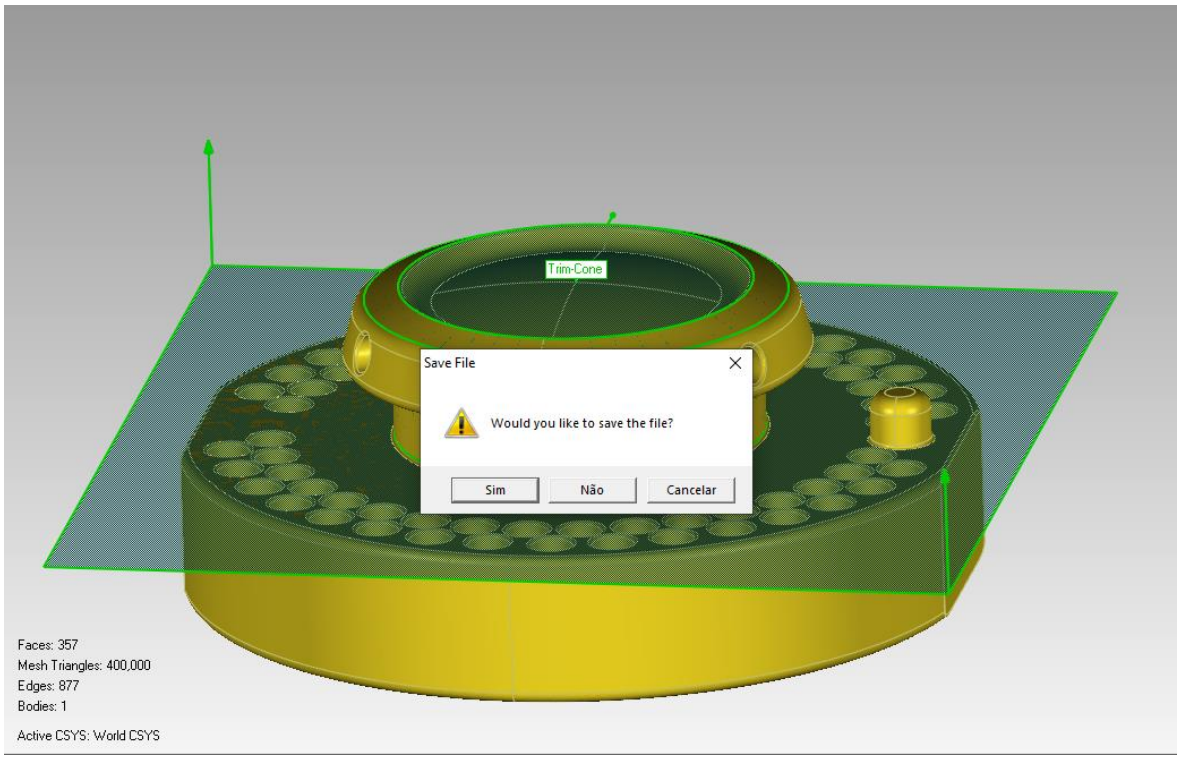

7. Start volume assessment

To begin the Volume Assessment script, its button should be pressed in the Bottle Mould Analysis tab.

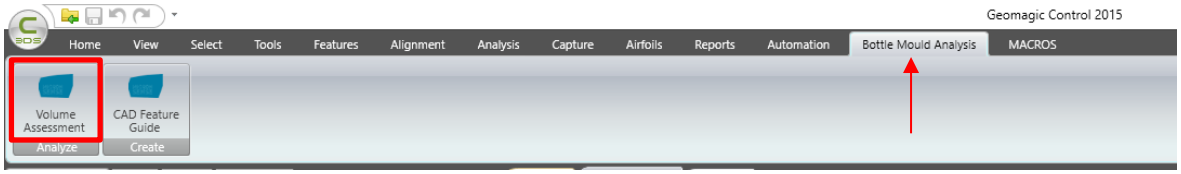

8. Input number of parts in the mould set/to be inspected

Pressing this button will clean the active environment and call a prompt to select the number of parts to be analysed in the mould set.

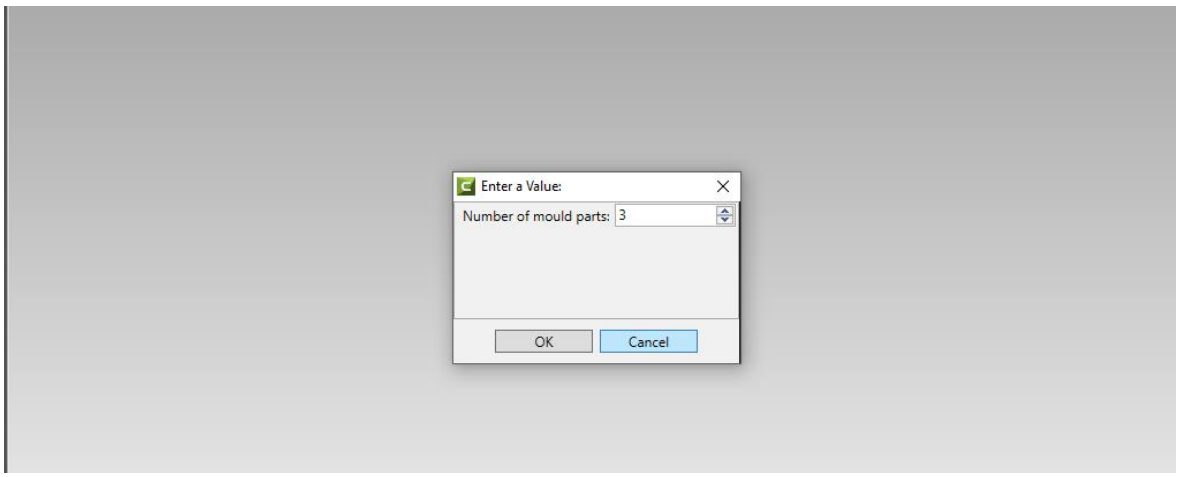

9. Load point clouds file with respective CAD

After selecting the amount, the point clouds file and its respective CAD model must be selected to then load into the environment.

10. Automatic operations from point cloud object to STL creation and feature creation

Following the loading, several automatic operations are executed without user input. These will be:

- The global registration of the point clouds to ensure the coincidental areas have overlap;
- The repair of the normal direction of the points;
- The combination of the several point objects into a single one;
- Following a general bestfit alignment to the CAD with a consequent fine adjustment only bestfit alignment to guarantee the models are sufficiently aligned for feature creation;
- The wrapping of the point cloud object to generate an STL mesh;
- Finally, the autocreation of the features in the STL mesh based on the ones that were created in the CAD guide script.

11. Create top plane by selecting points over mesh

By not having an accurate CAD model to represent the model, the top plane must be created via user input. This requires the selection of the triangles over the STL mesh to create the plane.

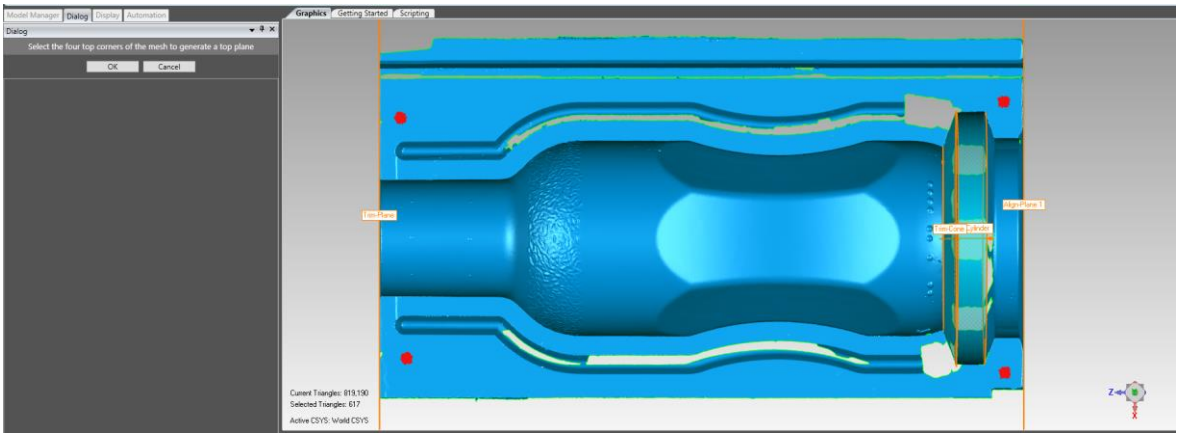

12. Auto trim

Having all the features created, the mesh is trimmed using the features created for this purpose.

13. Prompt to delete additional undesired triangles

Following the automatic mesh trimming, sometimes there can be leftovers or anomalous triangles still connected to the mesh which can be deleted to ensure the correct functioning of the script. The user is prompted to select any triangles fulfilling these cases to then be deleted after selection and by pressing Ok. Otherwise, if Cancel is pressed, the selected triangles will not be deleted. If the Ok button is pressed without having selected any triangles, the script will proceed as normal.

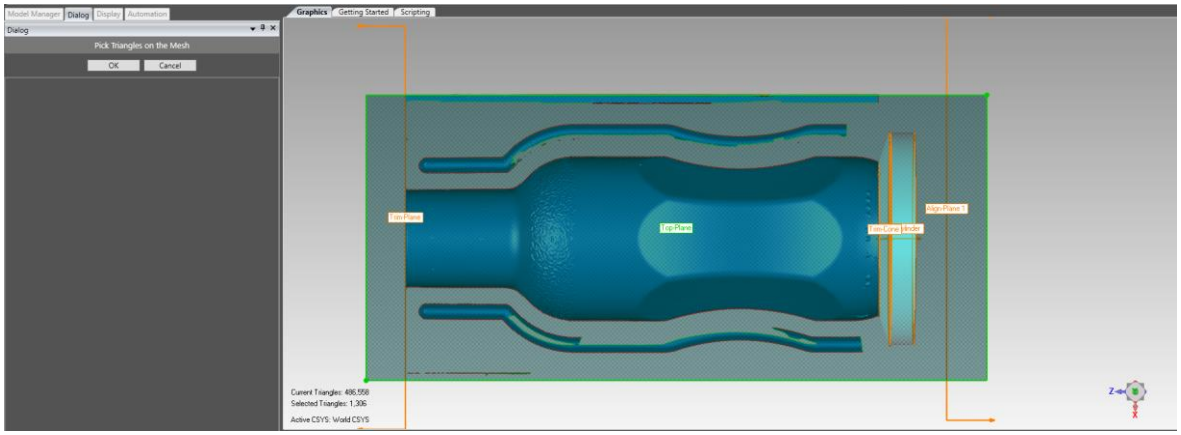

14. Auto feature align

By using the features with the Align mode attached, the STL mesh is aligned to the CAD to create a more accurate surface inspection.

15. Input auto or manual inspection points

Following the alignment, the user selects how the surface inspection is done. Either automatically, creating random points over the mesh, or manual where the user must select a file containing the coordinates of the inspection points. To accept the manual mode, the accepted keywords are: “”, “y”, “Y”, “ye”, “YE”, “yes” and “YES”.

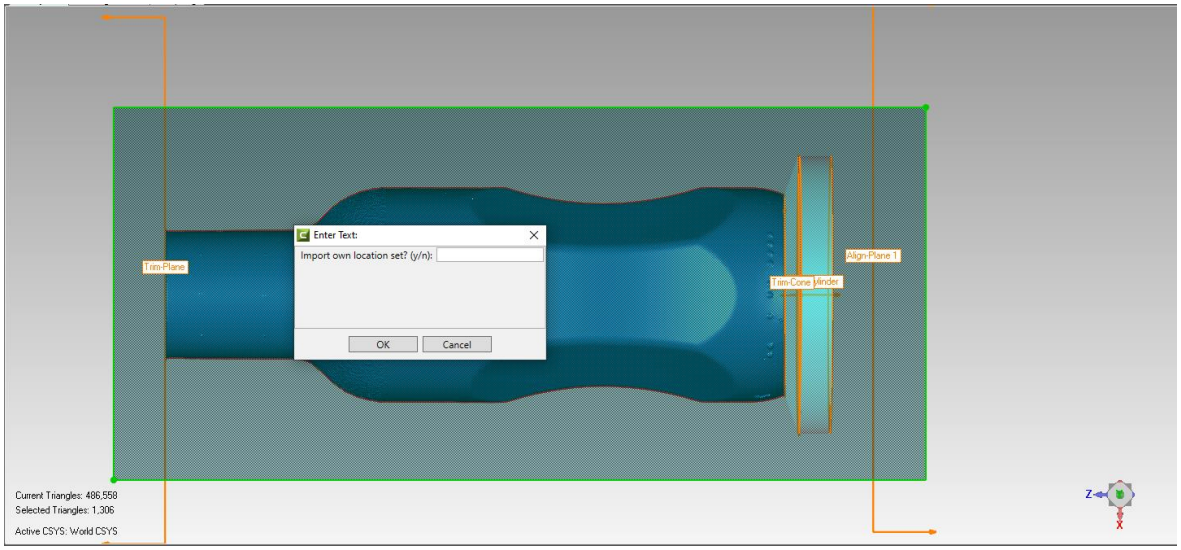

16. Surface inspection

The surface inspection is done based on the above choice with a max/min critical tolerance of ±0.2 mm and a max/min nominal of ±0.05 mm.

17. Save file destination

Following the surface inspection, the user then selects where he wishes to save the files. This location is stored to then load all the analysed parts of the mould set to produce a volume calculation.

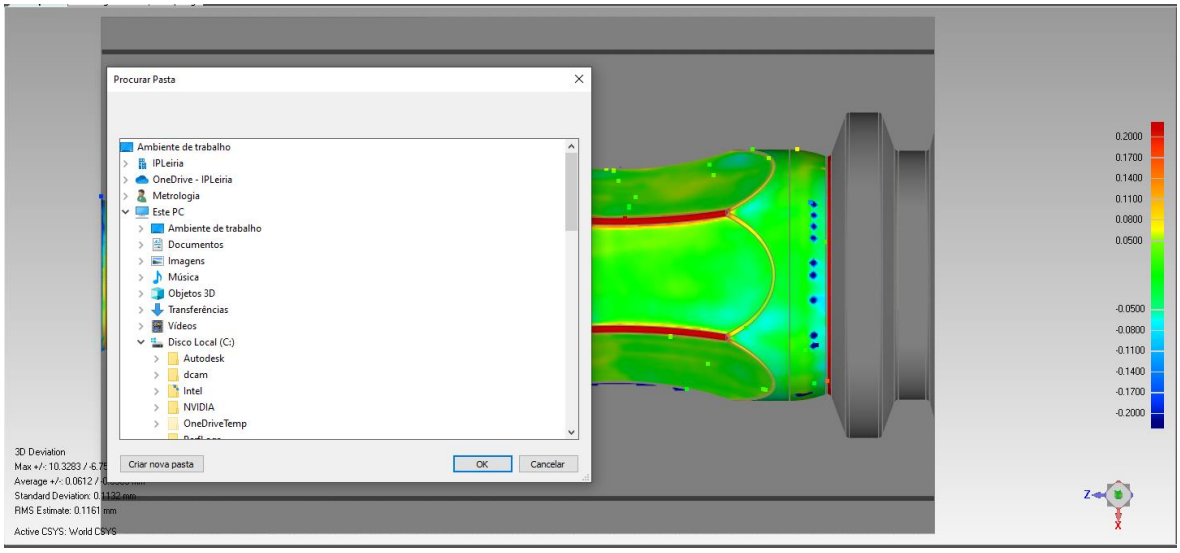

18. Volume calculation

The mesh files are loaded into the environment and are then aligned to each other. Following the alignment, they are merged, and their holes are closed, generating a closed bottle model. The volume is, thusly, calculated.

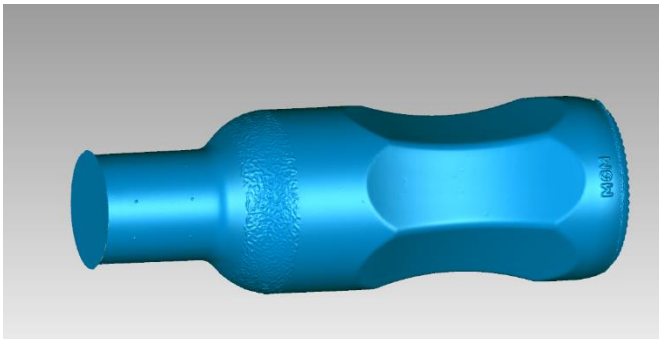

Appendix C – Input/output function blocks: User CAD guide script

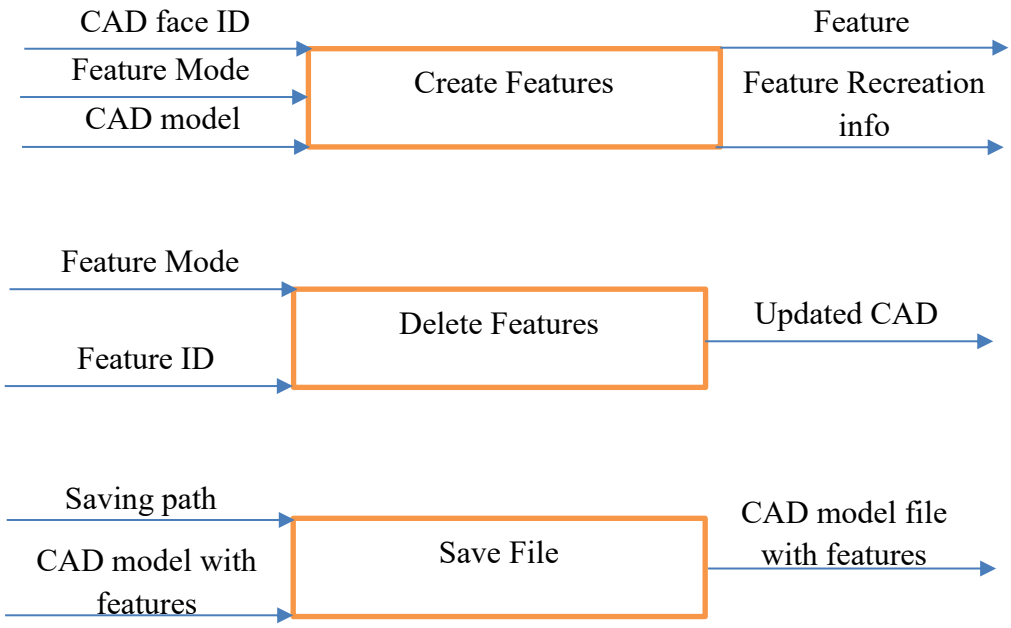

Appendix D – Diagram for the workflow of the volume assessment script

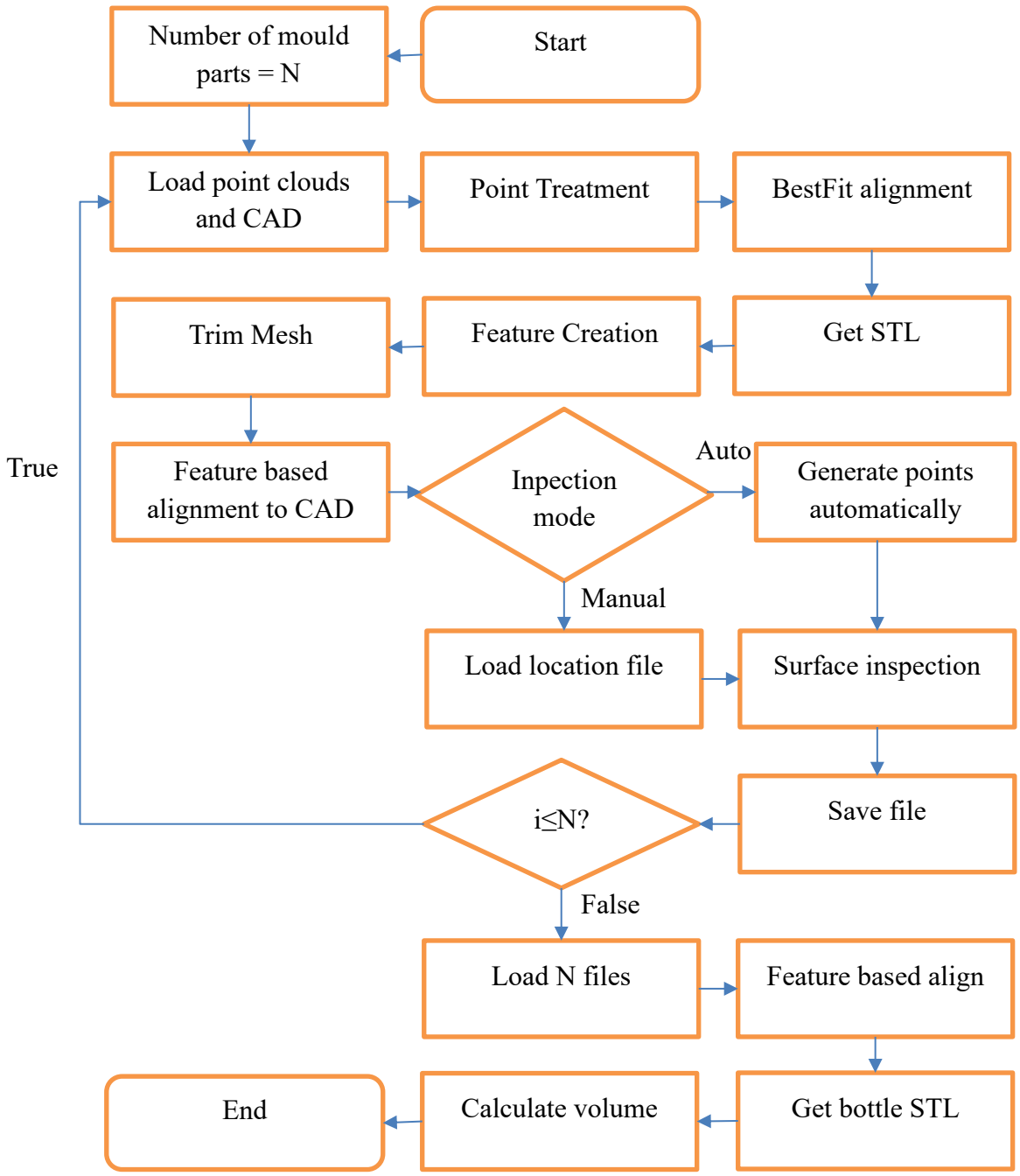

Appendix E – Input/output function blocks:

Volume Assessment script

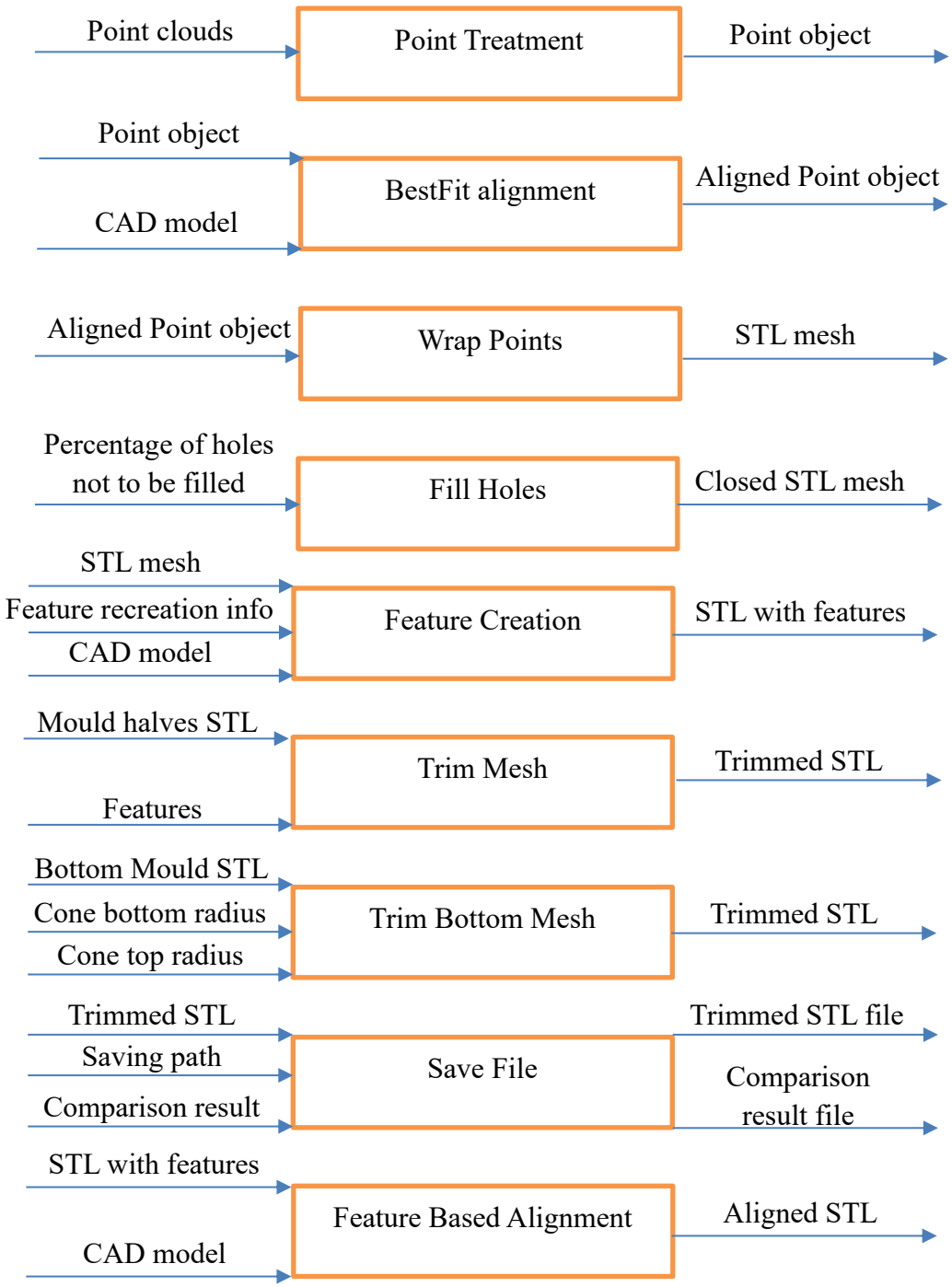

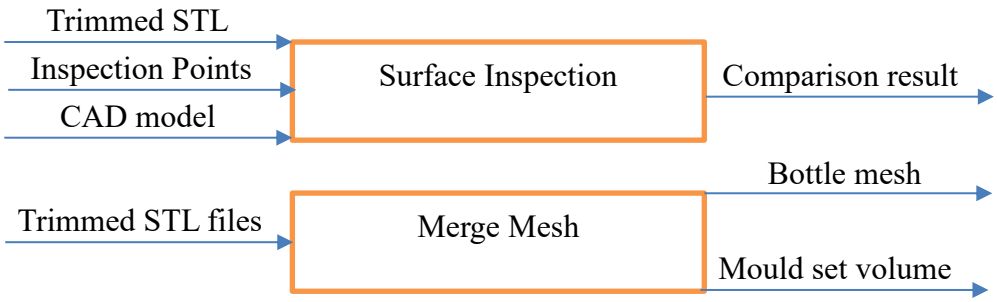
Trimmed STL
Inspection Points
CAD model
Surface Inspection
Comparison result
Trimmed STL files
Merge Mesh
Bottle mesh
Mould set volume